ผลงานตีพิมพ์ในวารสารวิชาการนานาชาติ

# FASCIOLA GIGANTICA: STUDIES OF THE TEGUMENT AS A BASIS FOR THE DEVELOPMENTS OF IMMUNODIAGNOSIS AND VACCINE

P Sobhon, S Anantavara, T Dangprasert, V Viyanant, D Krailas, ES Upatham, C Wanichanon and T Kusamran

Faculty of Science, Mahidol University, Bangkok 10400, Thailand

Abstract. The regument of bile-dwelling Fusciola gigantica is the interfacing layer that helps the parasite to maintain its homeostasis, and evade the hostile environment, including the host's immune attacks. The tegument is a syncytial layer about 10 mm thick, that is formed by the fusion of cytoplasmic processes of tegument cells, whose soma lie underneath the two muscle layers. The surface of the tegument is highly folded and invaginated into numerous ridges, pits and spines, which help to increase the surface area of the tegument for the absorption and exchanging of molecules, as well as for attachment. The outer membrane covering the tegument is a trilaminate sheet about 12 nm thick, and coated with a carbohydrate-rich glycocalyx layer that also bears high negative charges. Some host molecules may also be adsorbed onto this layer. These unique characteristics enable the parasite to evade the antibody-dependent cell-mediated cytotoxicity (ADCC) reaction exerted by the host. The outer membrane and glycocalyx is continuously replaced by the reserved membrane synthesized and stored in secretory granules of tegument cells, that are transported via cell processes towards the tegument by microtubules. The basal membrane of the tegument is trilaminate and invaginated to form membrane infoldings with closely aligned mitochondria. The tegument cytoskeleton is composed of a highly cross-linked network of 4-6 nm knobby microtrabecular fibers, bundles of intermediate filaments, microtubules that splay out from the tegument cells' processes. Major proteins of the cytoskeleton are actin, paramyosin and tubulin. The flukes' antigens that can elicit strong immunological responses in animal hosts are synthesized and released mainly from the tegument and the cecum. The majority of antigens derived from the surface membrane and the tegument are of MW 97, 66, 58, 54, 47 and 14 kDa, while those released from the occum are cysteine proteases of MW 27, 26 kDa. Monoclonal antibodies have been raised against some of these antigens, and have been employed in immunodiagnosis of the infection. From the protection conferred to animal models and the in vitro killing assays of young parasites by specific antibodies, candidate vaccines could be selected from these antigens, such as, an antioxidant enzyme, glutathione-S-transferase, the digestive enzyme cysteine proteases, the surface-tegument proteins, such as fatty acid binding protein (14kDa), membrane proteins (at 66 kDa), as well as muscle protein paramyosin, and hemoprotein. Ongoing research have been directed at deciphering the genetic codes and the syntheses of some of these antigens by recombinant DNA technology.

#### INTRODUCTION

Fascioliasis, a disease that infects both domestic and wild animals, is one of the major tropical diseases that afflict both the temperate and tropical regions of the world. The causative parasites in the temperate regions is Fasciola hepatica, while in tropical region is F. gigantica. Fascioliasis causes significant economic loss estimated at US \$ 2,000 million per annum from its effect on domestic and economic animals (Boray, 1985). The disease can also cross infect humans, and there are reports of increasing incidence world wide (Chitchung et al, 1982; Maurice, 1994; Anon, 1995). The prevalent rates are as high as 30-90% in Africa, 25-90% in Indonesia (Edney and Muchlis, 1962; Soesetya,

1975; Fabiyi, 1987). In Thailand the prevalence rates in cattle and buffaloes are 4-24%, with the highest incidents in the north and northeast and lowest incidents in the South (Photpark and Srikitjakara, 1989; Sukhapesna et al, 1990; 1994). It is clear that the disease is a major impediment to economic progress, which is exacerbated in the less developed countries, particularly towards small-scale farmers, who cannot mobilize limited resources to control, not to mention eradicate the disease.

Fascioliasis could be partially controlled by periodic treatments of the animals in the endemic area with a repertoire of drugs, among which triclabendazole was reported to be highly effective (Sukhapesna et al. 1992), eventhough incidence of resistance to this drug have been repeatedly reported

(Overend and Bower, 1995). In view of the cost and the possible mutation of the parasites which could compromise the drug's action, a better alternative would be the development of vaccines which could either completely prevent the infection or arrest the development of the parasite at certain stage of its life cycle, or even partially reducing the fecundity of infecting adult parasites.

# PARASITES' LIFE CYCLE AND HOST IMMUNOLOGICAL RESPONSES

The sound understanding of the parasites' life cycles together with their biology and hosts' immunological responses are the two most important corner stones for devising any rational vaccine. The life cycle of F. gigantica, which is putatively a single parasite that causes fascioliasis in Thailand, was studied in detail by Chompoochan et al (1976). The whole cycle needs about 158-175 days for completion. The prepatent period of F. gigantica eggs was 8-14 days, after which eggs are hatched into miracidia, whose longevity in water is about 24 hours. Miracidia penetrate intermediate snail hosts, Radix rubiginosa, and develop into sporocysts and rediae within 7-8 days. Cercariae develop from germ cells inside rediae and leave the snail hosts in 35-49 days from the time of miracidial penetration. Within 30-45 minutes, the cercariae settle on leaves of nearby grass or water plants, on which they shed the tails and transform into cysts. Metacercariae continue to develop inside the cysts and may lay dormant up to 60 days. After being ingested by animals or human, excysted juvenile flukes penetrate the gut wall and travel towards the liver via peritoneal cavity. Upon reaching the destination, the flukes penetrate the capsule and burrow themselves into liver parenchyma, and eventually reside in the biliary tree where they develop into adults and begin to lay eggs. Eggs are first found in feces of the cattle and buffaloes between 16-18 weeks and in sheep about 11 weeks after the infection, and reach the peaks about 24-28 and 17-26 weeks, respectively (Thammasart et al, 1996). The ensuing histopathological changes are marked by the progressive biliary cirrhosis due to the fibrosis and calcification of bile ducts. This liver failure leads to diarrhea, losses of appetite, weight and vigor (Sukhapesana et al. 1994), and meat or milk productions. The heavily infected animals, particularly the young ones, could succumb and die.

There are ample evidence which demonstrate that animals hosts mount both humoral and cellmediated immune responses against parasites. Antibody against F. gigantica infection in cattle and buffalocs were first detected at 2-4 weeks after the infection, and reached the peaks around 16 to 20 weeks before declining slowly (Thammasart et al, 1996). It is noticeable that the detection of antibody preceded the finding of eggs in feces by 12 to 14 weeks. This information attests that the devising of immunodiagnostic methods for detecting the early infection is one of key strategy that could benefit the monitoring and early treatment of the disease. Apart from causing antibody formation, the parasites can elicit eascades of antibody-dependent cellmediated cytotoxic (ADCC) reactions. Similar to the cases of schistosomiasis (reviewed by Sher and Coffman, 1992; Maizels et al, 1993; Capron and Capron, 1994), newly excysted juvenile F. hepatica could be coated and killed by antibodies and variety of host immune effector cells that attach to the tegument, including eosinophils, neutrophils, macrophages and mast cells, during their migration through the host's peritoneal cavity (Rajasekariah and Howell, 1977; Kelly et al, 1980; Doy and Hughes, 1982; Hughes, 1987). The release of hydrolytic enzymes and production of oxygen free radicals and nitric oxides by these effector cells on, or in the immediate vicinity of the tegument are the primary action that kill young parasites (James and Gleven, 1989; Smith, 1989; Golenser and Chevion, 1993; Liew and O' Donnell, 1993; Wynn et al. 1994). By contrast, the adult parasites hardly appear affected by the host immune reactions. This may be due to their fairly sequestered residence in the bile duct which has lower immunological activities, though the bile itself contains emulsifying agents and certain level of IgA antibody. Adult parasites may also possess counteracting reactions against oxygen free radicals and nitric oxides which are catalysed by a series of detoxifying or antioxidant enzymes, such as, superoxide dismutase, glutathione-S-transferase and glutathione peroxidase. In schistosomes, these enzymes are more concentrated in adult tissue than juveniles (Mei and Loverde, 1997). Adult parasites can also evolve an evasion mechanism by which their tegament can avoid the attachment of immune effector cells, and thus damage from ADCC reaction. In addition, they can release certain immunomodulating factors that compromise the cell-mediated immune response of the hosts. Studies showed that T cell proliferation and IL-2 production in cattle,

sheep and rats were suppressed during the course of infection by F. hepatica (Oldham and Williams, 1985; Zimmerman et al, 1983; Cervi et al, 1996). Thus any successful vaccine candidate should be directed primarily at preventing the infections by juvenile parasites, which have not yet develop any viable evasion mechanism.

# TEGUMENTAL STRUCTURE AND EVASION MECHANISM

The tegument is the interfacing layer between parasites and hosts that helps the parasites to maintain their homeostasis which is essential for their survival in the hostile biliary environment. Judging from its remarkable structural characteristics, which will be elaborated later, the tegument is probably playing key roles in the absorption and exchange of nutritive and waste molecules, and the regulation of osmolarity as well as ionic equilibrium between the interior of parasites' bodies and the surrounding fluid. In addition, evasion mechanisms, including many of the parasites' counteracting reactions against hosts' immune attacks, are probably generated in large part by the tegument. Any compromise on the integrity and normal functioning of the tegument such as the treatment by certain drugs, could facilitate and accelerate the killing action of hosts' immune effector cells. Thus one can perceive a delicate balance between counteracting actions between hosts' immunological responses and parasites' evasion mechanisms as a forever ongoing exercise. The complete understanding of structural organization and the roles played by the tegument is hence crucial in devising any rational vaccine.

# Observations of the adult parasite surface by scanning electron microscope (SEM)

When adult F. gigantica were observed under scanning electron microscope (Fig 1A-D) the tegument surface was characterized by the presence of numerous spines, except in the areas around the oral and ventral suckers. These spines were closely spaced and varied in shape and size depending upon the body parts. Some, especially those on the antero-ventral and lateral sides of the body, were large with serrated edges and directed backward. Others on the postero-ventral and dorsal sides tended

to be smaller with no serrated edges. The areas between spines appeared corrugated with series of grooves and folds which in turn were covered with small ridges invaginated with pits. The surface of the spines themselves was also highly ridged and pitted. Thus the surface area of the parasites were vastly increased by these structural characteristics. Groups of sensory papillae were also seen in the areas between spines, and each of them has dome shape, some with cilia on top. Large groups of papillae (up to 10-15 per group) tended to concentrate on the ventero-lateral aspect of the body.

# Observations of the tegument by transmission electron microscope (TEM)

Under TEM (Fig 1E-H), the tegument could be subdivided into 4 layers, based on the concentration of the organelles and the density of the cytoplasmic matrix. The outermost layer was a thin strip representing cross sections of ridges and invaginated pit, which together appeared like microvilli (Fig 1E; 1G). These ridges were covered by trilaminate outer membrane and their interior contained a dense network of cytoskeleton fibers. There were numerous pale-stained discoid bodies (about 30x200 nm) embedded within the cytoskeletal network, and some were fused with the overlying membrane (Fig 1G).

The second layer was a thin strip of cytoplasm that contained a high concentration of discoid bodies, lysozomes and spherical or ovoid bodies (Fig 1G, H). Spherical or ovoid bodies (about 160x190 nm) contained homogeneously dense matrix surrounded by the trilaminate membrane. Some of them were fused with the surface membranes at the bottoms of the pits, and hence probably released their content to form part of the glycocalyx coating the exterior of the surface membrane. Lysozomes were large dense spherical bodies (about 400 nm in diameter) that were arranged in rows in the inner part of the second layer.

The third layer was the widest zone of the tegument cytoplasm that contained a high concentration of mitochondria and dense scaffold of the cytoskeletal network. It contained evenly distributed discoid as well as spherical bodies, but with much lower concentrations than in the first two layers (Fig 1E).

The fourth layer was the basal zone where there

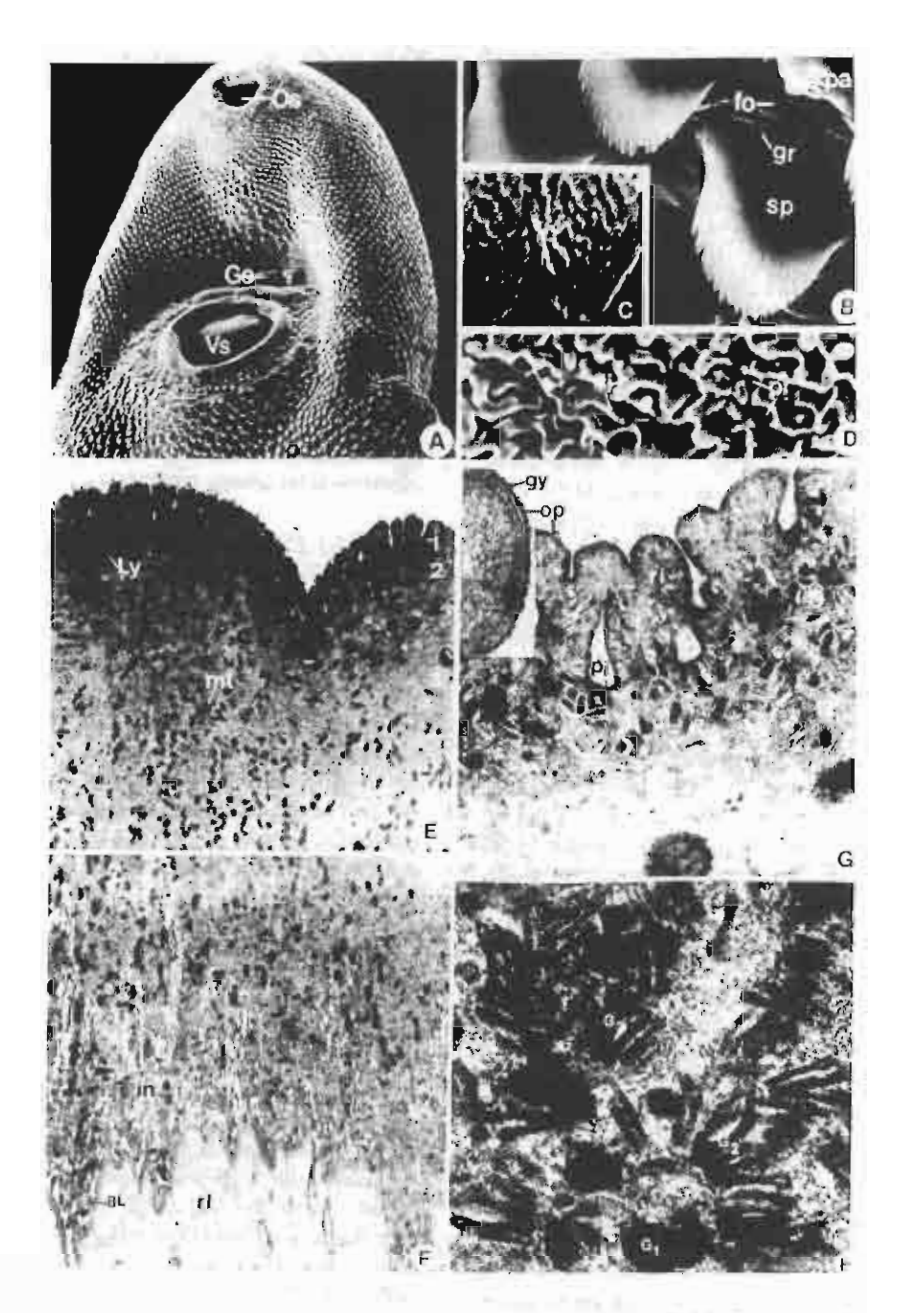


Fig. 1. A.-D.) Scanning electron micrographs, showing the surface characteristics of adult F gigantica. In A the anterior half of on an adult parasite showing oral (Os), wentral suckers (Vs), genital opening (Ge), and the surface studded with spines. In B and C, the spines have serrated edges with folded covering of the edges and spines main hodies. In D, the surface between spines is highly folded by ridges (ri) and pitted (pi).

E.F) Transmission electron micrographs showing the division of the tegument across its thickness into 4 layers (1-4) according to the following characteristics: the cross sections of ridges and pits in layer 1; the high concentration of tegumental granules and lysosomes (Ly) in layer 2, the high concentration of mitochondria in layer 3, and the extensive basal membrane in foldings in layer 4.

G.4) The first and second layer showing cross sectional profiles of ridges (ri) and pits (pi), and the high concentration of dense spherical granules (G1), ellipsoid granules (G2), and mottled spherical granules (G3) in layer 2. In set showing the triliminate surface membrane (Op) coated with a thick layer of glycocalyx (Gy).

390 Vol 29 No. 2 June 1998

were infoldings of the basal plasma membrane. The basal plasma membrane rested on the thick basal lamina which was coupled to the former by series of hemidesmosomes. Underneath the basal lamina was the reticular lamina that connected the tegument to the underlying muscle layers. There were numerous processes of tegument cells traversing the reticular lamina outwardly to join up with the tegument (Fig 1F). The tegument cells themselves lie in rows underneath the muscle layer, and there appears to be one type of tegument cell that is capable of producing all types of tegumental bodies.

Spines appeared as triangular crystalline lattice, whose interior was tightly packed. Their bases were firmly anchored to the basal lamina, while their peripheral boundaries adjoining the tegument cytoplasm exhibited no special condensation or anchoring fibers.

Earlier detailed electron microscopic observations by our group showed strong evidence that. both the discoid and spherical bodies might contain the content that were contributed to the formation of the surface membrane (Sobhon et al. 1994). The discoid bodies were actually vesicles of trilaminate membrane that were invariably fused with the surface membrane, and that most of them were concentrated in the layer 1 of the tegumental cytoplasm immediately underneath the membrane. Likewise, the spherical bodies might contribute both their dense matrix and surrounding membrane to the formation of the surface membrane and its glycocalyx coating, by fusing themselves with the latter at the bottoms of the invaginated pits. In schistosomes, the dynamics of membrane synthesis and renewal have been well documented. The so called membraneous bodies, which were spherical in shape, contained stack of presynthesized membrane held in reserve. Later they were added in toto to the surface membrane by direct fusion of the bodies with the overlaying surface membrane in Schistosoma mansoni (Hockley and McLaren, 1973; McLaren, 1980) or through semi-permanent membrane channels joining between the membraneous bodies and the surface membrane in S. japonicum and S. mekongi (Sobhon et al. 1984; Sobhon and Upatham, 1990).

The synthesis and packaging of tegumental bodies were carried out by the Golgi complex-RER system of the tegumental cells. It is still debatable whether the synthesis of all types of bodies is

carried out in a single or several cell types. In F. hepatica, Hanna (1980a,b,c) reported that there were at least 3 cell types responsible for the production of T<sub>1</sub> and T<sub>2</sub> bodies in adult, and T<sub>0</sub> in metacercariae and newly excysted juvenile parasites. In contrast our preliminary observation (Sobhon et al, 1994) demonstrated that in F. gigantica there was only one cell type responsible for the syntheses of all kinds of tegumental bodies, while those in metacercariae and newly excysted juveniles have not yet been studied. Following their syntheses in the tegument cells, tegumental bodies were transported to the tegument by the propelling action of microtubules localized in the cells' process and the second and third layers of the tegument cytoplasm. In schistosomes and Opisthorchis viverrini, it has been clearly demonstrated that this translocation was mediated by microtubules, since the treatment with tubulindepolymerizing drugs disrupted this transport process (Wilson and Barnes, 1974; Sobhon and Upatham, 1990; Sobhon and Apinhasamit, 1996). It can be concluded, therefore, that the synthesis/ secretory activity of the tegumental cells is the major source of replenishment and turn over of the surface membrane and tegument. This continuous process helps to repair damaged surface membrane as well as fending off the immune attacks by hosts. It remains to be proven whether under the influence of the latter insults, the process of membrane synthesis and replenishment is accelerated.

### SOURCES OF PARASITE ANTIGENS

Antigens of F. gigantica that causes antibody formation in hosts are generated and released principally from the tegument and the cecum as demonstrated by immunoperoxidase detection method (Sobhon et al., 1996).

# Tegument

The immuno-staining of the tegument exhibited four distinctive characteristics: the intense undulating outer rim of the tegument, the fine brownish granules being evenly distributed throughout the width of the tegument, the brownish attenuated processes between muscle cells, and the staining of the tegument cells' soma (Fig 2).

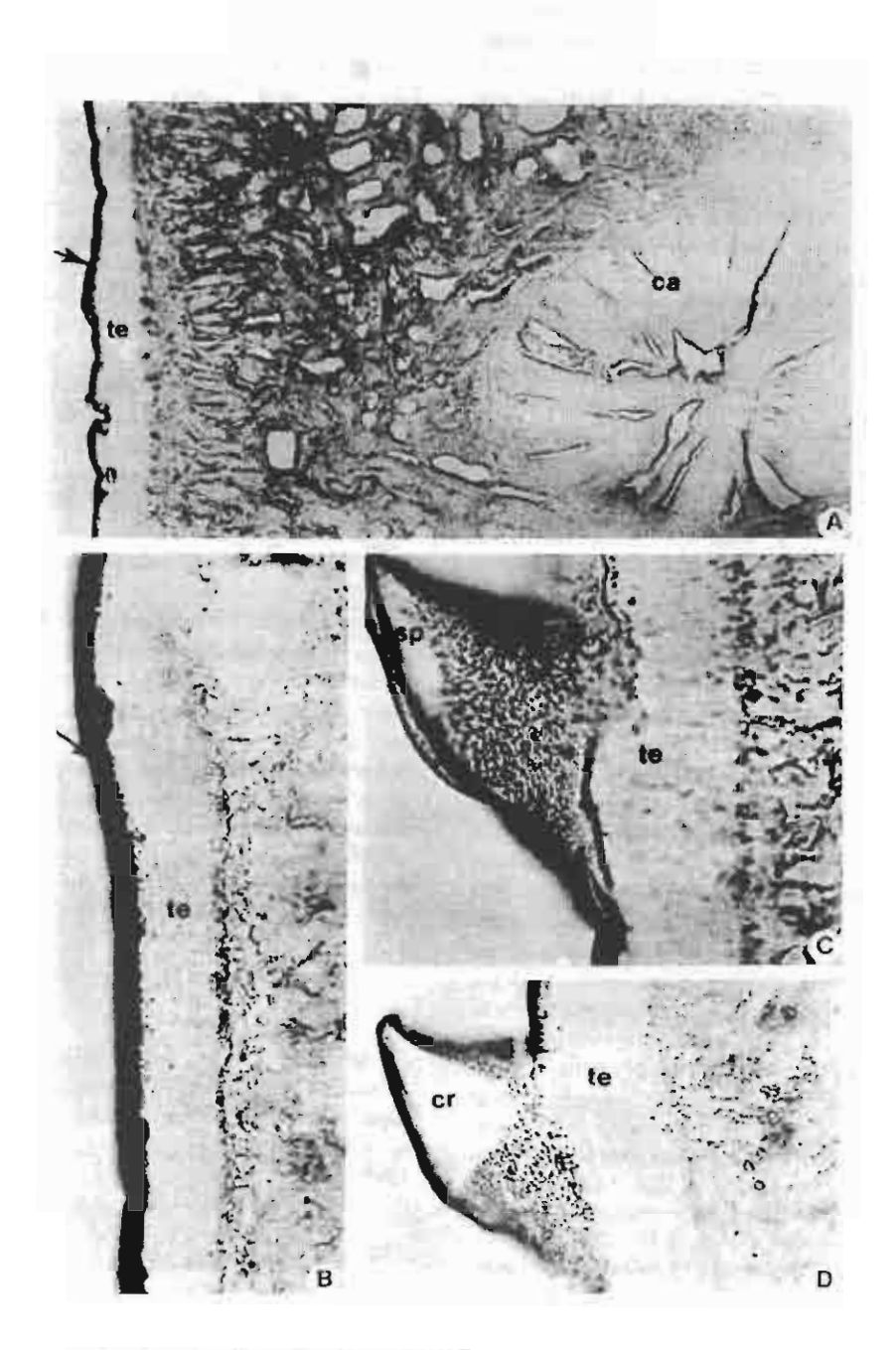


Fig 2 A) A cross section of an adult F. gigantica stained with immunoperoxidane technic, demonstrating the presence of dense deposit that indicate the locations of antigens on the surface membrane and outer rim (arrow) of the tegument (Te), and the apical membrane of cecal epithelial cells (Ca).
B) A high power micrograph of the tegument showing dense deposit on surface membrane and the narrow rim

(arrow) of tegument (Te).

C.D) The surface of a spine is densely stained with granules of dense deposit (in C), while the spine crystalline matrix (Cr-in D) is unstained.

At high magnification, it was revealed that the intensely stained outer rim was composed of a narrow zone of tightly packed brownish granules, as well as the deeply stained outermost thin line (Fig 2A,B). This narrow zone should correspond to the deeply-stained outer margin of the tegument's cytoplasm, containing the first and second layers of the tegumental cytoplasm as revealed by TEM observations. It was, therefore, interpreted that the deeply-stained outer thin line was actually the surface membrane and its coating of glycocalyx, while the thicker outer brownish rim was the layers 1 and 2 of the tegument's cytoplasm which have high concentrations of discoid and spherical granules. In other words, the immuno-staining reflected the antigenic content in the existing surface membrane and its constituents that were stored and held in reserved within the two types of granules.

The intense immuno-staining of the tegument cells' soma and their branches between muscle cells implicated that most antigens were produced in the cells and transported via their processes towards the tegument. Eventhough direct evidence such as gold labelling of the cells' soma is still lacking, it is believed that antigens were concentrated in the discoid and spherical bodies that were produced in the cells' soma. Within the tegument, both types of granules were scatterred throughout which corresponded to the patterns of distribution of brownish granules in the tegument exhibited in the immuno-stained tegument.

It was reported that eventhough portions of the surface membrane covering spines were intensely stained, the spine crystalline matrix themselves were not stained (Fig 2C,D). This implies that spines'material was not antigenic by nature, or more likely that spines were not shed and turned overlike the surface membrane, hence their content were not released into the hosts' circulation to stimulate the antibody production.

### The cecum

The immuno-staining of the cecum demonstrated that antigens were concentrated mainly in the luminal content as well as in the cecal epithelial cells. The staining of the cecal content, in most cases, was very intense and could represent the secreted products of epithelial cells in mixture with the food content. On the other hand the immuno-

staining of the apical zone of the epithelial cells' cytoplasm superimposed with the region where zymogen granules were mostly concentrated, and rough endoplasmic reticulum were highly dilated. Therefore, the antigens that were detected by the immuno-staining could be the enzymatic content already packed within zymogen granules as well as those still in the cisternae of rough endoplasmic reticulum, and those that were already exocystosed into the lumen.

Antigens from the cecum might be the most abundant among the excretory-secretory (ES) antigens, considering the mass of highly branching cecum in the adult parasites. F. gigantica lacks a circulatory system but the conveyance of digested nutrients to every part of the parasite's body is carried out directly by the extensive branching of the cecum, that is pervasive throughout the parasite's body. The nutrient molecules are absorbed by the layer of epithelial cells and passed directly to the surrounding tissues. In other species of helminth parasites, particularly F. hepatica, the cecal contents were also major antigens that were released from the parasites. Some of those so called ES antigens were proven to be the digestive enzyme cysteine protease (Dalton and Heffernan, 1989; Rege et al, 1989; Yamasaki, et al, 1989; 1992; McGinty et al, 1993; Smith et al, 1993; Dowd et al, 1994; Wijffels et al, 1994a). Direct evidence that the cecal antigens are the content of zymogen granules could be provided by the immunogold labelling of the zymogen granules in the Lowicrylembedded sections which is still under investigation by our group.

### ANTIGENS OF THE ADULT PARASITES

Analysis of proteins from homogenized whole body of the adult parasites showed that there were approximately 21 detectable bands, ranging in molecular weights (MW) from 110 to 14 kDa (Fig 3A). Eleven of these bands at MW 97, 86, 66, 64, 58, 54, 47, 38, 35, 19 and 14 kDa were present in the surface tegument (ST) fraction which was extracted from the parasites' bodies by Triton X-100. Most of these are believed to be proteins associated with the tegument cytoplasm and the surface membrane, because both light and electron microscopic examinations revealed that the basement membrane underlining the tegumental layer was generally still

intact, and pieces of the tegument were cleanly separated from the basement membrane. Besides, there was little extraction of the underlying tissues, such as, muscles, gut, excretory, reproductive tissues, as well as stromal tissues of the parasites' bodies. In contrast the excretion-secretion (ES) fraction which represented the proteins released in the in vitro culture were composed mainly of two prominent bands at MW 27 and 26 kDa, and lightly stained bands at 66, 64, 58 and 54 kDa. The latter group was also observed in the ST fraction, while the former group was not (Sobhon et al. 1996). Hence it is believed that 27 and 26 kDa proteins were most likely derived from the deeply-localized tissue, such as cecum which also continuously released its content to the exterior. The two proteins have been purified and characterized by our group for their amino acid composition and sequence, and are believed to be cysteine proteases (Kiatpathomehai et al, 1995). These enzymes were generally detected in other Fasciola species, such as F. hepatica (Dalton and Heffernan, 1989; Rege et al. 1989; McGinty et al. 1993; Smith et al, 1993; Dowd et al. 1994; Wiffels et al, 1994a) and in Schistosoma species (Rege, et al, 1992; Gotz and Klinkert, 1993). They are probably used in the digestion of hosts' tissues, such as epithelia of the bile ducts, and blood cells for the parasites to feed on. The enzymes could also be acting inside the parasites' bodies to break down the ingested mate-

In immunoblotting analysis, 14 from 21 bands in the whole body fraction were antigenic, while all 11 bands of tegumental-associated proteins in ST fraction were antigenic. Among the latter, the major antigens, judging from the staining intensity, were 4 bands at MW 66, 58, 54 and 47 kDa. These bands were also detected in the immunoblot pattern of ES fraction, albeit they were very lightly stained, in comparison to the major and more intensely stained bands at MW 27 and 26 kDa (Sobhon et al, 1996). Hence, in F. gigantica we have found that major antigens in adult parasites were the group at high MW at 66, 58, 54, 47 and the group at low MW at 27 and 26 kDa. The former group were most likely the tegument-associated antigens, while the latter group were cecal-uss ociated antigens. These data on F. gigantica were the first to be reported by our group. In comparison, there have been considerable work on F. hepatica. Itagaki et al (1995), using enzyme-linked immunotransfer blot probed by sera from experimentally and naturally infected

cattle, have found that the major antigens of adult Fasciola sp were at 64-52 kDa, 38-28 kDa, 17 kDa, 15 kDa, 13kDa and 12 kDa. 160 kDa antigens were detected only by sera from the early stage infection. The lower molecular weights antigens reported by these authors were within the same ranges of MW as reported in our findings, especially at MW 64-52 kDa (versus 66-54 kDa reported by us) and 38-28 kDa (versus 27-26 kDa reported by us). It is also reported that antigens at 64-54 kDa might be possible candidates for scrodiagnosis of fascioliasis in cattle. The work by our group also reported that antigens at MW 66, 58, 54 kDa were more speciespecific than the cecal-associated antigens at 27-26 kDa (Viyanant et al, 1997a,b).

In Schistosoma species, especially S. japonicum and S. mekongi, analysis by immunoblotting showed that there were 15-20 bands of antigens at MW 205, 158, 128, 116, 110, 105, 97, 86, 76, 68, 64, 56, 54, 50, 45, 43, 38, 28 and 26 kDa (Sobhon and Upatham, 1990; Sobhon et al, 1992). S. mansoni also showed common antigens with these species at MW 97, 86, 68, 50 and 38 kDa (Taylor et al, 1981). These antigens were believed to be mainly the surface and tegument-associated antigens because similar pattern were obtained when the parasites were isotopically labeled with 1251 and antigenic bands analysed by immunoprecipitation (Sobhon et al. 1987). It is most likely that isotopic label of living parasites could only attach to the external facet of the surface membrane, and that little would gain excess to the internal tissues such as cecal content.

# PRODUCTION OF MONOCLONAL ANTIBODIES (mAB)

Our group has attempted to produce monoclonal antibodies (mAB) against F. gigantica antigens (Fig. 3B,C) and found that mAB obtained from mice immunized with ES antigens recognized epitopes present in 54, 27, and 26 kDa proteins (Viyanant et al, 1997a). As mentioned earlier 27, 26 kDa proteins are the major antigens from the cecum that are detected in the excretory/secretory fluid of adult parasites which is also reported to be the case in F. hepatica (Fagbern and Hillyer, 1992; Wijffels et al, 1994a). Since these antigens have been proven to be a family of cysteine protease enzymes (Kiatpathomchai et al, 1995) that are widely dis-

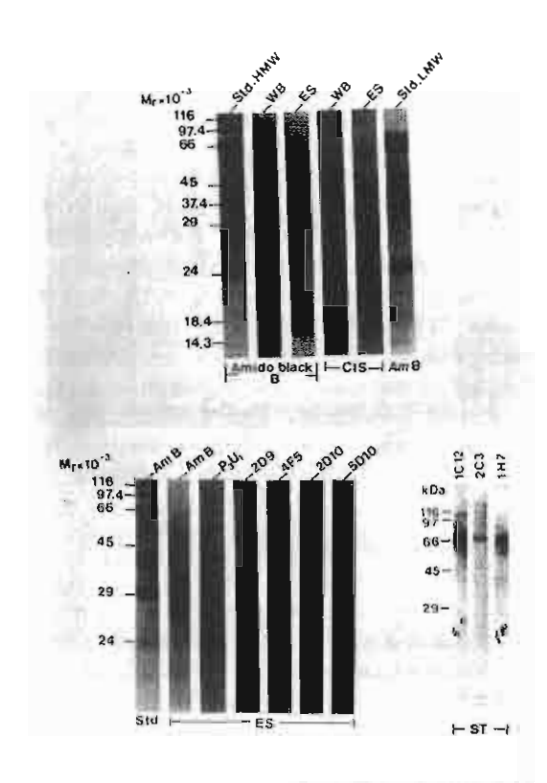


Fig 3-A) Proteins from adult F.gigantica suparated on 12.5% SDS PAGE, blotted on to nitrocellulose papers: whole body (WB), excretory-secretory (ES) antigens stained with Amide black dye (Am B), and immunblotted with cow infected serum (CIS).

B) Immunoblot of ES antigens against monoclonal antibodies from various clones of hybrid cells immunized by ES antigens (12D9, 4F5, 2D10, 5D10), and control culture medium (P3U1). Positive bands are at 26, 27 kDa (2D9, 4F5) and 54, 58 kDa (2D10, 5D10), Lanes 1 and 2 are standard molecular weights (Std), and ES stained with Amide black.

C) Immunoblot of surface and tegument antigens (ST) against monoclonal antibodies from various clones of hybrid cells immunized by ST antigens (IC12, 2C3, 1H7), indicates major positive band at 66 kDa.

tributed in trematode parasites including schistosomes, it is doubtful that their tack of specificity could be used for immunodiagnosis of fascioliasis. A monoclonal antibody that recognized a more specific surface tegumental antigen at 66 kDa could also be produced. This mAB has been used in ELISA-based immunoassay for detecting circulating antigens in the blood of cattle with up to 87% sensitivity (Viyanant et al., 1997b). In addition to

their immunodiagnostic protential, the parasite killing capabilities of these mAB against juvenile parasites are still being tested both in vitro and in vivo.

# VACCINE DEVELOPMENT STRATEGY AND CANDIDATE ANTIGENS

The rationale of vaccine design consists of 3 major strategies: first to identify parasites' antigens that are significantly different and do not cross react with those of hosts. These antigens may be molecules that are essential for maintaining the structural and functional integrity of parasites; or enzymes that are catalysing key reactions which are needed by parasites for acquiring nutrients, or for repairing damage done by various insults. Secondly, the molecules of choice should be able to elicit strong immunological responses in hosts, such that migrating juveniles could be immobilized or killed when they pass into the hosts' tissues. And thirdly, bulk synthesis of the antigens of choice should be feasible through the applications of recombinant DNA cloning technics.

Most vaccines may, however, not be as ideal as desired, because fasciola parasites are large and complex animals with substantial capacity to tolerate any insults and capability to repair themselves. Even partial vaccines that could impair the penetration and migration of newly excysted juveniles or those that could reduce the fecundity of adult parasites would have benificial effect for both the infected individual animals, and the proliferation of parasites in the endemic area. Recent research indicate that future prospect for the control of fascioliasis by immunological intervention appears brighter than previously thought. Candidate antigens from F. hepatica and F. gigantica that have shown vaccine potential during trials in cattle, sheep and rats are as follows:

## Fatty acid binding proteins (FABP)

FABP are probably a group of surface or membrane-associated proteins with molecular weights ranging from 12-14 kDa. These proteins were first isolated from F. hepatica by affinity chromatography using rabbit antisera against S. mansoni wholeworm extract (Hillyer et al. 1977). Thus they are proteins that share common epitopes between two trematode species. Furthermore, in schistosomes

they were found to be a major fraction with fastest migration in 12.5% SDS-PAGE gel, and their intensity is lessen by chloroform extraction (Sobhon and Upatham, 1990). These proteins were shown to confer cross protection for calves against F. hepatica (Hillyer, 1985; Hillyer et al, 1987), and for mice and hamsters against infection by schistosomula of S. mansoni (Hillyer, 1979; Hillyer et al, 1988a,b). A cDNA library has been made for these proteins from F. hepatica (Rodriquez-Perez et al, 1992; Chicz, 1994), and an almost identical group of proteins have been characterized and expressed in E. coli (Smooker et al, 1997). This protein fraction confers significant protection (31%) against F. gigantica infection in cattle ( Estuningsih et al., 1997). It is, therefore, quite optimistic to say that FABPs are one of the most promising vaccine candidate that could confer protection against at least two species of major parasitic trematodes.

#### 66 kDa surface membrane protein

Our group has discovered major antigens from the surface of tegument of adult F. gigantica at 66, 58, 54 kDa (Sobhon et al, 1996, Viyanant et al, 1997b). The 66 kDa antigens has been specifically localized and found to be concentrated in the surface membrane. And as already mentioned mAB has been produced against this antigen (Viyanant et al, 1997b). It is possible that this antigen is the major protein of the surface membrane and its potential as vaccine candidate should be explored, since hosts immunological attacks elicited by this protein may result in the disruption of the membrane and the tegument, which in turn could injure and kill the parasites.

#### Paramyosin

Another structural molecule that exhibits potential as a vaccine candidate is paramyosin, a muscle protein with molecular weight at 97 kDa. Paramyosin is one of the major proteins that ubiquitously present in invertebrate muscle cells, including that of trematodes (Laclette et al, 1991; Kalina and McManus, 1993). This protein is also found to be one of the cytoskeletal protein of the tegument in Schistosoma species (Matsumoto et al, 1988; Sobhon and Upatham, 1990). Paramyosin could be easily purified and obtained in large quantity, and it is known to induce high level of protec-

tion in mice infected with S. mansoni or S. japonicum (Pearce et al, 1988; Flanigan et al, 1989; Gressman et al, 1990; Ramirez et al, 1996). It is possible that the protective action of antiparamyosin is its damaging effect on the cytoskeletal component of the tegument as well as on the muscular layers that lie underneath. Consequently, this might lead to the impairment of the tegumental function and the decrease motility, which may affect the survival and migration of parasites, especially the juvenile stages. Library of cDNA for schistosome's paramyosin has been constructed and expressed in E. coli (Yang et al, 1992). While the protective action of paramyosin has been proven in schistosomiasis, it has not yet been proven positive in fascioliasis, especially against F. gigantica.

## Glutathione-S-transferase (GST)

An antioxidant enzyme, glutathione-S-transferase (GST) is another antigen that could be considered for vaccine candidate. GST actually consists of a large family of dimeric isoenzymes, whose monomeric units have molecular weight at 24-29 kDa. They are widely distributed in both animals and plants, in mammalian as well as parasites' tissues. GSTs comprise at least 4-5 main classes (Mannervik, 1985; Meyer et al, 1991). GSTs catalyse reactions that mop up oxygen free radicals and peroxides, hence preventing them from damaging parasites' surface. GSTs protective action has been shown in rats and mice against infection by S. mansoni and S. japonicum (Smith et al, 1986; Balloul et al, 1987; reviewed in Brophy and Pritchard, 1994), and against F. hepatica in sheep (Sexton et al, 1990) and cattle (Morrison et al, 1996). Evidently, cross protection by GSTs from the two species of parasites is also possible which implies that GSTs from different species may share common epitopes. Eventhough it has been shown recently that in one breed of cattle GSTs cannot confer protection against F. gigantica (Estuningsih et al, 1997), the potential of these molecules as vaccine candidates in other ruminants could not be ruled out, and should be exhaustively studied.

# Cysteine proteases

Cysteine proteases at 26-27 kDa is the main components of excretory secretory fluid of both species of fasciola (Dalton and Hefferman, 1989;

Yamasaki, Aoki and Oya, 1989; Smith et al, 1993; McGinty et al, 1993; Wijffels et al, 1994a,b; Kiatpathomchai et al, 1995; Sobhon et al, 1996). These enzymes are localized in the lumen and cecal epithelial cells (Sobhon et al, 1996; Creney et al, 1996; Viyanant et al, 1997a), and hence they presumbly are the secretory product of epithelial cells. cDNA library of fasciola cysteine proteases have been isolated, and to date a total of 6 complete sequences have been reported (Yamasaki and Aoki, 1993; Heussler and Dobbelaere, 1994; Wijffels et al, 1994a). Cysteine proteases are intensely immunogenic in cattle and sheep (Kiatpathomchai et al, 1995; Wijffels et al, 1994b) and have been used for immunodiagnosis with fairly high level of specificity (Yamasaki et al, 1989; Fagbemi and Goubadia, 1995; Silva et al, 1996). F. hepatica cysteine proteases have been tested as possible vaccine candidate in sheep and cattle. However, rather than decreasing the worm numbers fecal egg count were significantly decreased (Wijffels et al, 1994b; Dalton et al, 1996). Cysteine proteases from F. gigantica have also been tested in cattle, however, neither reduction of worm burden nor egg count was detected (Estuningsih et al. 1997).

9

# Hemoglobin-like antigen (Hemoprotein)

Recently a heme-containing protein has been detected in ES materials from adult F. hepatica (McGinty and Dalton, 1995). This is a high molecular weight protein at more than 200 kDa, with ability to bind oxygen molecules. Hence its role in concentrating and transporting oxygen to various tissues of the parasites' body is essential, especially in the low oxygen bile environment (Tielens et al. 1984). The high vaccine potential of this protein has been demonstrated, particularly in mixture with cysteine proteases (Dalton et al. 1996). The combined vaccine can greatly reduce the parasite fecundity, perhaps due to the decrease amount of nutrient materials and oxygen that must be delivered to the ovary and Mehlis gland for the egg shell formation (Bjorkmann and Thorsell, 1963; Dalton et al, 1996). Though this vaccine candidate cannot kill parasites and reduce the worm burden, the reduction of their fecundity help to alleviate the damaging effect on the hosts' liver, and may indirectly reduce or even eliminate parasites from the infected areas.

#### ACKNOWLEDGEMENTS

The research work in this review article were supported by Senior Fellowship Grant award to P Sobhon from the Thailand Research Fund, and Grant #CPT89B-1-05-173 from National Center for Genetic Engineering and Biotechnology, National Science and The Technology Development Agency.

#### REFERRENCES

- Anonymous Control of foodborne trematode infections. WHO Tech Rep Ser 1995; 849.
- Balloul JM, Grzych JM, Pierce RJ, Capron A. A purified 28,000 dalton protein from Schistosoma mansoni adult worms protects rats and mice against experimental schistosomiasis. JImmunol 1987; 138: 3448-53.
- Bjorkmann N, Thorsell W. On the fine morphology of the egg shell globules in the vitelline glands of the liver fluke (Fasciola hepatica). Exp Cell Res 1963; 32: 153-6.
- Boray JC. Flukes of domestic animals. In: Gaafar SM, Howard WE, Marsh RE eds. Parasites, pests and predators. New York: Elsevier, 1985: 179-218.
- Brophy PM, Pritchard DI. Parasitic helminth glutathione-S-transferase: An update on their potential as targets for immuno- and chemotherapy. Exp Parasitol 1994; 79: 89-96.
- Capron M, Capron A. Immunoglobulin E and effector cells in schistosomiasis. Science 1994; 264: 1876-77.
- Cervi L, Robinstein H, Masih DT. Involvement of excretion-secretion products from Fasciola hepatica inducing suppression of the cellular immune responses. Vet Parasitol 1996; 61: 97-111.
- Chicz RM. Submitted to the protein sequence database, August 1994: Accession A44638.
- Chitchung S, Ratananikom N, Mitranun W. Fasciola hepatica in human pancreas: A case report. J Parasitol Trop Med Assoc Thai 1982; 5: 113.
- Chompoochan T, Apiwattanakorn B, Seniwong V, Penpairatkul S. Study on the life cycle of liver fluke of cattle in Thailand. J Thai Vet Med Assoc 1976; 27: 43-7.

- Creney J, Wilson L, Dosen M, Sandeman RM, Spithill TW, Parsons JC. Fasciola hepatica: irradiation-induced alterations in carbohydrate and cathepsin-B protease expression in newly excysted juvenile liver fluke. Exp Parasitol 1996; 83: 202-15.
- Dalton JP, Hefferman M. Thiol proteases released in vitro by Fasciola hepatica. Mol Biochem Parasitol 1989; 55: 161-6.
- Dalton JP, McGonigle S, Rolph TP, Andrews SJ. Induction of protective immunity in cattle against infection with Fasciola hepatica by vaccination with cathepsin L proteases and hemoglobin. Infect Immun 1996; 64: 5066-74.
- Doy TG, Hughes DL. In vitro cell adherence to newly excysted Fasciola hepatica: failure to effect their subsequent development in rats. Res Vet Sci 1982; 32: 118-20.
- Dowd JA, Smith AM, McGonigle S, Dalton JP. Purification and characterization of a second cathepsin L proteinase secreted by the parasitic trematode Fasciola hepatica. Eur J Biochem 1994; 223: 91-8.
- Edney JM, Muchlis A. Fascioliasis in Indonesian livestock. Commun Vet 1962; 6: 49-52.
- Estuningsih SE, Smooker PM, Wiedosari E, et al. Evaluation of antigens of Fasciola gigantica as vaccine against tropical fasciolosis in cattle. Int J Parasitol 1997 (in press).
- Fabiyi JP. Production losses and control of helminths in ruminants of tropical regions. Int J Parasitol 1987; 17: 435-42.
- Fagbemi BC, Hillyer GV. The purification and characterization of a cysteine protease of Fasciola gigantica adult worms. Vet Parasitol 1992; 43: 223-32.
- Fagbemi B, Goubadia EE. Immunodiagnosis of fascioliasis in ruminants using a 28-kDa cysteine protease of Fasciola gigantica adult worms. Vet Parasitol 1995; 57: 309-18.
- Flanigan TP, King CH, Lett RR, Nanaduri J, Mahmoud AA. Induction of resistance to Schistosoma mansoni infection in mice by purified parasite paramyosin. J Clin Invest 1989; 83: 1010-14.
- Golenser J, Chevion M. Implication of oxidative stress and malaria. In: Aruoma OI. Free radicals in tropical diseases. Switzerland: Harwood Academic Publishers, 1993: 53-80.
- Gotz B, Klinkert MQ. Expression and partial characterization of a cathepsin B-like enzyme (Sm31) and a proposed "haemoglobinase" (Sm32) from Schistosoma mansoni. Biochem J 1993; 290: 801-6.
- Gressman Z, Ram D, Markovica A, et al. Schistosoma mansoni: stage-specific expression of muscle-specific gene. Exp Parasitol 1990; 70: 62-71.
- Hanna REB. Fasciola hepatica: Glycocalyx replacement in the juvenile as a possible mechnism for protection against host immunity. Exp Parasitol 1980a; 50: 103-14.

- Hanna REB. Fasciola hepatica: An immunofluorescent study of antigenic changes in the tegument during development in the rat and the sheep. Exp Parasitol 1980b; 50: 155-70.
- Hanna REB. Fasciola hepatica: Autoradiography of protein synthesis, transport and secretion by the tegument. Exp Parasitol 1980c; 50: 297-304.
- Heussler VT, Dobbelaere DA. Cloning of protease gene family of Fasciola hepatica by the polymerase chain reaction. Mol Biochem Parasitol 1994; 64: 11-23.
- Hillyer GV. Schistosoma mansoni: reduced worm burdens in mice immunized with isolated Fasciola hepatica antigens. Exp Parasitol 1979; 48: 287-95.
- Hillyer GV. Induction of immunity in mice to Fasciola hepatica with Fasciola/Schistosoma cross-reactive defined immunity antigen. Am J Trop Med Hyg 1985; 34: 1127-31.
- Hillyer GV, del Llano de Diaz A, Reyes CN. Schistosoma mansoni: acquired immunity in mice and hamsters using antigens of Fasciola hepatica. Exp Parasitol 1977; 42: 348-55.
- Hillyer GV, Haroun EM, Hernandez A, De Galanes MS. Acquired resistance to Fasciola hepatica in cattle using a purified adult worm antigen. Am J Trop Med Hyg 1987; 37: 363-69.
- Hillyer GV, De Galanes MS, Rosa MI, Montealegre F. Acquired immunity in schistosomiasis with purified Fasciola hepatica cross-reactive antigens. Vet Parasitol 1988a; 29: 265-80.
- Hillyer GV, Rosa MI, Alicea H, Hernandez A. Successful vaccination against murine Schistosoma mansoni infection with a purified 12 kDa Fasciola hepatica cross-reactive antigen. Am J Trop Med Hyg 1988b; 38: 103-10.
- Hockley DJ, McLaren DJ. Schistosoma mansoni: change in the outer membrane of the tegument during development from cercaria to adult worm. Int J Parasitol 1973; 3: 13-25.
- Hughes DL. Fasciola and fascioloides. In: Soulsby EJL, ed. Immune response in parasitic infection: immunology, immunopathology, and immunoprophylaxis. Vol II. Trematodes and cestodes. Florida, USA: CRC Press, 1987: 91-114.
- Itagaki T, Sakamoto T, Itagaki H. Analysis of Fasciola sp antigen by enzyme-linked immunotransfer blot using sera from experimentally and naturally infected cattle. J Vet Med Sci 1995; 57: 522-13.
- James SL, Gleven JA. Macrophage cytotoxicity against schistosomula of Schistosoma mansoni involves arginine-dependent production of reactive nitrogen intermediates. J Immunol 1989; 143: 4208-12.
- Kalina B, McManus DP. An 1gE (Fe gamma) binding protein of Tuenia crassiceps (Candida) exhibits sequence homology and antigenic similarity with schistosome paramyosin. Parasitology 1993; 106: 289-96.

- Kelly JD, Campbell NJ, Dineen JK. The role of the gut in acquired resistance to Fasciola hepatica in the rat. Vet Parasitol 1980; 6: 359-67
- Kiatpathomehai K, Chaichomelert S, Kusamran T, et al. Protein antigens of cattle liver-fluke Fasciola gigantica. In: Biopolymer and bioproducts: structure, function and applications. 11th FAOBMB Symposium. Bangkok: Samakkhisan 1995.
- Laclette JP, Landa A, Arcos L, Williams K, Davis AE, Shoemaker CB. Paramyosin is the Schistosoma mansoni (Trematoda) homoloque of antigen B from Taenia solium (Cestoda). Mol Biochem Parasitol 1991; 44: 287-95.
- Liew FY, O'Donnell CA. Immunology of leishmaniasis. Adv Parasitol 1993; 32: 161-259.
- Maizels RM, Bundy DA, Selkirk ME, Smith DF, Anderson RM. Immunological modulation and evasion by helminth parasites in human population. *Nature* 1993; 365: 797-805.
- Mannervik B, Alin P, Guthenberg H, et al. Identification of three classes of cytosolic glutathione-S-transferase common to several mammalian species: correlation between structural data and enzymatic properties. Proc Nat Acad Sci USA 1985; 82: 7702-6.
- Matsumoto Y, Perry G, Levine RJC, Blanton R, Mahmoud AAF, Aikawa M.Paramyosin and actin in schistosomal tegument. *Nature* 1988; 333: 76-8.
- Maurice J. Is something lurking in your liver? New Scientist 1994; 1917: 26-31.
- McGinty S, Dalton JP. Isolation of Fasciola hepatica hemoglobin. Parasitology 1995; 113: 209-15.
- McGinty A, Moore M, Halton DW, Walker B. Characterization of the cysteine proteases of the common liver fluke Fasciola hepatica using novel, active-site directed affinity labels. Parasitology 1993; 106: 487-93.
- McLaren DJ. Schistosomo mansoni: The parasite surface intrelation to host immunity. New York: John Wiley and Sons Research Studies Press, 1980.
- Mei H, Loverde PT. Schistosoma mansoni: The development regulation and immunolocalization of antioxidant enzymes. Exp Parasitol 1997; 86: 69-78.
- Meyer DJ, Colos B, Pemble SE, Gilmore KS, Fraser GM, Ketterer B. Theta, a new class of glutathione transferase purified from rat and man. *Biochem J* 1991; 274: 409-14.
- Morrison CA, Colin T, Sexton JL, et al. Protection of cattle against Fasciola hepatica infection by vaccination with glistathione-S-transferase. Vaccine 1996; 14: 1603-12.
- Oldham G, Williams L. Cell mediated immunity to liver fluke antigens during experimental Fascrola hepatica infection of eattle. Parasite Immunol 1995; 17: 503-16.

- Overend DJ, Bower FL. Resistance of Fasciola hepatica to triclabendazole. Aust Vet J 1995; 72: 275-6.
- Pearce EJ, James SL, Hieny S, Lanar DE, Shei A. Induction of protective immunity against Schistosoma mansoni by vaccination with schistosome paramyosin (Sm97), a nonsurface parasite antigen. Proc Nat Acad Sci USA 1988; 85: 5678-82.
- Pholpark M, Srikitjakara L. The control of parasitism in swamp buffalo and cattle in north-east Thailand. In: International Seminar on Animal Health and Production Services for Village Livestock, Khon Kaen, Thailand, 1989: pp 244-9.
- Zhou Y, Podesta RB. Effect of serotonin (5HT) and complement C3 on the synthesis of the surface membrane precursors of adult Schistosoma mansoni. J Parasitol 1989; 75: 333-43.
- Rajasekariah GR, Howell MJ. The fate of Fusciola hepatica metacereariae following challenge infection of immune rats. J Helminthol 1977; 51: 289-94.
- Ramirez BL, Kurtis JD, Wiest PM, et al. Paramyosin a candidate vaccine antigen against Schistosoma japonicum. Parasite Immunol 1996; 18: 49-52.
- Rodriguez-Perez J, Rodriguez-Medina JR, Garcia-Blanco MA, Hillyer GV. Fasciola hepatica: molecular cloning, nucleotide sequence and expression of a gene encoding a polypeptide homologous to a Schistosoma mansoni fatty acid binding protein. Exp Parasitol 1992; 74: 400-7.
- Rege AA, Herrera PR, Lopez M, Dresden MH. Isolation and characterization of a cysteine protease from Fasciola hepatica adult worm. Mol Biochem Parasitol 1989; 35: 89-96.
- Rege AA, Wang W, Dresden MH. Cysteine proteases from Schistosoma haematobium adult worms. J Parasitol 1992; 78: 16-23.
- Sexton JL, Milner AR, Panacco M. Glutathione-Stransferase: Novel vaccine against Fasciola hepatica infection in sheep. J Immunol 1990; 145: 3905-10.
- Sher A, Coffma RL. Regulation of immunity to parasites by T cells and T cell-mediated cytokines. Ann Rev Immunol 1992; 10: 385-409.
- Silva MLS, Dacosta JMC, Dacosta AMV, et al. Antigenic components of excretory-secretory products of adult Fasciola hepatica recognized in human infections. Am J Trop Med Hyg 1996; 54: 146-8.
- Smith DB, Davern KM, Board PG, Tiu WU, Garcia EG, Mitchell GF. Mr 26,000 antigen of Schistosoma japonicum recognized by resistant WEHI 129/I mice is a parasite glutathione-S-transferase. Proc Nat Acad Sci USA 1986; 83: 8703-7.
- Smith AM, Dawd AJ, McGonigle S, et al. Purification of a cathepsin L-like protease secreted by adult Fasciola hepatica. Mol Biochem Parasitol 1993; 62:1-8.

- Smith NC. Review article: The role of free radicals in the expulsion of primary infection of Nippostrongylus brasilliensis. Parasitol Res 1989; 75: 423-38.
- Smooker PM, Hickford DE, Vaiano S, Spithill TW. Isolation, characterization and expression of cDNA encoding a Fasciola gigantica fatty acid binding protein. Exp Parasitol 1997; (in press).
- Sobhon P, Upatham ES, Mclaren DJ. Topography and ultrastructure of the tegument of adult Schistosoma mekongi. Parasitology 1984; 89: 511-21.
- Sobhon P, Upatham ES. Snail hosts, life-cycle, and tegumental structure of oriental schistosomes. UNDP. World Bank/ WHO Special Programme for Research and Training in Tropical Diseases, 1990.
- Sobhon P, Panuwatsuk W, Tharasub C, Upatham ES, Kusamran T, Viyanant V. Identification of surface antigens in Schistosoma japonicum (Chinese & Philippine) by immunoprecipitation. Proceeding of His Majesty's Fifth Cycle Commemorative Conference of USAID Science Research Award Grantees, Nakhon Pathom Thailand 1987: 237-50.
- Sobhon P, Upatham ES. Viyanant V, Kusamran T, Mohthong V, Anantavara S. Identification and localization of surface antigens in adult Schistosoma japonicum and Schistosoma mekongi. National Research Council, USA, Aquaculture and Schistosomiasis. Proceedings of a network meeting held in Manila, Philippines, August 6-10, 1991. Washington, DC: National Academy Press, 1992: pp178-95.
- Sobhon P, Dangprasett T, Saitongdee P, Wanichanon C, Upatham ES. Surface topography and ultrastructure of the tegument of adult Fasciola gignatica. Elec Micros Soc Thai 1994; 8: 36-45.
- Sobhon P, Apinhasamit W. Opisthorchis viverrini: The effect of colchicine and cytochalasin B on the adult tegument. Southeast Asian J Trop Med Public Health 1996; 27: 312-7.
- Sobhon P, Anantavara S, Dangprasett T, et al. Fasciolagigantica: Identification of adult antigens, their tissue sources and possible origins. J Sci Soc Thailand 1996, 22: 143-62.
- Socsetya RHB. The prevalence of Fasciola gigantical infection in cattle in East Java, Indonesia, Malaysian Vet J 1975; 6: 5-8.
- Sukhapesna V. Tantasavan D. Sarataphan N. Sangiumfuksana S. A study on epidemiology of liver fluke infection in buffaloes. *That I Vet Med* 1990; 20: 527-34.
- Sukhapesna V, Sarataphan N, Tantasuvan D. Anthelmintic activity of triclabendazule against Fasciola gigantica in cattle and buffaloes. Bangkok: Thai Veterinary Medical Association Conference, 1992: 53.
- Sukhapesna V, Tantasuvan D, Sarataphan N, Imsup K. Economic impact of fasciolistis in buffalo production. J Thai Vet Med Assoc 1994; 45: 45-52.

- Tielens AG, van den Heuvel JM, van den Bergh SG. The energy metabolism of Fasciola hepatica in the final host. Mol Biochem Parasitol 1984; 13: 301-7.
- Taylor JW, Hayunga EG, Vannier WE. Surface antigens of Schistosoma mansoni. Mol Biochem Parasitol 1981; 3: 157-68.
- Thammasart S, Chompoochan T, Prasittirat P, Nithiuthai S, Taira N. Dynamics of ELISA titers in cattle, buffaloes and sheep infected with Fasciola gigantica metacercariae. J Trop Med Parasitol 1996; 19: 13-23.
- Viyanant V, Upatham ES, Sobhon P, et al. Development and characterization of monoclonal antibodies against excretory- secretory antigens of Fasciola gigantica. Southeast Asian J Trop Med Public Health 1997; Vol 28 (supp 1): 128-33.
- Viyanant V, Krailas D, Sobhon P, et al. Diagnosis of a circulating antigen using a monoclonal antibody.

  Asia Pacific J Allerg Immunol 1997b (in press).
- Wijffels GL, Panaccio M, Salvatore L, Wilson L, Walker LD, Spithill TW. The secreted cathepsin L-like protease of the trematode, Fasciola hepatica, contains 3-hydroxyproline residues. Biochem J 1994a; 299: 781-90.
- Wijffels GL, Salvatore L, Dosen M, et al. Vaccination of sheep with purified cysteine protesses of Fasciola hepatica decreases worm fecundity. Exp Parasitol 1994b; 78: 132-48.
- Wilson RA, Barnes PE. The tegament of Schistosoma mansoni: Observation on the formation, structure and composition of cytoplasmic inclusions in relation to tegament function. Parasitology 1974; 68: 239-58.
- Wynn T, Oswald IP, Eltoum IA. Elevated expression of Th1 cytokines and nitric oxide synthase in the lungs of vaccinated mice after challenge infection with Schistosoma mansoni. J Immunol 1994; 153: 5200-9.
- Yamasaki H, Aoki T, Oya H. A cysteine protease from the liver fluke Fasciola spp; purification, characterization, localization and application to immunodiagnosis. Jpn J Parasitol 1989; 38: 373-84.
- Yamasaki II, Kominami E, Aoki T. Immunocytochemical localization of a cysteine protease in adult worms of the liver fluke Fasciola sp. Parasitol Res 1992: 78: 574-80.
- Yang W. Waine GJ, Sculley DG, Lim X, McManus DP. Cloning and partial nucleosite sequence of Schistosoma japonicum paramyonin: a potential vaccine candidate against schistosomiasis. Int J Parasitol 1992; 22, 1187-91.
- Zimmerman GL, Kerkvliet NI, Brauner JA, Cerro JE. Modulation of host immune responses by Fasciala hepatica: reponses by peripheral lymphocytes to mitogens during liver fluke infection of sheep. J Parasital 1983; 69: 473-7

400 Vol 29 No. 2 June 1998

# CLASSIFICATION OF NEUROSECRETORY CELLS, NEURONS, AND NEUROGLIA IN THE CEREBRAL GANGLIA OF HALIOTIS ASININA LINNAEUS BY LIGHT MICROSCOPY

E. S. UPATHAM, A. THONGKUKIATKUL, M. KRUATRACHUE, C. WANICHANON, Y. P. CHITRAMVONG, S. SAHAVACHARIN, AND P. SOBHON<sup>2</sup>

Department of Biology
Faculty of Science
Mahidol University
Bangkok 10400, Thailand
Department of Anatomy
Faculty of Science
Mahidol University
Bangkok 10400, Thailand
Coastal Aquaculture Development Center
Prachuap Khiri Khan 77000, Thailand

ABSTRACT The gross anatomical study of the nervous system of Haliotts asimina reveals that it comprises a pair of cerebral ganglia, a buccal ganglion, a pleuropedal ganglion mass, and a visceral ganglion, connected together by nerve commissures and connectives. There are eight types of nerve cells in the cerebral ganglia on the basis of their histological characteristics and stain affinity, two types of neurosecretory cells, three types of neurosecretory cells are large and occur along the periphery of the ganglia. They contain neurosecretory granules in the cytoplasm that stained deep violet with paraldehyde-fuchsin. The neurose are the most numerous cell type and occur in various parts of the cortex. The neuroglia are small cells and contain spindle-shaped nuclei.

KEY WORDS: abalone, cerebral eaugin, Halien's asinina, histological study

#### INTRODUCTION

The abalone is one of the most primitive gustropods in form and structure. The central nervous system of abalone is of the streptoneurous type, with no concentration of neuronal mass, and it consists of several ganglia connected by connectives and commissures (Bullock 1965, Joosse 1979). Most ganglia are elongated and fiamened, and sheaths of ganglion cells usually extend to form flat commissures and connectives linking ganglia together (Crofts 1929).

The cerebral ganglia are the most anterior ganglia in the head. They are paired, lie above the esophagus or buccal mass, and are connected by a long commission (Dorsett 1986). The cerebral ganglia have connectives to the buccal, pleural, and pedal ganglia, and they send nerves to innervate the eyes, statocysts, and head tennecles (Crofts 1929, Bullock 1965), thus playing an important role in guiding the animals around their habitat.

The cerebral ganglin of several temperate abalone species have been extensively studied., e.g., Haliotis inherculara Linnaeus, Haliotis lamellosa Lamarck, Haliotis cracherodii Leach, Haliotis referens Swamson, Haliotis discus harmai Ino, and Nordotis discus Reeve (Crofts 1929, Miller et al. 1973, Halio 1994a, Yahata 1971) Several types of neurons and neurosceretory cells have been described in the ganglia (Miller et al. 1973, Yahata 1971, Halin 1994a). Yahata (1971) and Halin (1994a) reported that there were four types of neurons in the cerebral ganglia of N discus and H. discus hannai, which were designated as types A, B, C, and D. Type A and Type B cells were believed to be neurosceretory cells. This article reports on the gross anatomy of the nervous system and the classification, based on the histological characteristics of neurons and other cell types in the cerebral ganglia of Haliotis

asinina Linnaeus, which is a tropical abalone species native to Thailand.

## MATERIALS AND METHODS

Anatomical Study

Mature abaltone, H. annina, with a shell length of 4–5 cm were obtained from the Coastal Aquaculture Development Center. Klong Wan, Prachuap Khini Khim Province, Thailand, These animals were reared in a land-based aquaculture system in well-circulated and aerated seawater. They were given appropriate algal food ad libitum and kept under normal daylight. Abaltone were anesthesized with 5% MgCl, after which their shells were removed. They were then placed on a layer of paraffin wax poured on an enamel pag and immersed in 70% alcohol. The dissections were made under a stereomicroscope, which was also used to make drawings with the aid of a camera lucida.

#### Histological Study

The cerebral ganglia were dissected out and fixed in Bouin's flant in 0.14 NaCl for 12 h. Tissues were dehydrated through a graded series of ethanol, infiltrated with dioxane, and embedded in paraffin. Sections were cut at 5–6 µ m thickness and stained with hematoxylin-cosm (H&E), chrome-hematoxylin-phloxime (CH-P) (Gomori 1941), and parallehyde-fuchsin (PF) (Gomori 1950). Neurons and cells in the cerebral ganglia were observed and evaluated for their cell size and shape, nuclear size and shape, and staining affinity under an Olympus Vanox light microscope.

#### RESULTS

#### Anatomical Study

The nervous system of H. aximina consists of a pair of cerebral ganglia, a buccal ganglion, a pleuropedal ganglion mass, and a visceral or abdominal ganglion. These ganglia are connected by nerve commissures and connectives (Fig. 1). The cerebral ganglia are connected by dorsal and ventral cerebral commissures. Thus, the ganglia and commissures surround the anterior esophagus. The middle part of the ventral cerebral commissure swells into a small buccal ganglion. Two major nerves, i.e., the optic and tentacle nerves, join the cerebral ganglia separately (Fig. 1). Optic nerves innervate the eyes, whereas tentacle nerves innervate the tentacles. The cerebropleural and cerebropedal connectives leave the ventroposterior part of the cerebral ganglia and merge into a pleuropedal ganglion mass. Arising from this mass are two loops of nerve cords: the visceral cord and the paired pedal nerve cords. The visceral cord twists into a figure 8 around the visceral mass. At its posterior end is a single visceral ganglion that gives off many nerves going to digestive and reproductive organs. The paired pedal nerve cords run parallel along the midline of the foot muscle (Fig. 1). The two pedal cords are connected at several intervals by pedal cord commissures. From each pedal cord, many nerves arise to innervate the foot muscles (Fig. 1).

#### Histological Study

The paired cerebral ganglia are elongated and flattened (Fig. 2A). The ganglia are composed of two parts: the outer cortex and the inner medulla (Fig. 3A). Each ganglion is surrounded by a

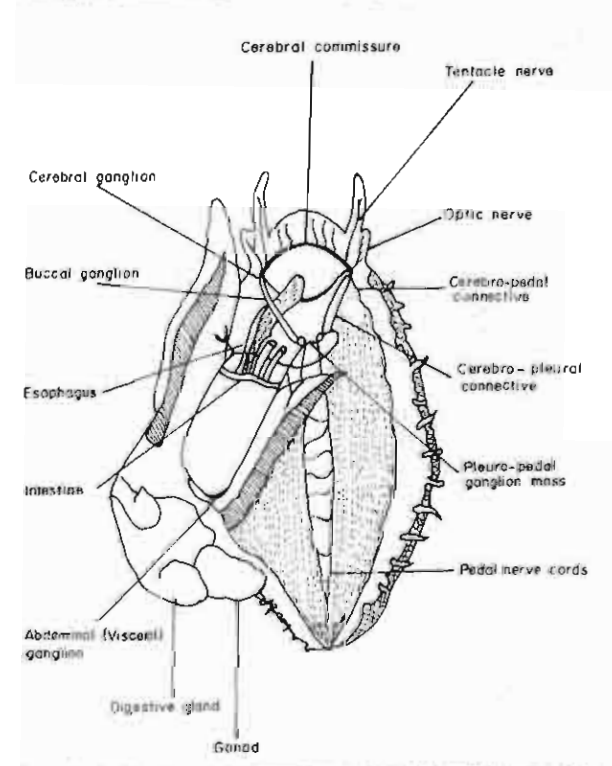
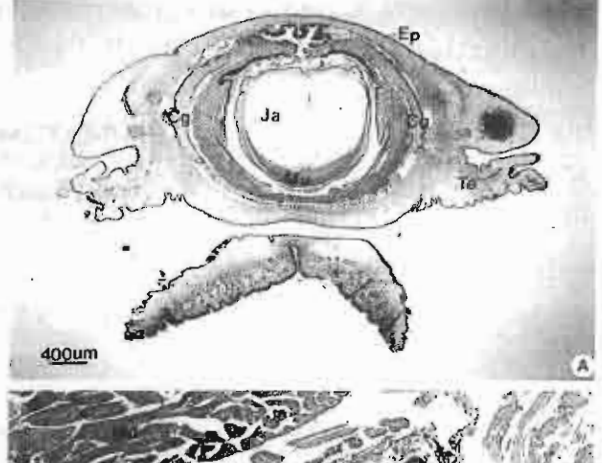


Figure 1. A diagram of the nervous system of *H. asinina*, showing various nerve ganglia linked together by nerve cords and connectives.



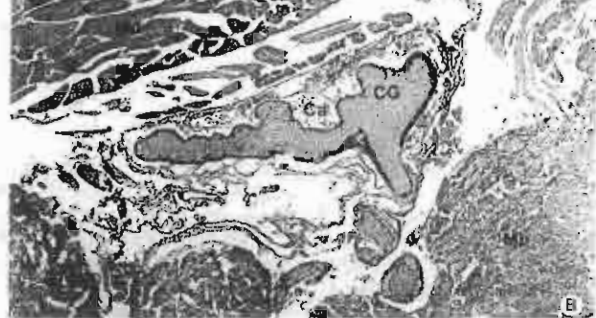


Figure 2. (A) Photomicrograph of longitudinal section showing location of cerebral ganglia (Cg) lying on both sides of jaw (Ja) and jaw muscle (Mu). Ep, epidermis; Te, tentacle, (B) A high magnification of longitudinal section of cerebral ganglion (CG). Ca, capillary.

loose connective tissue rich in collagen-like fibers and capillaries (Fig. 2B). In the cortex, there are numerous neurons, neurosecretory cells, and neuroglia. The outermost cell layer of the cortex is in close contact with the basement membrane of the ganglion capsule. Most of the medial part of the cortex is relatively thin and contains only two to three layers of cells, with only a few neurosecretory cells. In contrast, the dorsal, ventral, and lateral parts of the cortex of each ganglion are thick and contain four to five cell layers (Fig. 3A, see Fig. 5A). Although those neurosecretory cells are dispersed throughout these regions, there are especially high concentrations of these cells in the dorsal and ventral parts, or "horses" of the ganglion (Fig. 3A).

The cells in the cerebral ganglia can be classified into eight types on the basis of their histological characteristics and stain affinity to dyes (H&E, CH-P, and PF). There are two types of neurosecretary cells (NS<sub>4</sub> and NS<sub>2</sub>), three types of neurosecretary cells (NS<sub>4</sub> and NS<sub>2</sub>), three types of neurosetic (NR<sub>4</sub>, NR<sub>2</sub>, and NR<sub>3</sub>), and three types of neuroglia (NG<sub>4</sub>, NG<sub>2</sub>, and NG<sub>3</sub>).

## Type 1 Neurosecretory Cell (NS<sub>1</sub>)

These cells are very large in size (10 × 20 µm), with an oxal shape. Most cells occur along the periphery of the cortex, resting on the basement memorane (Fig. 20, see Fig. 6). The nucleus is round (8 µm in diameter) and is located toward one side of the cell. It contains mostly pule-stained eucliromatin with only a thin run of heterochromatin binding to the internal surface of the nucleus envelope (Figs. 3C and D and 4B). The nucleus, which is round in

shape, is very distinct (Fig. 4B and C). The cytoplasm is well preserved and shows a clear boundary. It stained reddish pink with H&E and pinkish purple with CH-P. There are numerous neurosecretory granules, which stained deep violet with PF and filled the entire cytoplasm.

# Type 2 Neurosecretory Cell (NS2)

These cells are smaller than  $NS_1$  and occur in the same layer as  $NS_1$  and also in the inner cell layer (Fig. 3D and 4A, see Fig. 6). The cell body is round or oval and of medium size ( $10 \times 12 \mu m$ ). The nucleus is round ( $10 \mu m$  in diameter), with most blocks of heterochromatin attached to its periphery with some in the center. Together, they resemble a clock-face pattern (Figs. 3C and D and 4C). The nucleolus is not as prominent as in  $NS_1$ . The cytoplasm contains fewer neurosecretory granules than those of  $NS_1$ , and they stained deep violet with PI:

#### Type 1 Neuron (NR<sub>1</sub>)

These cells are the largest neurons and have a pyramidal shape  $(15\times30~\mu\text{m})$  (Figs. 3D, 4D, and 5C). The nucleus is round  $(10~\mu\text{m})$  in diameter) and contains almost entirely euchromatin with eccentrically located nucleolus (Fig. 3D). The basal portion of the cell is flattened and lies on the basement membrane. Their slimmer cytoplasmic processes extend inward to the medulla of the ganglion (Figs. 3D, 4D, and 6). The cytoplasm stained homogeneously pink with H&E and CH-P. There are no neurosecretory granules in the cytoplasm.

#### Type 2 Neuron (NR2)

These cells are the most numerous among neuronal cells. They are concentrated mostly in the middle cell layer of the cortex (Figs. 3D and 6). They have a round to oval shape (4-6 µm in diameter)

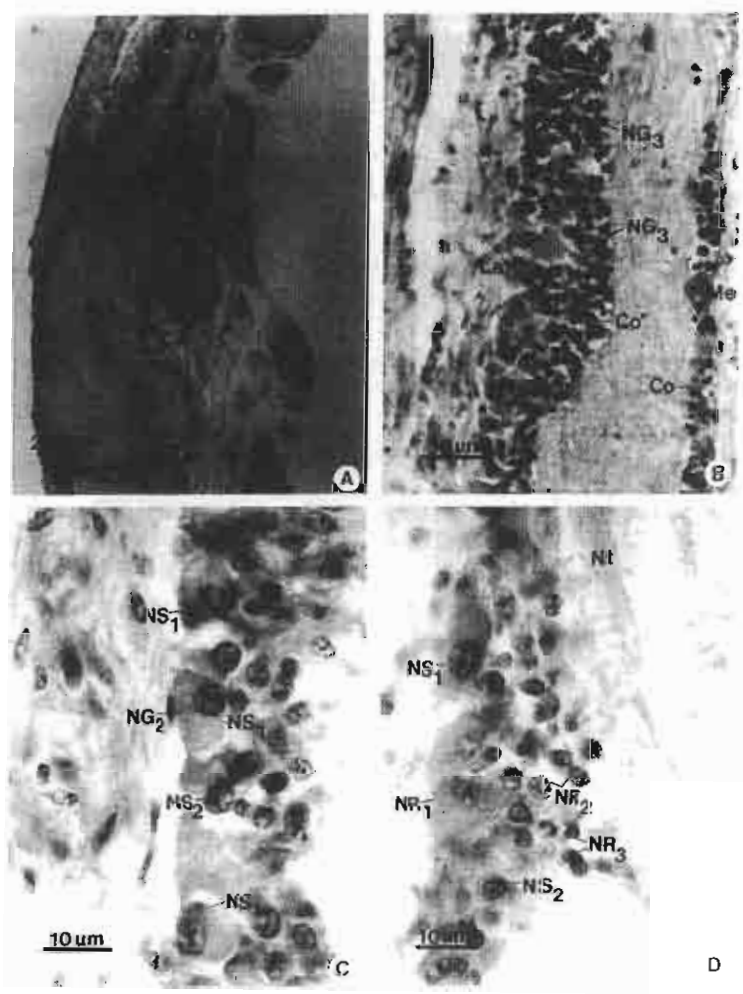


Figure 3. (A) A low-power micrograph showing longitudinal section of the upper half of a cerebral ganglion stained with H&E. Co. cortex; Co. capillary; Do. dorsal; Me. median; La. lateral. (B) A medium-power micrograph showing longitudinal section of the cerebral ganglion stained with H&E. Notice thicker cell layers on the lateral (La) than medial (Me) sides. NG<sub>3</sub>, Type 3 neuroglia. (C) A high-power magnification showing various types of nerve cells in the cortex stained with H&E. NS<sub>1</sub>, Type 1 neurosecretory cell; NS<sub>2</sub>, Type 2 neurosecretory cell; NG<sub>2</sub>, Type 2 neuros; NR<sub>3</sub>, Type 1 neuron; NR<sub>4</sub>, Type 1 neuron; NR<sub>5</sub>, Type 2 neuron; NR<sub>7</sub>, Type 3 neuron; NR<sub>7</sub>, Type 3 neuron; NR<sub>7</sub>, nerve tract.

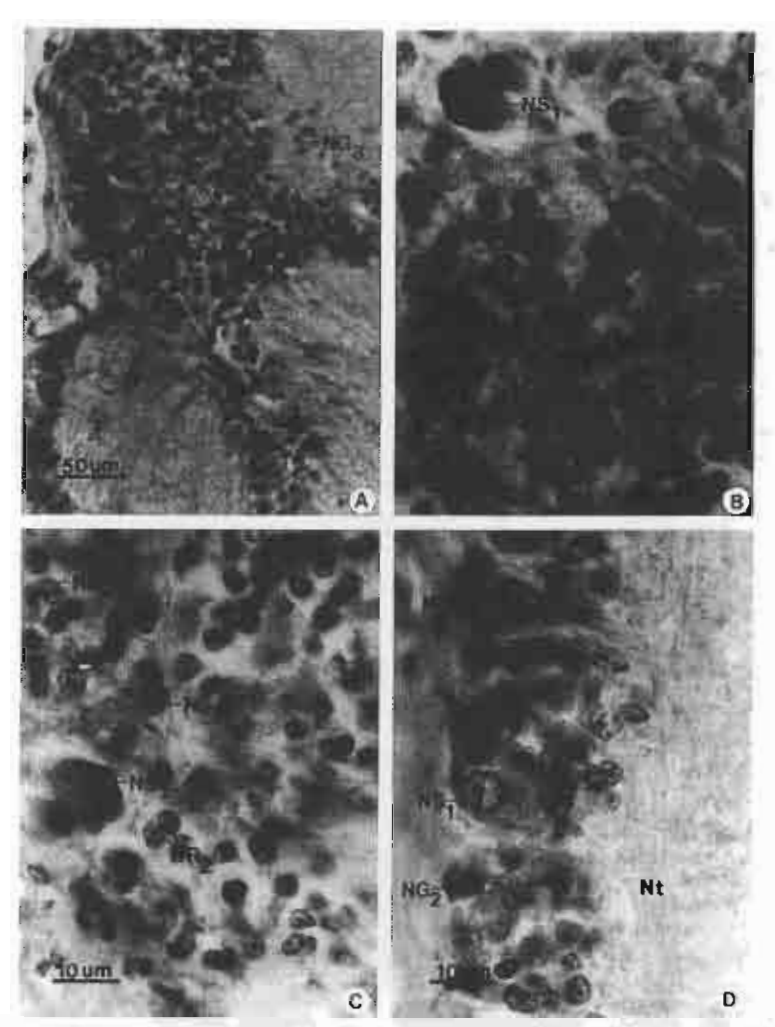


Figure 4. Medium-power (A) and high-power (B-D) micrographs showing various types of nerve cells in the cortex stained with H&E. NS<sub>2</sub>, Type 1 neurosecretory cell; NS<sub>2</sub>, Type 2 neurosecretory cell; NS<sub>2</sub>, Type 2 neurosecretory cell; NR<sub>3</sub>, Type 1 neuron; NR<sub>2</sub>, Type 2 neuron; NG<sub>3</sub>, Type 3 neuroglia; NG, nerve tract.

and contain round nuclei (4-6 µm in diameter) with patchy heterochromatin. The cytoplasm is extremely thin and does not contain neurosecretory granules (Figs. 3D and 4B and C).

## Type 3 Neuron (NR<sub>3</sub>)

These cells are a little smaller than  $NR_2$ , about 4  $\mu m$  in diameter. They occur in the innermost cell layer of the cortex (Figs. 3D and 6). The nucleus is elliptical (4  $\mu m$  in diameter) and contains completely dense heterochromatin (Fig. 3D). There are no neurosecretory granules in the cytoplasm.

# Type I Neuroglia (NG,)

These cells are scattered throughout the cortical region of the gaughton (Figs. 4B and 6). They are small (3-6 µm in diameter) and contain a spindle-shaped nucleus (Fig. 4B). The nuclear membrane is a little crenated, with a thin rim of beterochromatin attached to its inner surface, whereas most of the remaining chromatin is euchromatic (Fig. 4B).

# Type 2 Neuroglia (NG<sub>2</sub>)

The cell body and nuclear size of these cells are similar to those of NG<sub>1</sub>, but they show completely dense chromatin (Figs. 3C and 4D). NG<sub>2</sub> lie in a single row on the basement membrane (Figs. 4D and 6).

### Type 3 Neuroglia (NG.)

These are small cells with spindle-shaped nuclei (2-3 µm) that contain completely dense heterochromatin. They are scattered among nerve bundles of the medulla (Figs. 3B, 4A, 5D, and 6).

#### DISCUSSION

The anatomy of the nervous systems of the tropical abalone, H. asimina, is similar to those of primitive prosobranchs and other species of abalone described by Crotts (1929) and Fretter and Graham (1962). Crofts (1929) reported that in H. tuberculata, H. lamellosa, and H. cracherodii, the cerebral gangia sent the nerves to supply the epipodia, tentacles, eyes, and statocysts. Through

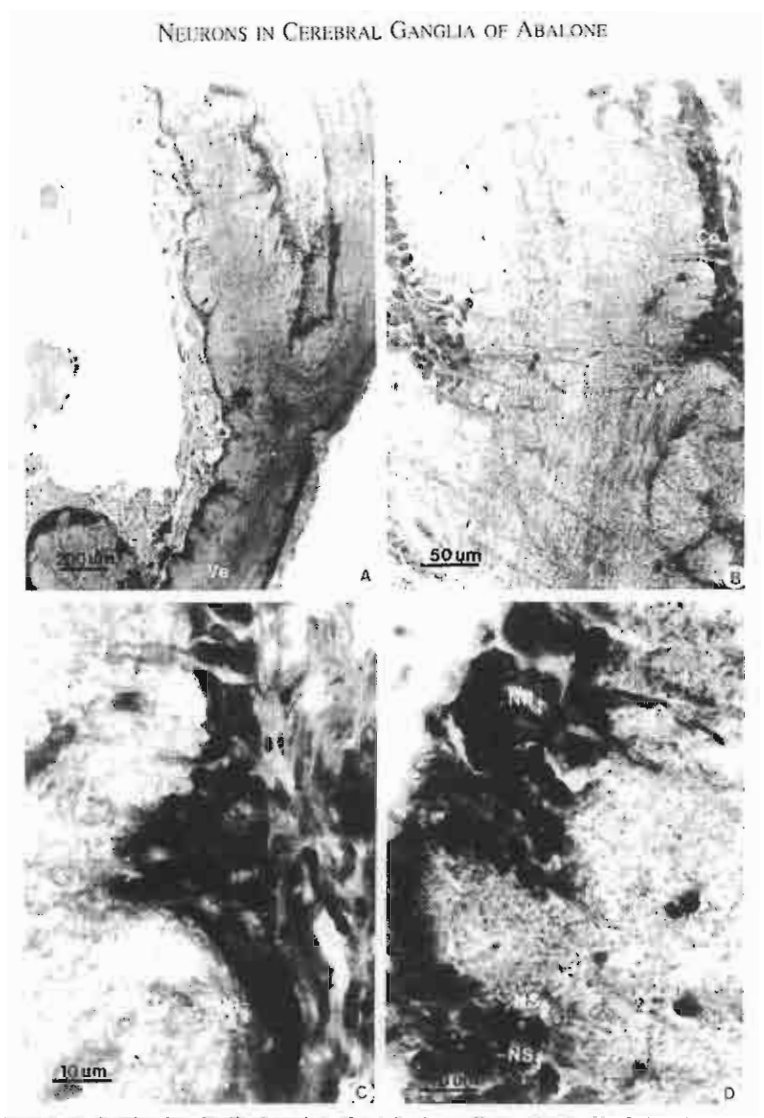


Figure 5. A low-power micrograph showing longitudinal section of cerebral gauglion stained with CH-P. Do, dorsal; I.a, lateral; Ve, ventral. (B-D) Medium-power (B) and high-power (C and D) micrographs showing longitudinal sections of cerebral gauglion stained with CH-P. Co, cortex; Np, neuropil; NG<sub>3</sub>, Type 3 neuroglia; NS<sub>1</sub>, Type 1 neurosecretory cell; NS<sub>2</sub>, Type 2 neurosecretory cell; NR<sub>3</sub>, Type 1 neuron; NR<sub>2</sub>, Type 2 neuron; NG<sub>3</sub>, Type 3 neuroglia.

these nerves, the animals receive chemosensory, mechanosensory, and visual input from their environment. Hence, the cerebral ganglia are probably the most important center for nervous integration, comparable to the brain in higher animals. The cerebral ganglia in *H. asinina* are also connected with the buccal ganglion and plenropedal ganglion mass. It was, therefore, suggested that the cerebral ganglia could serve as a center for coordinating and modulating various functions mediated by the rest of the nervous system (Jahun-Parwar and Fredman 1976).

The cerebral ganglia of *H. asinina* are surrounded by a loose connective tissue that is rich in collagen-like fibers, threaded with capillary plexuses. This connective tissue sheath is quite different from that of *Helix aspersa* Muller, which is composed of two layers, the outer layer being pucked with globuli cells and the inner being dense and lamellated (Fernandez 1966). The histological andy presented here of the corebral ganglia of *H. asinina* revealed that they contain eight cell types: two types of neuroecretory cells, three types of neurons, and three types of neuroglia. Yahata (1971)

and Hahn (1994a) described four types of neurons in N. discus and H. discus hannar. They are called Type A. Type B, Type C, and Type D cells. Type A and Type B cells are neurosceretory cells. On the basis of the similarities in size and shape and their nuclear characteristics, distribution, and staining affinity, the neurosceretory cells Type 1 (NS<sub>1</sub>) and Type 2 (NS<sub>2</sub>) in this study should correspond to Type A and Type B cells, respectively, as reported by Yahata (1971) and Hahn (1994a). In N. discus, Type A cells were further divided into Type A-I cells, which contain neurosceretory granules stained with PF and CH-P, and Type A-II cells, the secretory granules of which stained with phloxime but not CH-P. Type A-II cells of H. discus hannai appear to be larger (20–32 μm) than the NS<sub>2</sub> of H. discus hannai (20 μm). However, the cell bodies of both Type A cells (Hahn 1994a) and NS<sub>2</sub> stained with PF

Neurosecretory cells are found in large quantities and variety in mulluscan ganglia, which are the principal source of hormones. The functions of neurosecretory cells in the cerebral ganglia are

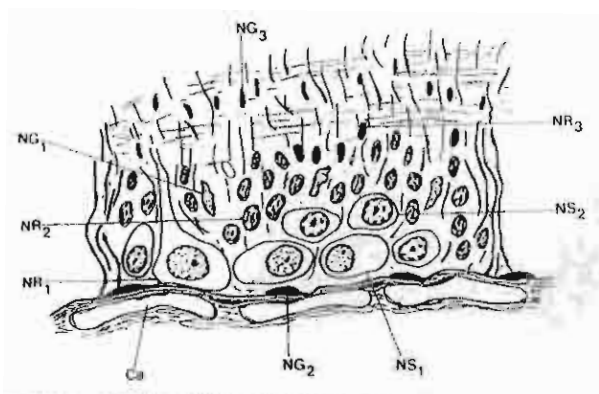


Figure 6. A diagram illustrating structure and cellular composition of the cortex and medulla of cerebral ganglion.  $NS_1$ , Type 1 neurosecretory cell;  $NS_2$ , Type 2 neurosecretory cell;  $NR_1$ , Type 1 neuron;  $NR_2$ , Type 2 neuron;  $NR_3$ , Type 3 neuron;  $NG_1$ , Type 1 neuroglia;  $NG_2$ , Type 2 neuroglia;  $NG_3$ , Type 3 neuroglia; Ca, capillary.

thought to be related to reproduction (Yahata 1971, Yahata 1973, Hahn 1994a, Hahn 1994b). Yahata (1971) found that Type A and Type B cells in the cerebral ganglin of N discus showed seasonal changes in the staining intensity of PF. These cells began to accumulate PF granules in June, when the gonads started to mature, and the PF stain intensity continued to increase until it reached a maximum in September, which was the month of spawning Hence, the rise and fall of the neurosecretory material coincided with gonadal maturation (Yahata 1971). However, the injection of crude homogenate of the cerebral ganglia into ripe females, N. discus, did not induce spawning, but there was a considerable gain in the mean body weight from the increase in water uptake (Yahata 1973).

Hahn (1994a) reported that the neurosecretory activities in Type A and Type B cells in the cerebral ganglia of H. discus hannai, as reflected by the staining intensity of cytoplasmic material, varied with the reproductive cycles. The neurosecretory activity of Type A cells was correlated with vitellogenesis in the

ovaries of females, but not with gonal maturation and spermatogenesis in males. The neurosecretory activity in Type B cells in both sexes did not show any correlation with gametogenesis, vitellogenesis, or spawning. Further studies are clearly needed on the neuroendocrine activities and functions of neurosecretory cells of cerebral ganglia in abalone, including NS, and NS<sub>2</sub> cells in H. assinia.

There are three types of neurons in the cerebral ganglia of H. anning, whereas only two types of neurons (Type C and Type D cells) were described in N. discus and H. discus humai (Yahata 1971, Hahn 1994a). On the basis of the size and shape of cells and their nuclei, NR, are quite similar to Type C cells, whereas NR, probably correspond to Type D cells. These cells did not have any neurosecretory granules in their cytoplasm. NR, cells have not been reported in N. discus or H. discus hannai (Yahata 1971, Hahn 1994a). These cells are the largest neurons in the cerebral ganglia of H. asinina. They are pyramidal and multipolar in shape with a round nucleus, and no neurosecretory granules are observed in the cytoplasm. Compared with the classification of neurons in the nervous systems of higher vertebrates, it is possible that NR<sub>1</sub> may be concerned with motor activities because of their large size and multipolarity, whereas NR3 and NR3 are most likely to be associated neurons.

Three types of neuroglia were observed in the cerebral ganglia of *H. asinina*. To the best of our knowledge, there has not yet been any classification of neuroglia in any species of abalone. NG<sub>1</sub> are probably the general glia cells of the cortex because of their uniform distribution in all cell layers of the cortex. NG<sub>2</sub>, because of their unique lining of the basement membrane, could be a part of the blood-nerve barrier that gates out the undesirable factors from the blood supplied by the capillaries. NG<sub>3</sub>, on the other hand, are glia cells of the neuropil of the medullary region. It remains to be proved whether they are involved in the synthesis of the myelin-like structure surrounding the nerve fibers in the neuropil.

# ACKNOWLEDGMENT

This study received financial support from the Thailand Research Fund

# LITERATURE CITED

- Bullock, T. H. 1965. Mollusca: Gastropoda. pp. 1283-1386. In: T. H. Bullock and G. A. Horridge (eds.). Structure and Function in the Nerveus System of Inversebrates. Precimal Syn Francisco.
- Crofts, D. R. 1029 Habous. Liverproof Mar. Blad. Committee Memoirs, 29:1–174.
- Dorselt, D. A. 1986. Brains to cells: the neuroanatomy of selected gastropod species. pp. 101–187. In: The Mollisca. A. O. D. Willows (ed.), vol. 9. Academic Press, New York.
- Fernandez, J. 1966. Nervous system of the snail Helis aspersa I. Structure and histochemistry of ganglionic sheath and neuropha. J. Comp. Neural, 127:157-181.
- Finter, V. & A. Graham, 1962. British Prosobnurch Molluscs. Barthelongew Press, Darking, pp. 299–320.
- Gomori, G. 1941. Observations with differential stains on human falets of Langernans. Am. J. Pathol. 17: 395–406.
- Gomori, G. 1950. Aldehyde fuelisin: a new stain for elustic tissue. Am. J. Clin. Pathol. 20:065–660.
- Hahn, K. O. 1994a. The teamsecretory staming in the cenebral ganglia of the Japanese afialone (crowwabi). Halloris discus hanneti, and its relationship to reproduction. Gen. Comp. Endocrinal, 93:295–303.

- Hahn, K. O. 1994b. Gametogenic cycle of the Japanese abalone (ezoawabi), Haliotis descus hamas, during conditioning with effective accumulative temperature. Aquaculture. 122:227–236.
- Jalun-Parwar, B. & S. Fredman. 1976. Cerebral ganglion of Aphymiccellular organization and origin of nerves. Comp. Biochem. Physiol. 54A:347–357.
- Juosse, J. 1979. Evolutionary aspects of the endocrine system and of the hormonal control of reproduction of molluses: pp. 119-157. htt E. J. W. Barrington (ed.). Hormones and Evolution, vol. 1. Academic Press, New York.
- Miller, W., R. S. Nishioka & H. A. Bern 1973. The "juxtaganglionic" tissue and the brain of the abatone. Hultoris reference Swainson. Veliger. 16:125–129.
- Yahata, T. 1971. Demonstration of naurosecretory cells in the cerebral gaughtm of the abalence, Nordatis discus Reeve, Bull. Fac. Fish, Hakkathle Univ. 22:207-214.
- Yahata, T. 1973. Demonstration of neurosecretory cells in the cerebral ganglian of the abalone, Nordotis discus Reeve infected with ganglional suspensions. Bull. Ipn. Soc. Sci. Ersh. 39:1117-1122.

# SCANNING ELECTRON MICROSCOPE STUDY OF RADULAE IN HALIOTIS ASININA LINNAEUS, 1758 AND IIALIOTIS OVINA GMELIN, 1791 (GASTROPODA: HALIOTIDAE)

# YAOWALUK P. CHITRAMVONG, <sup>1</sup> E. SUCHART UPATHAM, <sup>1</sup> MALEEYA KRUATRACHUE, <sup>1</sup> PRASERT SOBHON, <sup>2</sup> AND VICHAI LIMTHONG <sup>2</sup>

Departments of Biology and Anatomy Faculty of Science Mahidol University Rama VI Road Bangkok 10400, Thailand

ABSTRACT The middle parts of the radula ribbon of 10 mature smalls of Haliotis asinina and Haliotis ovina were studied by scanning electron microscopy. In each transverse row, the numbers of the central and lateral teeth of H. asinina and H. ovina are I and 10, respectively. The number of the marginal teeth of H. asinina and H. ovina ranges from 108 to 128 and 214 to 236, respectively. The central and lateral teeth of Haliotis spp. are uniticistic spp. are uniticistic, in H. asinina, the anterior cusps are broad, short, and blunt ended in the central and first lateral teeth; long, narrow, and tapered in the second lateral tooth, spade shaped in the third to fifth lateral teeth; and with one large central and several lateral denticles on the inarginal teeth. The radula marphologies of H. asinina and H. ovina are basically the same, with the differences in the middle part of the base of the central tooth, the size of the central tooth, the shape of the first and second lateral teeth, and the shape of the lateral denticles of the marginal teeth.

KEY WORDS: SEM, radula, abalone, Hallotis asinina, Haliotis ovina, Thailand

#### INTRODUCTION

Three species of abalone are found in Thailand: Haliotis asinina Limmeus, 1758, Haliotis ovina Gmelin, 1791, and Haliotis varia Limmeus, 1758 (Nateewathana and Hylleberge 1986, Nateewathana and Bussawarit 1988, Tantanasiriwong 1978). The average shell length and width in centimeters is 8 and 4 in H. asinina, 5 and 4 in H. ovina, and 4 and 3 in H. varia, H. asinina and H. ovina are cocktail-sized abalone and are potential commercial species. The prices as well as their market demand are high.

There have been several reports on the radulae of abalone, notably those on Haliotis tuberculata Linnaeus, 1758 (Crofts 1929), Hallotts rufescens Swainson, 1822 (Hickman 1984), Haltotis rugosa Lamarck, 1822 (Herbert 1990), and Haliotis unilateralis Lamarck, 1822 (Geiger 1996). In H. tuberculata, each transverse row of radula is characterized by a large central tooth, whereas the lateral ones are in three distinct series (Crofts 1929). The marginal teeth are too numerous to count; hence, the radula formula is  $= (3 + 2) \cdot 1 \cdot (2 + 3) \cdot = (Croft 1929)$ . Herbert (1990) described the radula formula H. ragona to be  $\approx \pm 5 + 1 + 5 + \infty$ . The radula ribbon contains a rachidism tooth, lateral teeth with one innermost lateral, our second lateral and three outer laterals, and numerous marginal teeth (Herbert 1990). To date there has been no published work on the radula of the Thai abstore. Hence, the objective of this study is to perform a comparative study on the radulae of two potential commercial species of Thai abalone -II. asinina Linuxeus. 1758 and IE. ovina Greelin, 1791-asing scanning electron microscopy (SEM).

## MATERIALS AND METHODS

H. asinina and H. ovina were obtained form Prov Bay, Rayong Province, and from the Coastal Augustuliare Development Cortex. Prachasp Khari Khan Province. Ten matters smalls of each species were collected. The average shell length and width of mature snath in these samples were 66.6 and 31.6 mm for H. asinina and 56.4 and 43.1 mm for H. ovina, respectively. Each specimen was an-

esthesized with 5% MgCl<sub>2</sub> and three to four menthol crystals for 3-4 hours in a small, round plastic bowl (12 m in diameter and 6.5 cm in height), covered with a piece of glass. The entire buccal mass of the well-relaxed small was extracted and submerged in boiling 10% sodium hydroxide for 20-25 min to dissolve the tissue surrounding the radula before being washed three times in distilled water. The entire radula was mounted on a SEM stub with double-stick tape. The SEM stub was placed in a dessicator for 7-10 days and then coated with platinum and palladium for 3 min two times. Specimens were examined with the secondary electron detector and 15-KV accelerating voltage (S-2500 Hitachi). For each specimen, the central, lateral, and marginal teeth of 15 transverse rows in the middle part of the radula ribbon were examined.

### RESULTS

Radula of H. asinina

The radula of H. aximing is a very long and ribbon-like structure. It normally extends from the anterior and of the buotal mass through about one-third of the upper exophagus. Each transverse row of the radula ribbon has a central tooth in the middle. The lateral and marginal teeft lie, respectively, on both sides at the central tooth (Fig. 1A). The central and lateral teeth are unixaspic, and the ranging teeth are avulticispid. All types of teeth lack basel denticles.

The number of teeth ine ach transverse row of adult *H. asinima* (average shall length and width of 66.8 and 31.6 mm, respectively) ranges from 119 to 139. The average widths of the cusual and the base of the central tooth are approximately 1%6.2 and 288.5 µm, respectively. The unicuspid central tooth is large, bread, shart, and blant at the cutting edge. The base of the central tooth is strongly curved in the middle, containing thick and long pointed ridges at the lateral negles, creating a vertical groove, and in less than twice as wide as the base of the anterior cuspid (Fig. 2A and B). The first lateral tooth is moderately long and slender (its average width is 201.6 µm) (Fig. 2A and C). The anterior cuspid is

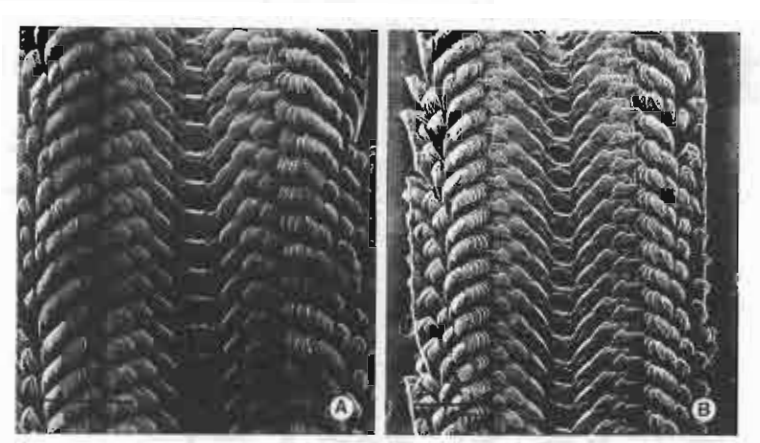


Figure 1. Scanning electron micrographs of the radula of *H. asinina* (A) and *H. avina* (B) showing the teeth of 15 transverse rows. Each transverse row is bilaterally symmetrical, with a central tooth in the middle. The lateral teeth lie next to and on both sides of a central tooth. The inner marginal teeth are spadeshaped and lie next to the left and right lateral teeth. The outer marginal teeth are the autermost teeth on the transverse row of the radula. The sides of the outer marginal teeth are comb-like. The radula of *H. avina* has the same arrangement of types of teeth in a transverse row.

broad, blunt, and short. The width of the base of the first lateral tooth is about the same as that of the anterior cuspid. In addition, it has thickened ridges with long pointed ends at the lateral angles, like the base of the central tooth. The second lateral tooth is equipped with a distinct shaft. The cuspid is long and narrow with a relatively rounded cutting edge (Fig. 2A and C). The third to fifth lateral teeth are similar in shape (Fig. 2E). They are broad and spadeshaped, with sharply pointed cutting edges, decreasing in size from the third to fifth (Fig. 2E). The marginal teeth are long and slender with moderately round cutting edges. They are multicuspid with several small denticles on each side (Fig. 2F). These denticles are triangular with sharply pointed ends. The base of the marginal tooth is very long and slender and has a stalk-like appearance (Fig. 2F).

# Radula of H. ovina

The radula of H. avina is similar to that of H. asinina. The number of teeth in each transverse row of adult H. ovina (average shell length and width of 56.4 and 43.1 mm, respectively) ranges from 225 to 247. The average widths of the cuspid and the base of the central tooth are approximately 150 and 225 µm, respectively. The central tooth is similar to that of H asining but is generally more narrow. The middle part of the base of the central tooth has a knob-like appearance (Fig. 3A and B). The lateral teeth of H. ovina are similar to those of H. asinina. However, the shape of the first lateral tooth of H. oving is more broad and short (with an average width of 290.9 µm) than in H. axinina (Figs. 2C and 3B). The cutting edge of the second lateral tooth of H. ovma is more pointed than that of H. asinina (Figs. 2C and 3C). The shapes of the third to fifth lateral teeth and the marginal teeth of H. ovina are the same as those of H. asinina (Figs. 2D-F and 3D-F). The number of the third to the fifth lateral and the marginal teeth on each side of the central footh are 3 and approximately 109, respectively. The lateral denticles of the marginal teeth are relatively long, narrow, and triangular, with sharply pointed ends (Fig. 3F):

#### Differences of radulae of H. asinina and H. ovina

Differences in the radular teeth of H. asmina and H. pvima are:
(1) the number of the outer marginal teeth in each transverse row

ranges from 108 to 128 in *H. asinina* and 214 to 236 in *H. ovina*; (2) the size of the central tooth is relatively large in *H. asinina* and is relatively small in *H. ovina*; (3) the base of the central tooth is strongly curved in *H. asinina* (Fig. 2A and B) and has a knob-like appearance in *H. ovina* (Fig. 3A and B); (4) the shape of the first lateral tooth is rather long and slender in *H. asinina* (Fig. 2C) and is broad and blunt in *H. ovina* (Fig. 3A and B); (5) the cutting edge of the second lateral tooth is tapered in *H. asinina* (Figs. 2A and C) and is strongly pointed in *H. ovina* (Fig. 3C); and (6) the shape of the lateral denticles of the outer marginal teeth is triangular and moderately long in *H. asinina* (Fig. 2F) and is triangular, but very long and narrow in *H. ovina* (Fig. 3F).

#### DISCUSSION

Information on the radular structure along with shell morphology is suitable to distinguish *H. asinina* from *H. ovina*. The radular structure may provide functional information related to the feeding habits and appropriate food types of *H. asinina* and *H. avina*.

The structure of the radials has received annel attention in the taxonomy of various groups of marine archaeogastropods (Thiele 1929, Wenz 1938-44. Fretter and Graham 1962, Burch 1982). The number of teeth, the number of cuspids on each type of tooth, and the shapes of these structures were observed in this study. Radular dentition patterns may provide useful information, especially if observations on the teeth are standardized. We chose to study the middle part of the radular ribbon because it is easy to locate, the teeth are fully formed, and they are not badly worn. The unterior radula is unsuitable because its teeth are worn. Haliotis have a rhipidoglossan type of radala (Crofts 1929, Fretter and Graham 1962, Burch 1982, Hickman 1984, Herbert 1990, Geiger 1996). Similar to other species of abalone, H. asinina and H. ovina have a typical rhipidoglossan type of radulae. Hickman (1984) studying H. rufescens, considered the three large teeth on either side of the central tooth to be modified marginals. In agreement with many other authors (Crofts 1929, Thiele 1929, Herbert 1990. Geiger 1996), we believe the laterals to be distinct from the marginals, common to the Vetigastropoda. In the middle part of the radular ribbon in H. asminic and H. ovina, each transverse row contains a central tooth and five lateral teeth. As stated above, the

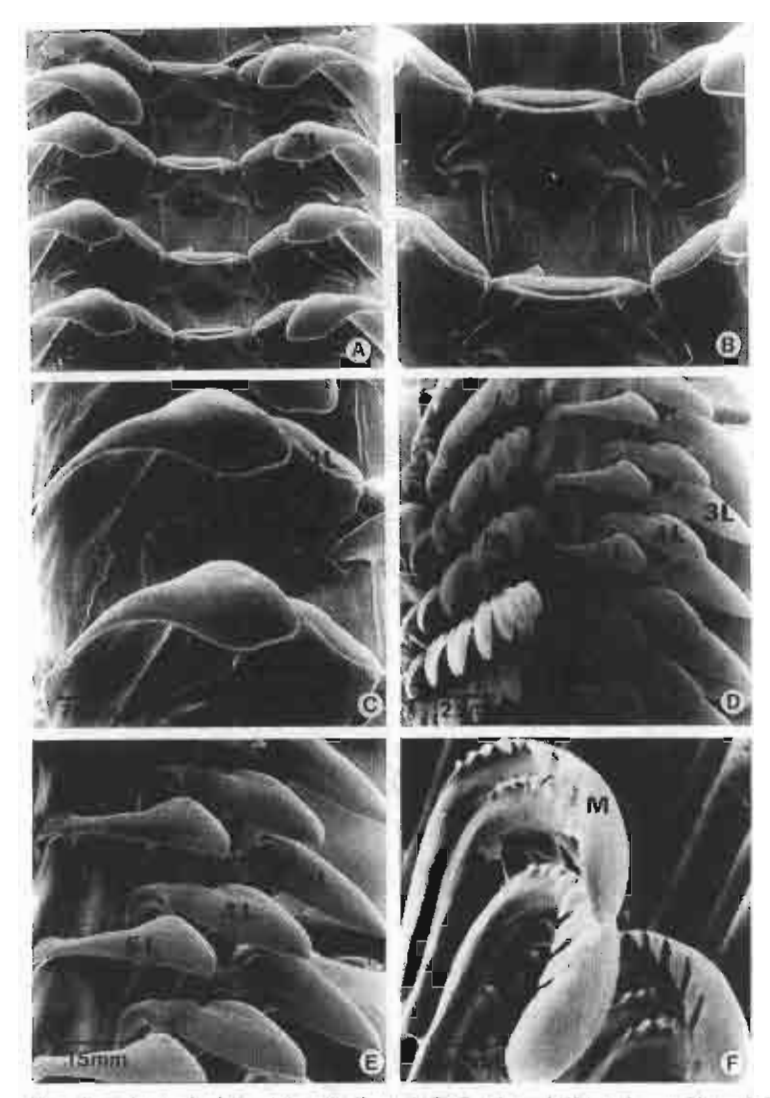


Figure 2. Higher magnifications of radular teeth of *H. asinina*, (A) Central (C), first lateral (1L), and second lateral (2L) teeth; (B) central tooth (C); (C) first lateral (4L), and second lateral (2L) teeth; (D) third lateral (3L), fourth lateral (4L), fifth lateral (5L), and marginal (M) teeth; (E) third lateral (3L), fourth lateral (4L), and fifth lateral (5L) teeth; (F) marginal teeth (M).

number of marginal teeth in *H. asinina* ranges from 108 to 128, whereas that for *H. osima* ranges from 214 to 236. Crofts (1929) and Herbert (1990) also reported numerous marginal teeth in *H. suberculata* and *H. sugosa*, respectively.

In general, it appears that the morphologies of tachdar teeff in habitids are relatively similar with some manor differences in different species. The central or rachidian tooth was reported to be ominospid in H. Intervalante (Crofts 1929). H. Intervalante (Heckman, 1984). H. Intervalante (Crofts 1990), and H. Intervalis (Geiger 1996). H. contina and H. oring also have a unicuspid central tooth Defeated study of the base of the central tooth revealed that H. contina used H. control both cowarin a vertical groove similar to that found in the central teeth of H. milateralis (Geiger 1996). The middle part of the base of the central tooth is strongly curved in H. oring and has a knowledge appearance in H. oring.

There are certain small efficient the mosphology of latenal teeth among various species of Haliotis (Hickman 1984, Herbert 1990, Geiger 1996). Among the five laterals, the innermose or first good the second laterals are different in shape, whereas the faird to the fifth laterals are similar in shape. In H. ragram and H. unilateralis, the first lateral is broad and blunt (Herbert 1990, Geiger 1996). Geiger (1996) reported that it had a corning edge with a distinct ridge. In H. resulting and H. owima, the first lateral is also broad and blunt with a distinct ridge on the autting edge. Similar to the second lateral of H. regions (Herbert 1990), H. unintur possesses a second lateral with a distinct shaft and relatively rounded cutting edge, whereas that of H. owima has a very pointed cutting edge. The third to the fifth laterals are relatively similar in shape in H. rafe-sons (Hickman 1984), H. ragosa (Herbert 1990), H. unilateralis (Geiger 1996), H. asinina, and H. ovima. They are spadeshaped and similar to each other but decreasing in size from third to lifth.

In H. unilateralis, Geiger (1996) divided the marginal weeth into inner, middle, and outermost marginals. We could not distinguish these subdivisions in the marginal teeth in H. assuma and H. ovina.

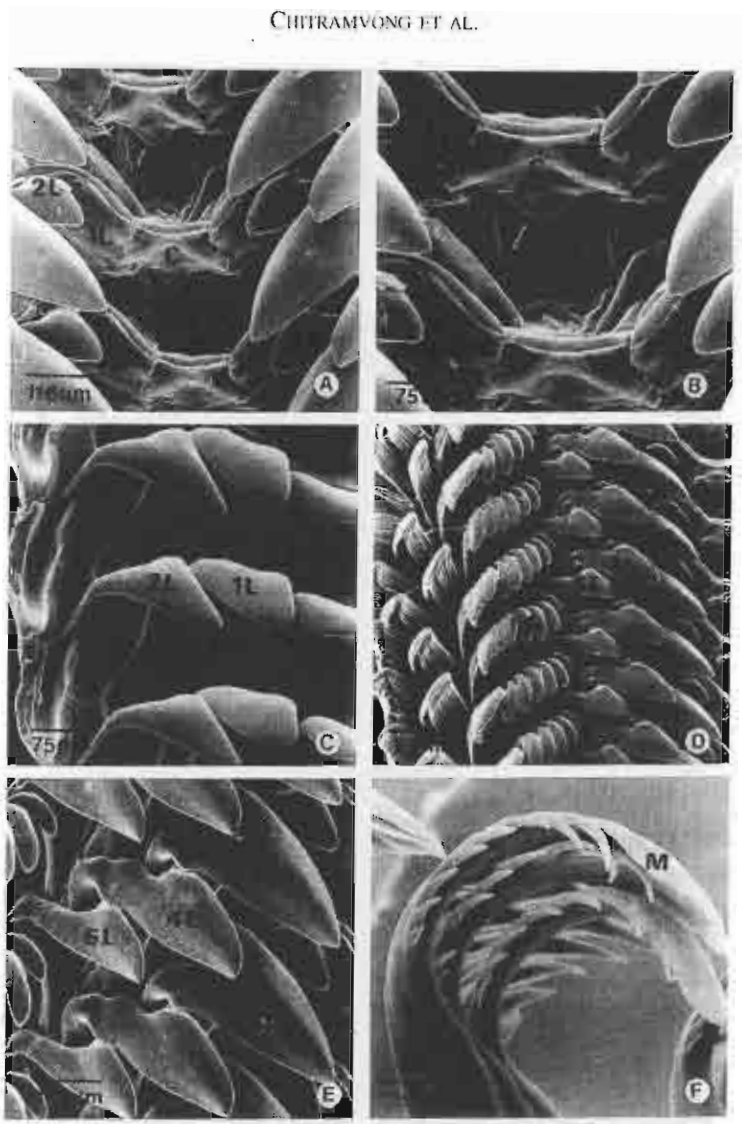


Figure 3. Higher magnifications of radular teeth of *H. ovina*. (A) Central (C), first lateral (IL), and second lateral (2L) teeth; (B) central (C) and first lateral (IL) teeth; (C) first lateral (IL) and second lateral (2L) teeth; (D) third lateral (3L), fourth lateral (4L), fifth lateral (5L) and marginal (M) teeth; (E) third lateral (3L), fourth lateral (4L), and fifth lateral (5L) teeth; (F) marginal teeth (M).

However, similar to the nurginals of *H. rufescens* (Hickman 1984), *H. rugosa* (Herbert 1990), and *H. unilateralis* (Geiger 1996), those of *H. asimina* and *H. usina* are slender in shape with rounded cutting edges and denticulated with several small projections on the sides.

Some differences in the radular structures and the number of teeth in each transverse row may indicate the capacity of radula for collecting and grinding up tood. Matthews and Cook (1995) reported that abalone postlarvae (Haliotis midar Linnaeus, 1758) preferred to graze on prostrate diatoms. Fallu (1991) stated that young abalone use their radulae to graze on microalgae and rupture; their trustules and cell walls, whereas adult abalone use the radula

to shave off pieces of macroalgae. Crofts (1929) suggested that abalone use their radulae with strong lateral teeth for rasping, whereas the numerous marginal teeth with serrated edges probably serve as cogs to help food fragments move along the buccal cavity. In addition, they act as combs, working with the jaws to prevent the entrance of large fragments (Crofts 1929).

#### ACKNOWLEDGMENTS

This project was funded by the Thirdand Research Fund.

## LITERATURE CITED

Hurch, J. B. 1982. Firstlywater smalls. (Mollinga: Campopoda) of North America. Environmental Monitoring Support Laboratory, Off. Res. Develop, U.S.Environmental Protection Agency, Cincomat. EPA 600/3-82-020, 294 pp.

- Crofts, D. R. 1929. Haliotis. Liverpool Mar. Biol. Committee Memoirs. Typical Br. Mar. Plants Animals. 29:1–174.
- Fallu, R. 1991. Abatone Farming. Fashing New Books. Blackwell Scientific Publications Ltd., Oxford. 195 pp.
- Fretter, V. & A. Graham, 1962. British Prosobranch Molluscs. Ray Society, London. 755 pp.
- Geiger, D. 1996. Habitats in the Red Sea, with neotype designation for Halions unilateralis. Lamarck, 1822 (Gastropods: Prosobranchia). Rev. Suisse Zocal, 103:339–354.
- Herbert, D. G. 1990. Designation of lectotype and type locality for Haliotis rugosa Lamarck, 1822 (Mollusca: Gastropoda: Haliotidae). Ann Natal Mas. 31:207–213.
- Hickman, C. S. 1984. Implications of radular tooth-row functional integration for Archaeogastropod symmetries. *Malacologia*. 22:143–160.
- Matthews, 1. & P. A. Cook. 1995. Diatom diet of abalone post-larvae

- (Haliotis midae) and the effect of pre-grazing the diatom overstorey. Mar. Freshwater Res. 46:545-8.
- Nateewathana, A. & S. Bussawarit, 1988. Abundance and distribution of abalones along the Andaman Sea Coast of Thailand. Kanetsart J. (Nat. Sci. 1, 22:8-15 (in Thail).
- Nateewarhana, A. & J. Hylleberge. 1986. A survey on Thai abatones around Phuket Island and feasibility study of abalone culture in Thai land. Thai Fish. Greette 39:177-190.
- Tantanasiriwong, R. 1978. An illustrated checklist of marine gastropods from Phuket Island, adjacent mainland and offshere island, Western Peninsula, Thailand. Phuket Mar. Biol. Center. Res. Bull. 21:1–22.
- Thiele, J. 1929. Handbuch der Systematischen Weichterkunde. vol. 1. Gustav Fischer, Juna. 376 pp.
- Wenz, W. 1938-44. Castropoda, Prosobranchia. In: O. H. Schindewolf (ed.) Handbuch der Palaozoologie. Borntraeger, Berlin. 1639 pp

# Classification of Germ Cells, Reproductive Cycle and Maturation of Gonads in *Haliotis asinina* Linnaeus

Prasert Sobhon°, Somjai Apisawetakan°, Malee Chanpoo°, Chaitip Wanichanon°, Vichai Linthong°, Amporn Thongkukiatkul°, Padermsak Jarayabhand°, Maleeya Kruatrachue<sup>h</sup>, Suchart E Upatham° and Tanate Poomthong°

- Department of Anatomy, Faculty of Science, Mahidol University, Bangkok 10400, Thalland.
- Department of Biology, Faculty of Science, Mahidol University, Bangkok 10400, Thailand.
- Department of Biology, Faculty of Science, Burapha University, Chonburi 20131, Thailand.
- Department of Marine Science, Faculty of Science, Chulalongkorn University, Bangkok 10330, fhailand.
- Coastal Aquaculture Development Center, Department of Fishery, Ministry of Agriculture and Cooperatives, Klong Wan, Prachuabkirikhun 77000, Thalland.

Received 25 Jan 1999

ABSTRACT Germ cells in the gonads of *Haliotis asinina*, a species of abalone found along the coast of Thailand, were classified basing on light and electron microscopies. Germ cells in oogenetic units could be classified into six stages according to their histological and ultrastructural characteristics: oogonium and five stages of oocytes, ic, Oc, with light to intense basophilia and abundant polyribosomes, with some in large aggregates; Oc, with intense basophilia, oil droplets, numerous well developed Golgi complexes and rough endoplasmic reticulum, but little secretory granules; Oc, with a few yolk granules and 2 types of cortical granules; Oc, with increasing number of yolk granules, numerous cortical granules and thin jelly coat; and Oc, is the mature ovum with 2 types of yolk granules, numerous cortical granules and fully formed jelly coat. The cells in spermatogenetic units could be classified according to the pattern of chromatin condensation into thirteen stages: spermatogonium, five stages of primary spermatocytes, secondary spermatocyte, four stages of spermatids and two stages of spermatozoa.

The gonads of adult *II asinina* reared in land-based culture system exhibit five phases of reproductive cycle during the year: these are proliferative, premature, mature, spawning and spent phases. Gonads in proliferative and premature phases contain primarily gonial cells, early oocytes, and spermatocytes, while mature phase contains mainly late stage cells, ic, oocytes, in ovary and spermatids and spermatozoa in testis. The spawning phase occurs at least twice during each year: from March to April and August to October in females, and with similar intervals but slightly prolonged duration in males. Spent phase, occurring after the period of spawning, is characterized by a complete discharge of gamete cells and the breakdown of connective tissue stroma. It takes approximately 5 to 6 months for gonads to regenerate their connective tissue stroma and germ cell population, and finally become repleted with mature cells again.

In developing H asinina definitive gonads appear to be clearly separated from hepatopancreas at 2 months. Histologically, gonal cells appear at 2 months, early spermatocytes and spermatids at 4 months; early oncytes  $(Oe_{1,2})$  at 6 to 7 months. While completely mature spermatozoa could arise in the gonads as early as 6 to 7 months, mature oocytes  $(Oe_{1,2})$  occur much later at 10 to 11 months. The male animals tend to reach full sexual maturity and start normal reproductive cycle as early as 7 to 8 months, while female animals reach sexual maturity and start reproductive cycle around 11 to 12 months.

KEYWORDS: Haliotis asinina, gametogenesis, germ cells, reproductive cycle, gonad development.

## INTRODUCTION

There are three species of abalone along the Thai coasts, namely, if usinina, if usina, if usina, if vina, if v

I to 7 m. 1.10 Among the three species, It asinina has the largest size and the most economic potential because of their maximum proportion of flesh? and good taste. It asinina is primarily found off the eastern coast of the Gulf of Thailand around Chomburi, Rayong and Trad provinces. 60 Since collection from natural habitat could not keep pace with narket demand, an efficient aquaculture system for this abalance is required. However, certain aspects

of knowledge that could aid the large scale production of larvae for aquaculture are still lacking. These are.

1) the probable spawning periods and the frequencies of spawning of land-culture broodstocks during the year; 2) the age when the abalone reaches full sexual maturity and could be used as broodstocks; and 3) the possibility of using artificial means to induce spawning when the gonads are fully developed in order that mature gamete cells from both sexes could be obtained simultaneously.

Among abalone species found in Thailand, preliminary study of 11 varia around Bon Island, Phuket, revealed that spawning occurred at several intervals throughout the year during January-February, April-May, June-July and November-December." Gametogenic cycle was also studied in another species, H ovina, at Khangkao Island, Chonburi province, to in which the spawning occurred between June and November. So far there has not yet been any studies of the gametogenic cycle as well as the development of reproductive organs in Hasinina. Therefore, the aims of the present study are to investigate the reproduction of H asining that have been reared in land-based culture system with respect to 1) the gonadal histology and the gametogenic processes, especially the classification of various stages of germ cells in the testis and ovary based on light and electron microscopic observations; 2) possible cyclical pattern of gonadal histology during different months of the year; and 3) the development of the gonads and the age of full sexual maturity in both sexes. The findings could be applied in determining the appropriate time for induction of spawning, and to increase gamete production leading to the improvement of aquaculture system of this abalone species.

## MATERIALS AND METHODS

### Collection of abalone specimens

Abalone from land-based culture system are provided by the Coastal Aquaculture Development Center, Prachaubkirikhum province, and Marine Biological Station, Chulalongkorn University, Angsila, Chonburi province. They are kept in concrete tanks housed in the shade and well flushed with mechanically circulated filtered sea water as well as air delivery system to maintain the controlled environment. The optimum level of sallmity is about 22.5-32.5 ppt and the temperature is about 22.26°C.7 They are fed with macroalgae (usually Gracilaria spp. and Laminaria spp.), supplemented with striffcial food for abalone.

For the study of the gonadal histology, ultrastructure and the cyclical changes during the year, adult abalone, aged at least 24 months, were collected monthly for a period of one year. The fixed gonads were prepared for light and electron microscopic observations by the paraffin, semithin, and conventional TEM methods.

For development of the gonads, samples of juvenile abalone reared in the closed-culture system as mentioned above were collected monthly from the age of 1 to 12 months, and the gonads were processed for light microscopic observations.

# Light Microscopy

Abalone were anesthetized in 5% magnesium chloride (MgCL) for one hour, for paraffin sections the gonads were cut and fixed in either Bouin's solution, or 3% glutaraldehyde in 0.1M sodium cacodylate buffer pH 7.4, at 4°C, for overnight. The tissue blocks were then washed in 70% ethyl alcohol for removal of the Bouin's fixative, and glutaraldehyde fixative was removed by washing with phosphate buffer three times. Then, the specimens were dehydrated in graded series of ethyl alcohol (70-100%) for 30 minutes each, cleared with dioxane, infiltrated and embedded in paraffin wax. Blocks of specimens were sectioned at 5-micron thick, and finally stained with heamatoxylin-cosin, or PAS-heamatoxylin, and observed in an Olympus Vanox light microscope.

#### Transmission Electron Microscopy

For semithin sections and TEM studies, gonads were cut into very small pieces and fixed in a solution of 3% glutaraldehyde in 0.1M sodium cacodylate huller pH 7.4, at 4"C, for overnight. The specimens were post-fixed in 1% osmium tetroxide in 0.1M sodium cacodylate buffer, at 4°C, for 2 hours. Then, they were dehydrated in graded series of ethanol (50-100%) for 30 minutes each, cleared in two changes of propylene oxide, infiltrated in a mixture of propylene oxide and Araldite 502 resin at the ratios of 3:1 for 1 hour, 2:1 for 2 hours and 1:2 for overnight, then embedded in pure Araldite 502 resin for at least 6 hours, and finally polymerized at 30°C. 45°C and 60°C for 24, 48 and 48 hours, respectively. Blocks of specimens were sectioned at 1-micron thickness by ultramicrotome and stained with Methylene blue for light microscopic observations, and ultrathin sections were entand stained with lead citrate-uranyl acetate and viewed under a Hitachi TEM H-300 at 75 kV.

# ٠...-

ες, ed

ds pic

> nd of

im in

ns n's

m

loi tol a d

ng he

ιth ιx.

> on in,

us

ds on uc

:n,

of os

in C, ly.

ly. .m .th

ts,

# RESULTS

# 1. Gonadal Histology

The conical organ consists of the hepatopancreas surrounded by the testis or ovary (Fig 1C,D). At the base of the organ, the hepatopancreas appears large and occupies most of the cross-sectional profile (Fig 1C); while it becomes smaller towards the tapered end of the organ where most of the tissue belongs to the gonads (Fig 1D). Both testis and ovary are surrounded by a capsule which is composed of the outer single layer of epithelial cells, and the inner layer of dense collagenous fibers mixed with smooth muscle cells (Fig 1K, 2D). The thickness of this capsule varies according to the gonadal cycle during the year.

The connective tissue from the capsule extends perpendicularly into the interior of the gonad to form septa or trabeculae that are branched, and connected at the innermost ends with the thin loose capsule of hepatopancreas. As a result, the gonads are partitioned into small compartments, each containing various stages of maturing germ cells (Fig. JE, 11). Within the connective tissue of each trabecula, there are small vessels running through its whole course (Fig 1F, IL,M), which may be capillaries that are branched out from the larger subcapsular vessels. Around the capillaries and parallel to the long axis of the trabeculae, there are packs of smooth muscle cells and collagen libers that are intermingled with small cells exhibiting dense ellipsoid nuclei (Fig 1K, 1M). Some of the latter may be fibroblasts, while others may be follicular or supporting cells that surround oogonia and developing oocytes. Some small cells show similar characteristics as endocrine cells by containing granules.

Each trabecula acts as the axis on which growing germ cells are attached (Fig 1E,F, IJ,M). Early stage cells, such as spermatogonia, initial stages of primary spermatocytes and organia, are closely adhered to the trabeculae. Middle stage germ cells, such as secondary spermatocytes and developing occytes, are more detached and appear further away from the trabeculae; while late stage cells, such as spermatozoa and mature occytes, are completely detached and move to the outermost region from the axis. Such an appearance gives rise to a discrete group of germ cells surrounding each trabecula, which is termed spermatogenic or oogenic unit.

#### 2. Classification of Germ Cells

Germ cells appraring in the gonads could be classified, according to their structural features as observed under the light and transmission electron microscopes, as follows:

2.15permatogenic cells Based on the nuclear characteristics and the cell sizes, the male germ cells of *H* asinina can be classified into 13 stages.

Spermatogonium (Sg). (Fig 1G) Sg is a spherical or oval-shaped cell with diameter about 8-10 µm. Its nucleus is round or slightly indented with diameter about 6-7 µm. The nucleus contains mostly euchromatin with only small chromatin blocks attached to the inner surface of nuclear envelope. The nucleolus is prominent and stands out from the rather transparent nucleoplasm. Sg are bounded to trabeculae.

Primary spermatocytes (PrSc). (Fig 1G-H, 4A-C) PrSc consists of 5 stages, ic, leptotene (LSc), zygotene (ZSc), pachytene (PSc), diplotene (DSc), and diakinetic or metaphase (MSc) stages. The early cells (from LSc to PSc) are round and become increasingly larger, then they (from DSc to MSc) are gradually decreased in size. The distinctive differences among various stages of PrSc are the pattern of chromatin condensation and the relative amount of euchromatin versus heterochromatin.

Leptotene spermatocyte (LSc). (Fig 1G, H, 4A) These round-shaped cells are larger than Sg with diameter about 10-12 µm and also contain large round nuclei, each with diameter about 8 µm. There is a thin rim of heterochromatin along the nuclear envelope and small blocks of heterochromatin scattered evenly throughout the nucleus. The nucleolus is still present but not as prominent as in Sg.

Zygotene spermatocyte (ZSc). (Fig 1G, H, 4A) ZSc has approximately the same size as LSc. The distinguishing leatures of ZSc is the heterochromatin blocks which are increasing in size and density, and they are coupled at many points by synaptonemal complexes. The nucleolus disappears completely.

Pachytene spermatocyte (PSc). PSc still shows round shape with slightly smaller size than those of LSc (about 8 µm in size and 5 µm in nuclear diameter). Under LM (Fig 1G, H) it is characterized by the heterochromatin which appears as long threads or thick libers that are entwined into "bouquet pattern", and becoming visible throughout the nucleus. Under TEM (Fig 4A-C) these chromatin "threads" are actually thick blocks consisting of tightly packed 30 nm fundamental chromatin libers.

Diplotene spermatocyte (DSc). (Fig. 1G, 11, 4A-C). This cell resembles USc, except the nucleus becomes smaller (about 4 pin), and the chromatin blocks become increasingly thicker and packed

closer together in the denser nucleoplasm than in earlier stages.

Diakinetic and Metaphase spermatocytes (MSc) (Fig 111, 4B,C) These stages exhibit thick chromosomes that move to the equatorial region, while the nuclear membrane disintegrates and completely disappears in MSc.

Secondary spermatocyte (SSc). (Fig 4B,C) SSc is a small round cell about 7 µm in diameter with the nucleus about 4 µm. They show thick chromatin blocks that are crisscrossing one another, thus appearing as checker-board or XY figures. The individual chromatin fibers in the block are loosened up, and each still maintains the size of 30 nm.

Spermatids (St). (Fig 1F-H, 4B,C) There are 4 stages of spermatids, ic, spermatid I (St<sub>2</sub>), spermatid III (St<sub>3</sub>) and spermatid IV (St<sub>4</sub>) depending on the size, chromatin granulation and condensation. All stages are round or oval, and ranging in size from 6  $\mu$ m in St<sub>4</sub> to 3  $\mu$ m in St<sub>4</sub>.

Spermatid I (St<sub>1</sub>). (Fig 1G) St<sub>1</sub> can be distinguished by their chromatin which appears as fine granules under LM, that are uniformly spread throughout the nucleus. As a result, the whole nucleus appears moderately dense without any intervening transparent areas of nucleoplasm. Under TEM the 30 nm chromatin fibers becomes loosely packed and uniformly distributed throughout the nucleus.

Spermatid II (St<sub>2</sub>). (Fig 1G,H) The general features of St<sub>2</sub> are similar to those of St<sub>3</sub> but the nucleus, which remains round, decreases in size and is located eccentrically within the cell. As a result, the chromatin fibers become more closely packed, and the nucleus appears denser but still uniform.

Spermatid III (St<sub>3</sub>). (Fig 1G,H, 4B,C) The cell becomes smaller and assumes more oval shape with eccentrically-located and clongated nucleus. The chromatin begins to condense into dark blocks with intervening light area of nucleoplasm, individual chromatin fiber is enlarged to 40 nm.

Spermatid IV (St<sub>4</sub>). (Fig 1H) The cell becomes smallest but still appears oval. Its chromatic becomes completely condensed, thus the nucleus appears rather opaque; however, the outlines of individual chromatin fibers could still be observed, and each is enlarged to 60 nm.

Spermatozoa (S.z.). (Fig 11'-1,4D) There are 2 stages of spermatozoa: S.z., is the immature spermatozoon that begins to show highly clongated nucleus with completely dense chromatin, thus the outlines of chromatin granules are barely discernible. There is a cap-like structure apposing on one side of the ellipsoid nucleus, which is the maturing acrosome.

The tail is short with a pair of centrioles moving to the neck region, from which the axonemal microtubules start to form.

In mature spermatozoa (Sz<sub>1</sub>) (Fig 11, 4D) the nucleus is fully elongated and slightly tapered at the anterior end, with the size about 1x3 µm. The chromatin is completely dense and the anterior portion of the head is covered by acrosome with central core element (Fig 4D). Five globular mitochondria surround the centrioles in the neck region. Zig-zag microtubules link mitochondria to the plasma membrane covering the distal half of the nucleus. The tail is lengthened, and consists of 9+2 axonemal microtubule doublets surrounded by plasma membrane. Both immature and mature sperm are completely detached from the germinal epithelium and come to lie in the space between adjacent spermatogenic units (Fig 11, 4B,D).

2.2 Oogenetic cells. There are 6 stages of female germ cells of *Hasinina*, including oogonium and five stages of growing oocytes.

Oogonium (Og). (Fig 1K,L) Og is a round or oval-shaped cell, whose size is about 10-12 µm. Its nucleus is round and about 7 µm in diameter. It contains small blocks of heterochromatin attached to the inner surface of nuclear envelope, with the remaining majority appearing as euchromatin. The nucleolus is present but may not be as prominent as in 5g. The cytoplasm is stained light blue by heamatoxylin-eosin and methylene blue, which implies its basophilic property due to the presence of moderate amount of ribosonies. Og are attached to the capsular side of trabeculae and usually are concentrated in groups (Fig 1K,L). Each Og is surrounded by flat, squamous-shaped follicular cells.

Stage I Oocyte (Oc,). (Fig. IK,L,5A-C) Oc, is a round or scallop-shaped cell that is closely adhered to the trabecula. It is about 15-24 µm in size, with a round nucleus about 12 µm in diameter. The nucleus exhibits densely packed chromatin in the form of numerous lampbrush chromosomes. The nucleolus is present but tends to be obscured by the rather dense chromatin and nucleoplasm. The exteplasm is stained deep blue with heamatoxylin-cosin and methylene blue, which indicates its intense bas while property, reflecting the presence of numerous polysomes, newly developed rough endoplasmic reticulum (RER) and Golgi complexes (Gc) as observed in TEM (Fig 1C). Newly released ribosomes are packed into large mass around murdear envelope (Fig 5B). There is very few secretory grupules. Due to its cularged size each Oe, is surrounded by few followiar cells.

l i i

1 ( ;

; ; ;

} ! .

> ( ( !

¿

i V a I i

i \ :1 1

44

199)

ιω nal

the the the

ith lar eck

the 0+2 by

rm nal cen

.-~\c .1∨C

lor Its : It ied the

The tas by ich

ied are ; is ils.

h a cus of lus

her sm ind isc of igh xes

sed car ary is

Stage II Oocyte (Oc<sub>2</sub>). (Fig 1K,L, 5D, 6A) Oc<sub>2</sub> becomes larger and transforms into columnar shape, with the cell size around 30x55 µm, and nuclear size about 22 nm. It is still attached to the connective tissue of trabecula by the narrow part, and each Oc, is surrounded by several follicular cells. The nucleus exhibits increasingly decondensed chromatin and nucleolus. Thus the nucleolus and nuclear membrane are clearly distinct due to the more transparent nucleoplasm and the presence of mostly cuchromatin. The cytoplasm is stained light blue similar to Og, and contains cluster of clear lipid droplets (Fig 5D). At TEM level it was observed to contain numerous well-developed Gc, RER and still abundant ribosomes. There are 2 types of secretory granules: SG<sub>1</sub> and SG<sub>2</sub> (~330 and 450 nm in diameter) with electron lucent and electron dense matrix, respectively (Fig oA,B).

Stage III Oocyte (Oc.). (Fig 1M, 6B) This cell becomes increasingly larger and assumes flask or pear shape, with the narrow side or base still attached to the connective tissue of trabecula. The cell size is about 35-70 µm, with the nuclear size about 20 µm. The nucleus contains mostly cuclifornatin, as most of the lampbrush chromosomes become almost completely unraveled, and the nucleoplasm is quite transparent. The nucleolus is distinct and becomes enlarged due to the uncoiling of nucleolar chromatin. In addition to increasing number of clear lipid droplets, the cytoplasm begins to show reddish yolk platelets (Fig.1M) which are electron dense under TEM. Fine blue granules representing SG, and SG, are evenly distributed between lipid droplets and yolk platelets. At TFM these granules are seen concentrated around Ge (Fig 6B). Follieular cells surround both the cell body and its base near trabecula.

Stage IV Oocyte (Oc.). (Fig 2A,C, oc.) This cell is large and assumes a pear or polygonal shape, but still attached to trabecula by slender cytoplasmic process. The cell size is about 60-80 µm, with nuclear size about 35 µm. The nucleus contains mostly eachtomatin and completely transparent nucleoplasm (Fig 2A, C, 6C). Hence the nucleolns is clearly visible, and it also becomes enlarged due to the complete uncoiling of its chromatin. The cytoplasm is filled with reddish and electron dense yolk platelets (each about 1500-2500 nm in diameter) mixed with numerous lipid droplets (each about 1500-3000 nm in diameter) (Fig. 6C). Fine blue-stained granules which represent SG, and SG, are decreased in central area of the cytoplasm, since most are probably translocated to the area underneath the plasma

membrane. A thin layer of jelly coat begins to form on the outer surface of the cell membrane (Fig 2C). This coat is PAS positive and may be formed by the released content of SG<sub>1</sub>, which were seen exocytosed at the oocyte's plasma membrane (Fig 6D). The coat is in turn surrounded by follicular cells.

Stage V Oocyte (Oc3). (Fig 2B-D) This is the fully mature oocyte before being released from the adult female. Oc, is the largest cells with polygonal or round shape, with the cell size about 80-140 µm and the nuclear size about 40 µm. The nucleus exhibits similar characteristics as that of Oc,, but with completely enlarged and clear nucleolus. Oc, could be divided into 2 subgroups based on the characteristics of yolk platelets observed under LM (Fig 2D). The first subgroup contains small and similar size yolk platelets that are scattered evenly throughout the cytoplasm. In the second subgroup, the yolk platelets are variable in size, and most are large bodies that could be formed by the coalescence of the smaller yolk platelets Stripe of fine blue granules are also located underneath the cell membrane as in Oc, (Fig 2C,D). The thick PAS positive jelly coat attains its maximum thickness and is uniform around the outer surface of the cell membrane, but without the surrounding layer of follicular cells. Under TEM jelly coat appears fibrous in comparison to the amorphous appearance in Oc, (Fig 6D). All Oc, are completely detached from the connective tissue of trabeculae.

# 3. Reproductive Cycle

The reproductive cycle of *H asinina* was assessed by observing the changes in the gonad histology, especially the characteristics of cellular association during one year period. The stages of gonad maturation during one reproductive cycle of the abalone cultured in a closed land-based system could be classified into 5 distinct phases as follows.

Proliferative phase. (Fig 2E-1) This is a period in which gamete cells begin to regenerate to commence a new reproductive cycle. At the initiation of this phase, the gonads contain mainly early stage cells, and all of them are closely attached to the trabeculae. The ovary (Fig 2E,F) contains primarily Og, which usually form clusters near the capsular side, and Oc, and Oc, which are rapidly increased in number. In the testis (Fig 2G-1) there are mostly Sg and PrSc, but neither St nor S2 are present. The clusters of these early stage cells are located around the short and dilated trabeculae. The hepatopancreas is quite large in size and occupies most of the cross sectional profile of the conical organ when compared

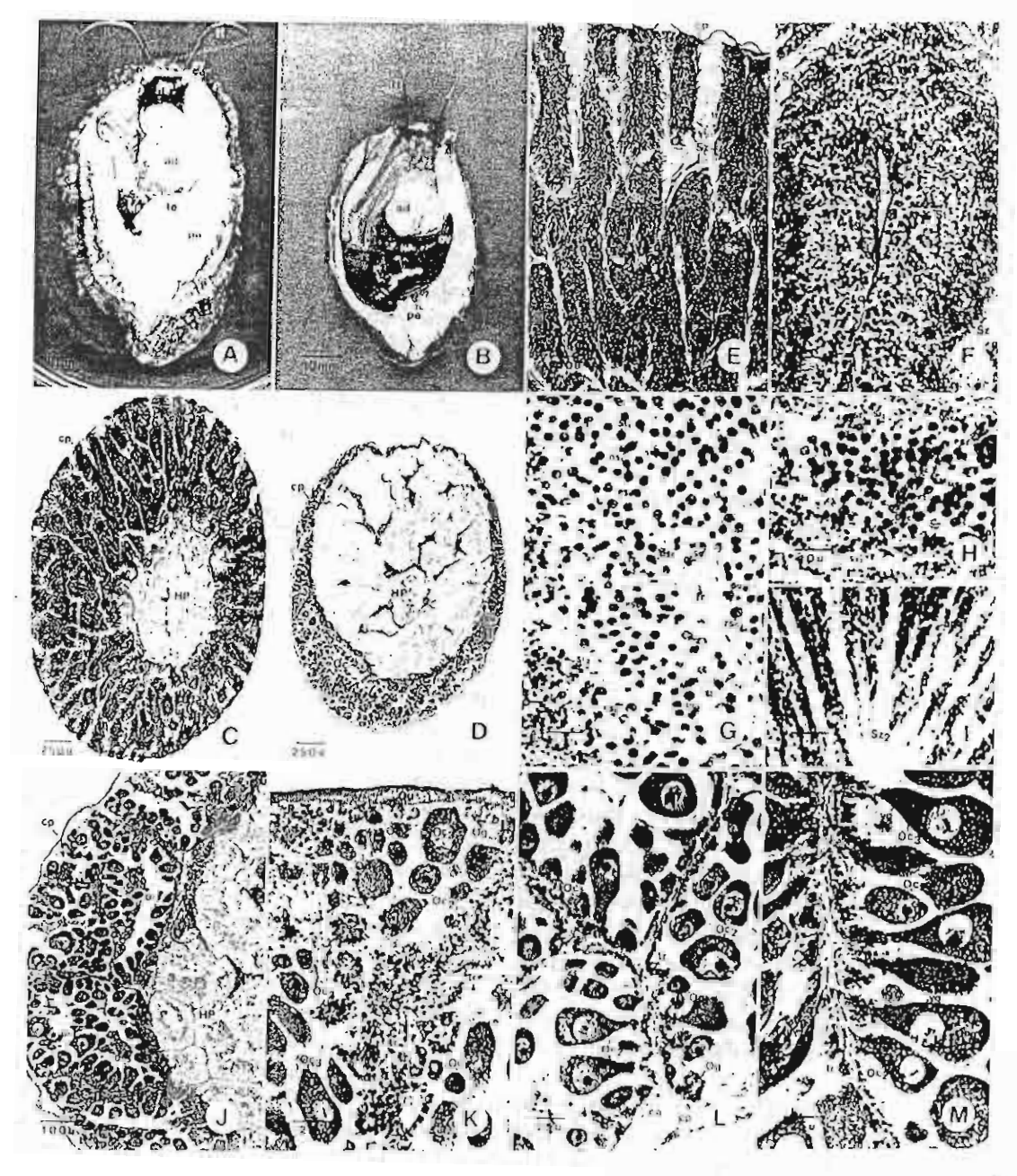


Fig 1 Toward views of shell-freed male abilitine (in A) and female abilitine (in B) showing tests (ie), overy (iw), freparopancies (HP), addition muscle (ad), pedal muscle (pe), head (be), eyes (ey), and remade (ii). C) A cross-section of the tests showing be paropaneiras (HP) surrounded by a thin councetive tissue capside (ep); D) a cross-section of the overy showing be paropaneiras (HP) surrounded by overantissic and filmous capside, E,P) aspectialogeneigh (iii) is present fusible each trabeculae (iii) arising from capside (iii), surrounded by various stages of gent cells, is F a capillary (iii) is present fusible each trabeculae, and surressive mainting trapes of gent cells he at different distance from the councetive trabeculae (Se spermanocyte, St-spermand and Se-spermanocyte). Gettions showing various stages of male gent cells surrounding early trabeculae; they are spermand (Sq.) primates spermanocyte (De-leptoneir, ASe-zygorine, ASe-purbaneir, DSe-diplotene; MSe metaphase stage), spermand (St.), and spermatozoa (Sz.), in I there are towered tilly mature operated (ii) with closely analysis of an axis of trabeculae (ii) with closely analysis age socytes (Or.). The hilly mature operates (the fair reference of cosmophilic yielk granifes (arrows) in the sympletic and trabeculae (iii) with closely analysis of an axis of the compartment paratroned off by alparint trabeculae (iii) with closely and the operation of the compartment paratroned off by alparint trabeculae (II) was showing the presence of cosmophilic yielk granifes (arrows) in the sympletic action in the former stage (iii) the property of cosmophilic yielk granifes (arrows) in the sympletic action is to be not stage (iii) the lower stage (iii) and the cosmophilic yielk granifes (arrows) in the sympletic action is not property to the compartment of cosmophilic yielk granifes (arrows).

12

))

14

vc

dis

1.1

ll;

Fig 2. A-D) Sections showing stage IV and V (O<sub>1</sub>, 2) notice the him appearance of a thin polycom (c), which is tAS positive and increasing miniber of cosmodule yell strandes (vg) in O<sub>2</sub>. The increasing amount of cuchromatin, which is pake stained, and the enlargement and vesiculation of mediculus are also noticeable. This straps underteath the notyte's plasma mentioning failured committee in the constraint of the lower cell (2) shows large platelet of yolks 1-D Sections of 'profilerative place', showing the regeneration of gamete cells after spaining and spent plases. The texts (G-D contains mostly Sg and I Sections of 'profilerative place', showing the reason minutes is. The texts (G-D contains mostly Sg and I Sections of 'profilerative place', showing flown in spent place', short to regenerate and appear short and direct J M) 'sections of 'profilerative', showing rapid increase in numbers and agent of various cells. The owny (J,K) contains mostly carles stage socytes (O<sub>2</sub>, 2) and late stage occytes (O<sub>2</sub>, 2) and the stage occytes (O<sub>2</sub>, 2) and the stage occytes (O<sub>2</sub>, 3) and the stage occytes (O<sub>2</sub>, 4) and the stage occytes (O<sub>2</sub>, 5) and the occute of the stage occytes (O<sub>2</sub>, 5) and the occute of the stage occytes (O<sub>2</sub>, 5) and the occute of the occute occute

10 ScienceAsia 25 (1999)

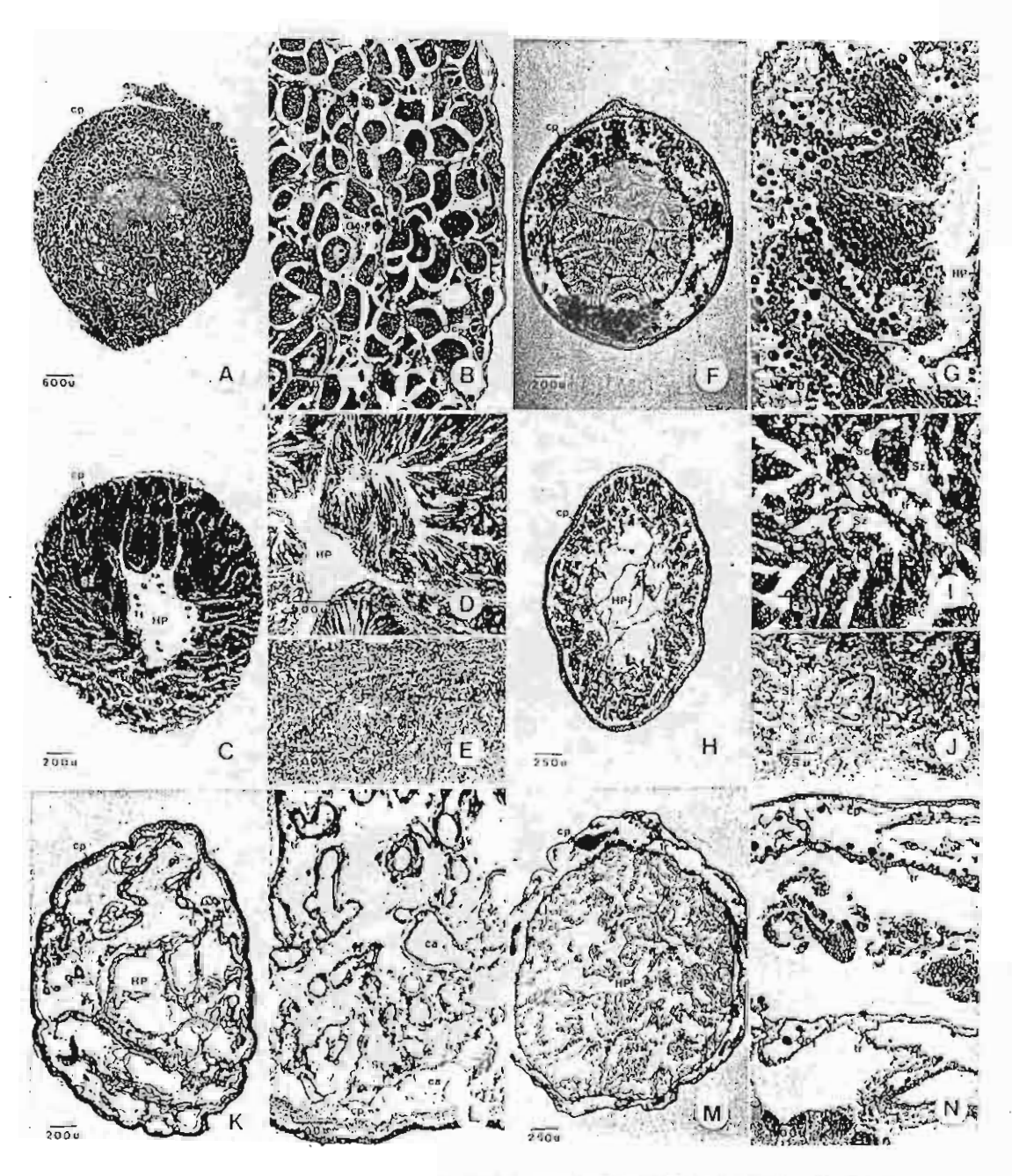


Fig 3. A-E) Sections of "nature phase", showing rapid growth of the gonads. The overy (A,B) contains primarily fully mature Oc, with only a few widely scattered early stage cells (Oc.). The section (C,C) contains mostly has specimentals (St) and specimentals (St) and specimentals (St) and specimentals (St) which lie is now and at low power appear streaky (D). Finally they become dispersed and released into luminal area of the test) (F-f). Sections of "speciment phase—disposed the period when allalone release the viable speciment riggs from the ground. The overy (F,C) contains only the ewiler stage over resolute have still attached to the dilated trabecular. Some yellowish granular substances (atrow) is present in the overland human. The tests (H-f) contains only early stage of male grant cells with a lew of spermatures (Sc), K-N) sections of "sperm phase" sharing the complete discharge of gaustic cells, and the breaking down of trabecular and associated connective tissues in both sexes. Notice the hepatopanicies which becomes larger in relative are

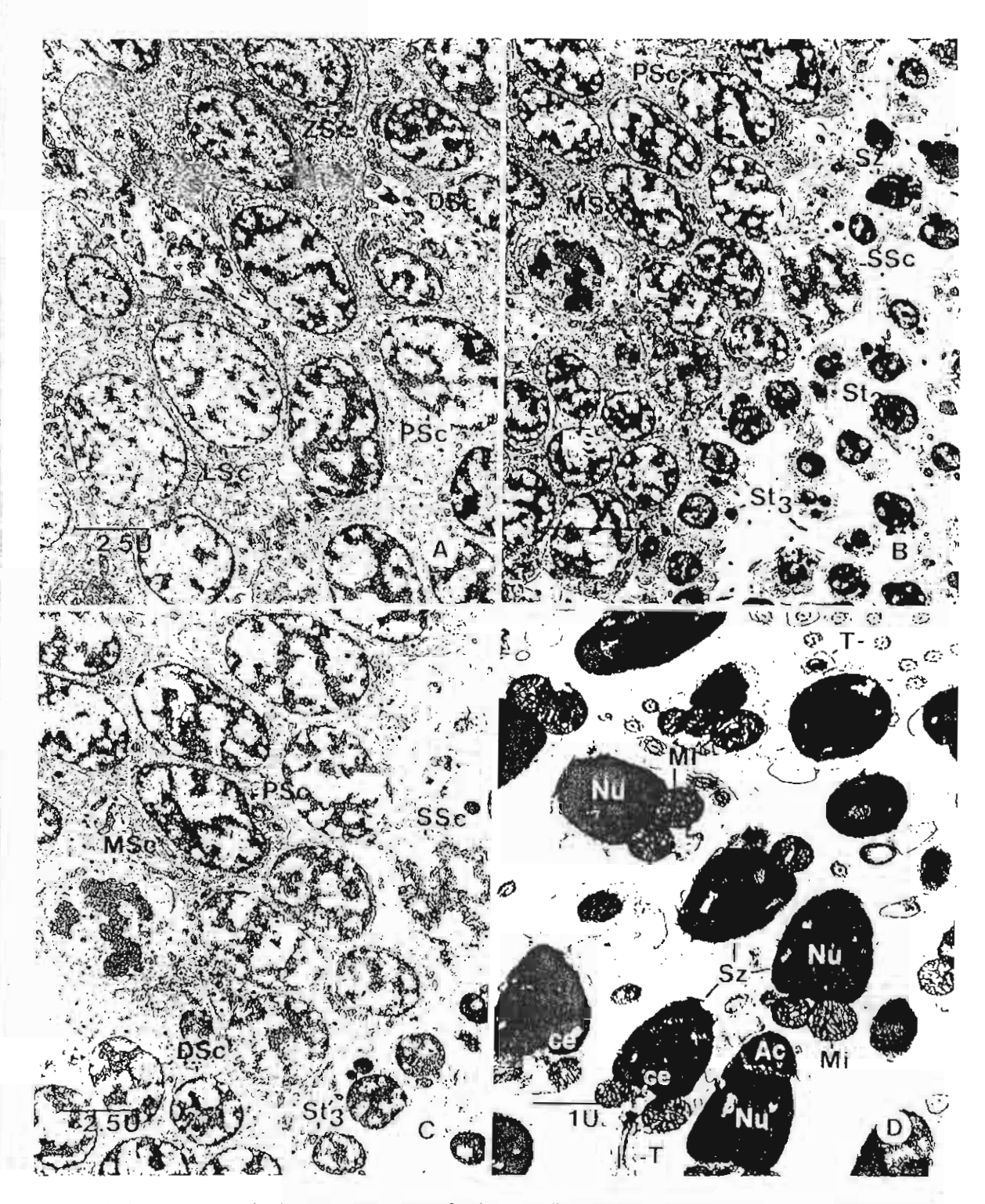


Fig 4. A-C) Electron micrographs showing various stages of male germ cells, including leptotene (ESc), zygotene (ZSc), pachytene (PSc), diplotene (DSc), secondary spermatocyte (SSc), spermands (St), D) Spermatozoa exhibiting dense nucleus (Nu), acrosome (Ac), globular mitochondria (Mi), centrole (ce), and tails (T) with axonemal complexes.

e Oc, tozoa rea of n the avish with aking lative

THE PROPERTY OF THE PROPERTY OF THE PROPERTY OF THE PARTY OF THE PARTY

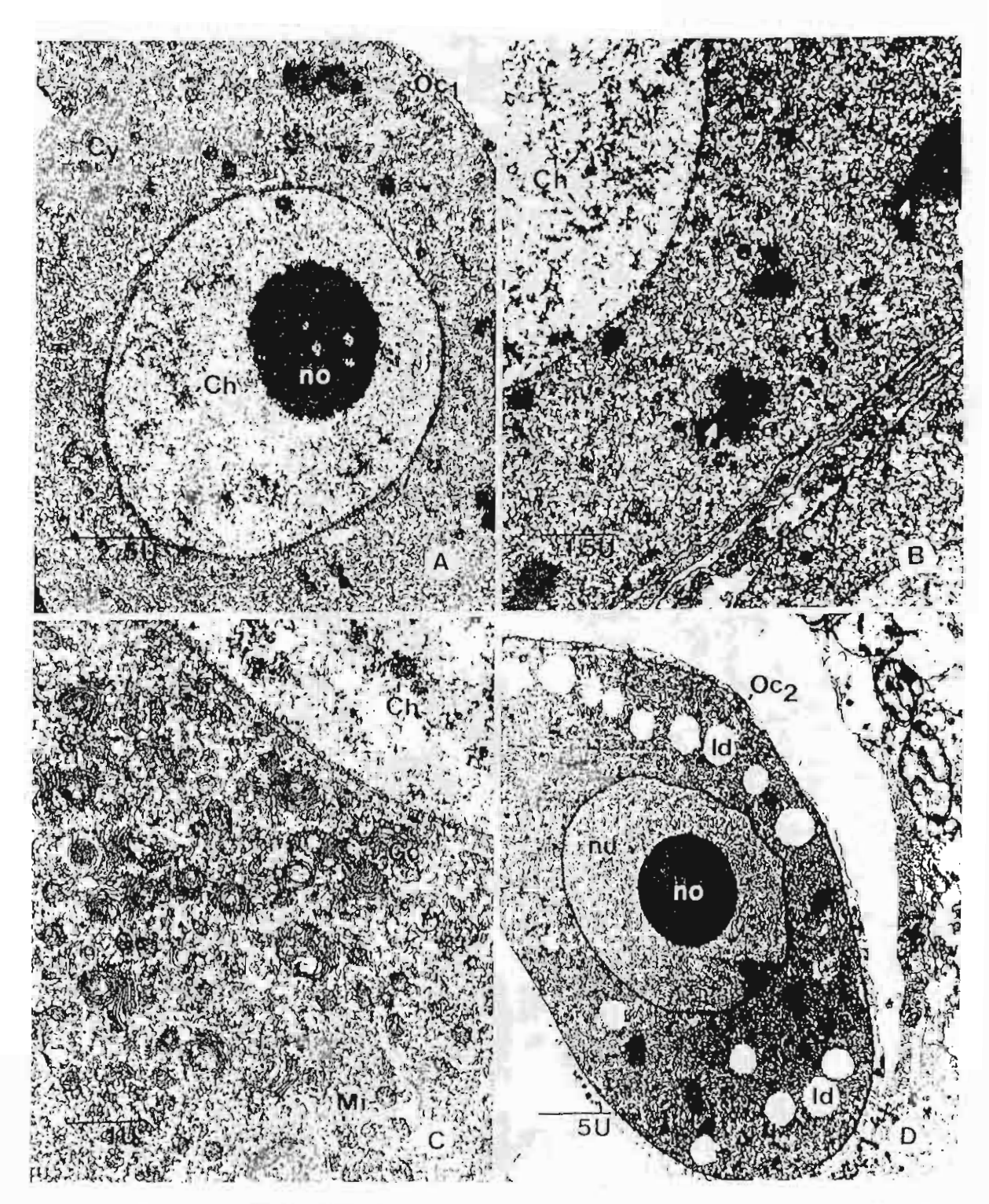


Fig. 5. A.B) Early stage I occur (Or.), exhibiting analous with Limpboosh chiramosomes (Cht. dense nucleolus (no), and cytoplasm (Cy) with abundant (thosomes, some of which are aggregated in crystal-like bodies farrows). Chang Or., exhibiting the extensive development of Golgi complexes (Ge) and minochoodina (Mil. D) Stage II encycle (Or.), exhibiting lipid droplets (Gd), multipus with univoked and elear elementary and micholos (no).

asin , the alm

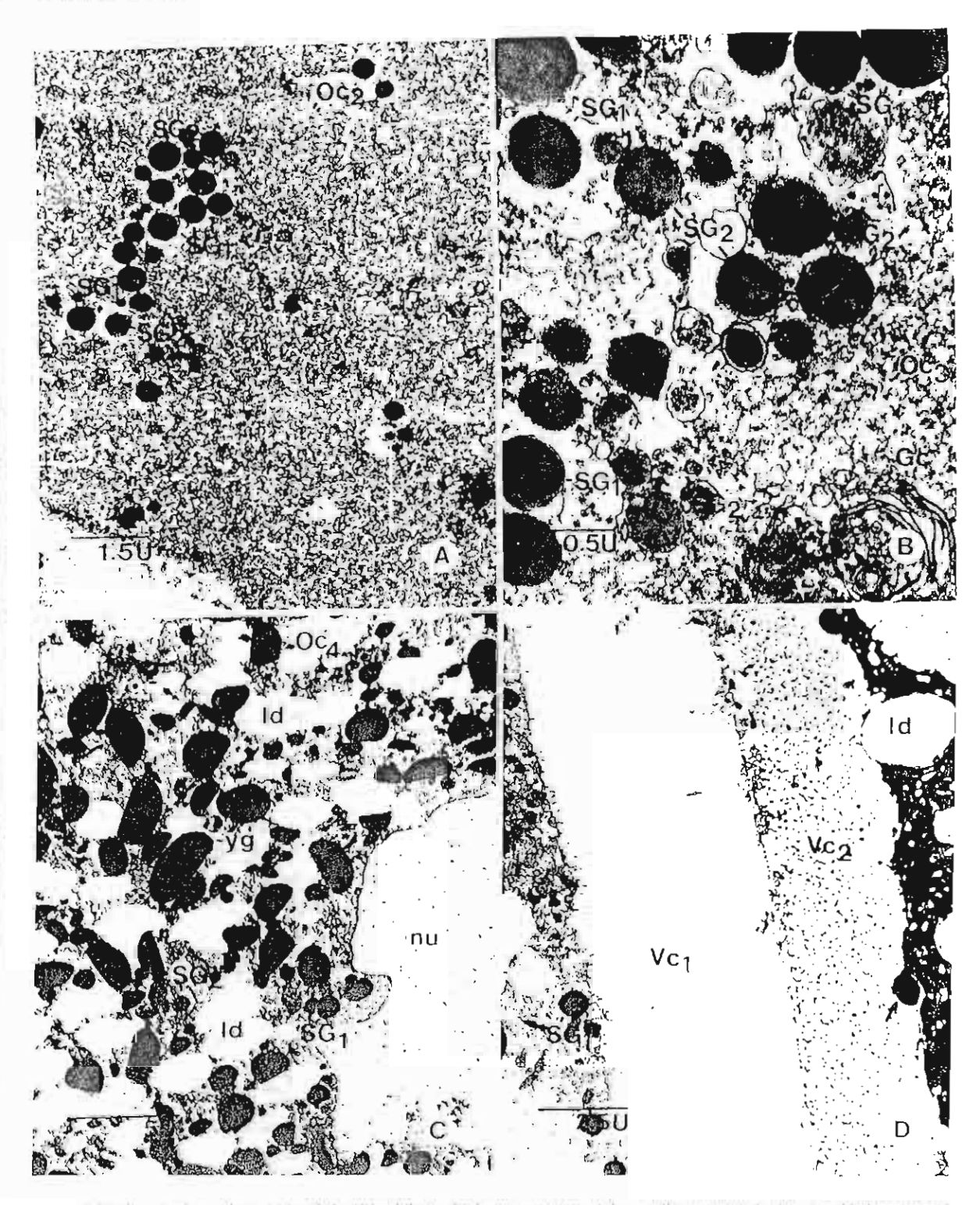


Fig. 6. A,B) I be symplasm of Or, (A) and C), (B) exhibiting highs interallmented device jelly contiguousles (M., Vasel lighter control of granules (S), around Golgi remplaces (G). (A) Fourth stage sowers (Oc, ) exhibiting viry light models is (not five to completely uncoded chromatin. The certaphen common nonerous large yells grounds (Cg), small SG, and SG, and SG, grandes. (D) The bostons necessary the roat of Oc, (Ve<sub>1</sub>) and fibrous jelly coat of Oc, (Ve<sub>2</sub>). Notice the exercises of SG, and plants Ve<sub>1</sub> farms.)

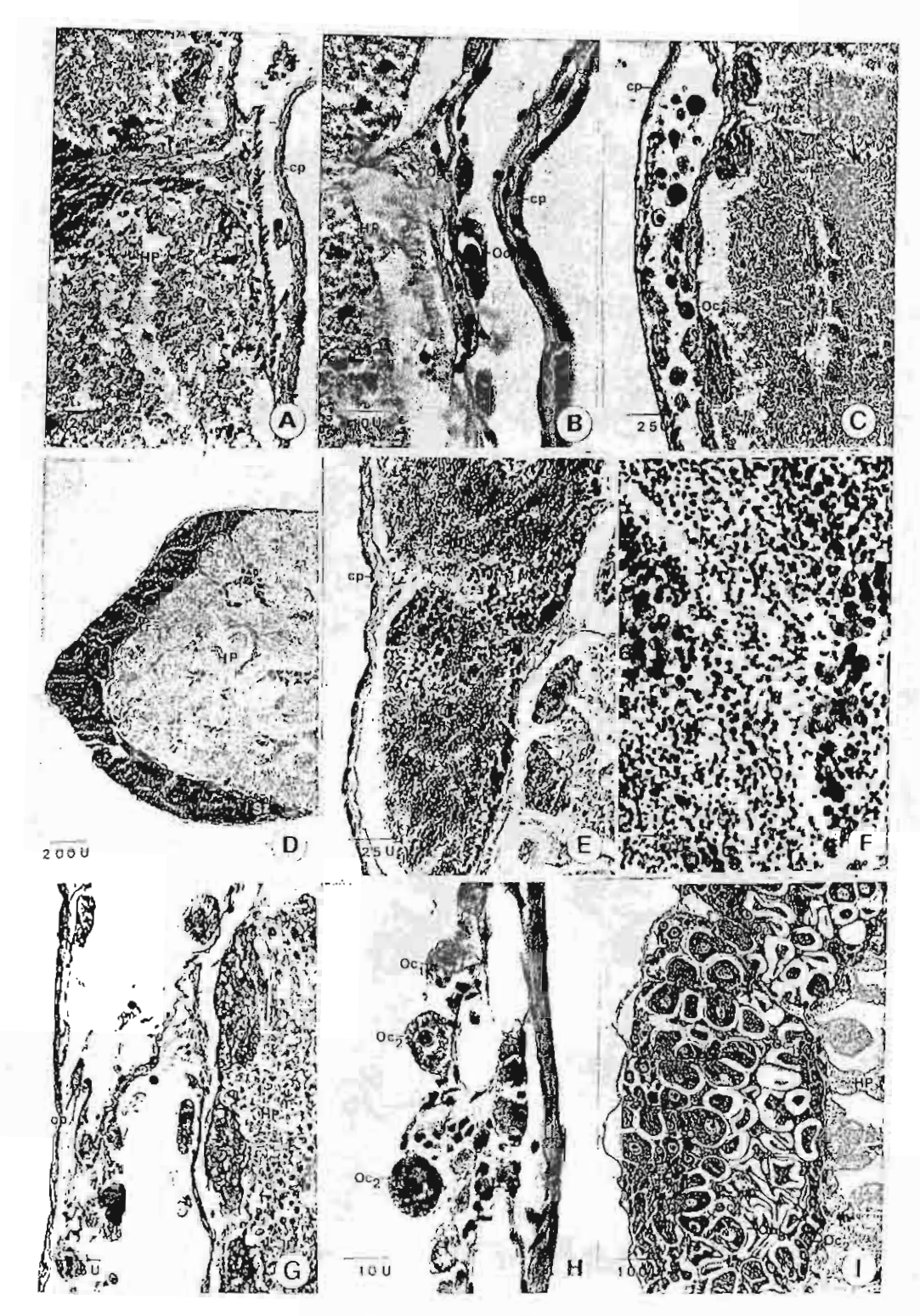


Fig.7: The development of gonals: A) the separation of gonalal cupsule (cp) from hepatopaneress (HP) at 2 minths, B) the presence of organia (Og) and possibly Oc; on the gonalal cupsule bordering the hepatopaneress (HP). C) the ovary at 6 months showing the presence of early onergies, mostly Oc; D,E,F) the testis at 4 months (in D) and 6 months (in F) showing full range of specimetocytes (Sc), specimenals (Sc) and some specimenomic (Sc), G,H) ovary at 7 months showing the formation of trafficula (ii) and the possence of early occytes, mostly Oc; and the all means at 11 months in mature phase, containing mostly Oc; and a few Oc;

to the total gonad area. This phase usually occurs immediately after the spawning, and lasts for 2 months around April to May and October to November.

Premature phase. (Fig 2J-M) This phase is the period when gametogenesis proceeds at full speed with rapid increase in numbers and sizes of various cells, while hepatopanereas is slowly reduced in its relative size; the gonads become enlarged in volume and trabeculae become thinner. At the beginning, the ovary (Fig 2J,K) contains Og, Oc, Oc, and predominantly Oc, most of which are still attached to the trabeculae; and later Oc, and Oc, cells occur. The testis (Fig 2L,M) contains mainly Sg, PrSc, increasing number of St and a few of Sz, all of which aggregate around the trabeculae. This phase lasts about 1 months following the proliferative phase. usually around May to June and January to February in lemale; and it takes place around April to May and December to January in male.

Mature phase. (Fig 3A-E) This phase is a period of rapid growth of gonads which are reflected by striking differences in color between the two sexes. The rates of cells proliferation start to diminish, and the gonads contain primarily late stage germ cells, while only a few of the early stage cells are still present and restricted to area immediately around traheculae. Hepatopancreas is further decreased in size, and trabeculae become slimmer. In the ovary (Fig 3A,B) there are abundant Oc, but only few remaining and widely scattered Oc. All of Oc, appear fully mature and are liberated into the lumen of oogenetic compartment. In the testis (Fig. 3C-E) there are mostly late stage male germ cells, ie, St and Sz. The most noticeable characteristics of the testis in this phase is the vast number of Sz, which lie in rows that in turn surround the earlier cell stages which are still closely attached to the trabeculae (Fig. 3D). As a result the testis appears to have maximum density of late stage cells. Prior to spawning, all of 5z, are dispersed into gonadal lumen and intermingled with other late stage cells (Fig 3E). Thin bands of Sg and PrSc surrounding the trabeculae are still evident. This phase lasts for 2 months usually from June to July and Vehruary to March in both

Spawning phase. (Fig 3F-J) This is the period when abalone are ready for breeding, during which the completely mature and viable eggs or sperm are released from the gorads. The gonads are significantly decreased in size, and the gonadal wall becomes wrinkle when compared with the former phase (Fig 3H). Mostly ripen sperm or eggs are discharged while the earlier stages of gamete cells are still attached to

the dilated trabeculae. After spawning, the yellowish granular substances (Fig 3G) remain in the lumen of gonadal compartments in both sexes. Spawning phase occurs at least twice during the one year period of observation, usually from August to October and March to April in female, and around August to November and February to April in male. In addition, partial spawning could be observed throughout the year in some males.

Spent phase. (Fig 3K-N) This is the period after spawning when fully mature gamete cells are completely discharged. The gonads exhibit the breaking down of connective tissue stroma, and gametogenic activity momentarily cease. However, there are still clusters of gonial cells remain attached to parts of the gonads' capsule. As a result the gonads are greatly decreased in size and become creamy in color in both sexes. These quiescence gonads show small cross-sectional profiles in contrast to those of the hepatopancreas, which becomes very large in relative size (Fig 3M). This phase occurs after spawning around September to November and February to April in both sexes.

#### 4. Maturation of Gonads

In developing H asinina, definitive gonads appear during 2 months. The initial sign is the separation of hepatopancreatic capsule into 2 separate layers with clusters of gonial cells start to appear in the space between the two layers of capsules. Early spermatocytes (PrSc, SSc) and spermatids (St, 4) could be detected at 4 months, while the ovary could be distinguished from the testis by the presence of few Og in contrast to fairly numerous primary spermatocytes. Spermatocytes, spermatids and mature spermatozoa are increasing in number during 6 to 7 months. While testis are rapidly enlarging and surrounding almost half of the circumference of the conical organ, ovary is much less developed and contains only oogonia and early oocytes (Oc.,). By 8 to 9 month the testis becomes enlarged to almost completely surround the hepatopanereas, and it already contains fully mature spermatozoa; while the ovary tends to be delayed in development and contains only early docytes (De j.). By 10 to 11 month the testis appears fully developed, while the ovary starts to enlarge substantially and mature oocytes (Oc., ) begin to appear. Thus the male animals tend to reach full sexual maturity and start normal reproductive cycle as early as 7 to 8 months, while female animals reach sexual maturity and start reproductive cycle around 1) to 12 months (Table 1, 1·ig. 7).

ScienceAsia 25 (1999)

Table 1. Summary of the key features during the course of development of gonads in Haliatis asinina.

Age (months)	General Structure	Gamelogenic Unit	Cell Types	Phases of Cycle
	Separation of ganadal consula from hepatapancreatic (HP) capsule. Development of few muscle cells in ganadal capsule. rexually inclutinguishable.	none	only few undifferentiated gardal cells attached to capsules	none
	-male: testicular tissue covering a quarter of HP capsule.	Incomplete	Sg. PrSc. SSc. St.,	proliferative
	of miceptate.  -female: overy shows as further developmentsexually distinguencoin.	none	Og	none
	-male: testis covering half of HP capsule. -female: ovary still small and not well developed.	none	Sg. PrSc. SSc. St <sub>1.4</sub> . Sz <sub>1</sub> Og. Oc <sub>1</sub>	premature none
	-male: testis covering half of HP capsule. -female: ovary still mail.	complete begin to develop from sprouting trabeculae	Sg. PrSc, SSc, SI <sub>14</sub> , Sz <sub>12</sub> Og, Oc <sub>1</sub> , Oc <sub>2</sub>	mature very early proliferative
	<ul> <li>male: festis covering slightly over half of HP capsule.</li> </ul>	complete	Sg. PrSc. SSc. St <sub>1.4</sub> , Sz <sub>1.2</sub>	mature
	-female: ovary covering about a quarter of HP capsule	Incomplete	Og, Oc <sub>1</sub> , Oc <sub>2</sub> , Oc <sub>3</sub>	early proliferative
	male: festis covering all HP copiule. female: overy covering half of HP capsule.	complete incomplete	Sq. PiSc, SSc. St., 57.2, Cg. Oc., Oc., Oc.	mature proliferative /premature
	-male: testls covering all HP copsule and much thickened.	complete and numerous complete and	Sg. PrSc. SSc. St 1.4. Sz 1.2	mature
7	-female: ovary covering signify over half of HP capsule.	Increasing in number	Og. Oc <sub>1</sub> , Oc <sub>2</sub> , Oc <sub>3</sub> , Oc <sub>4</sub> , Oc <sub>5</sub>	mature

# DISCUSSION

# Gonadal Structure and Classification of Cells in Gametogenesis

The first accounts of reproductive biology on an abalone species, H tuberculata, was published by Stephenson<sup>11</sup> since 1924, and Croft<sup>12</sup> in 1929, who showed that the basic framework of the gonads is composed of fibrous capsular and trabecular supports, from which germ cells appear to generate. Similar histological studies in other species were later performed by many investigators. 1122 More recently, a fine structural study of the ovarian cells in the red abalone. H rufescens, was also undertaken by Martin et al.23 All of these studies confirmed similar pattern of structural organization of the gonads; however, there are some disagreements on the classification of the stages of germ cells in the oogenetic and spermatogenic processes. 15,16,18,20 Utilizing a high resolution TEM to study the relative abundance of various organelles, particularly ribosomes and the development of rough endoplasmic reticulum and Golgi complexes in the cells, Martin et al 21 suggested that there were 5 stages of female germ cells in H infescens, which they termed oogomum, presynthetic obcyte, synthetic oocyte, early postsynthetic oocyte and fully developed postsynthetic oocyte. We feel that the classification based on size alone, as adopted by many investigators, is not a good criterion for dividing cells in a single line of differentiation into

various stages, because in reality these cells are undergoing continuous development. A better criterion would be to divide the cells according to the changes in histological and ultrastructural leatures which reflect the beginning of different synthetic activities in various developmental stages. In our study of II asinina, light and electron microscopic characteristics have been used for dividing the stages of lemale germ cells: 1) the appearance of nucleus and nucleolus especially with regard to the uncoiling of chromatin, as reflected by the clarity of the two structures; 2) the clarity of nuclear membrane which is the result of the density difference between the condensed chromatin in the nucleus and the surrounding cytoplasm; 3) the basophilia or the bluishness imparted to the cytoplasm of the cells by basophilic dyes which reflect the abundance of ribosomes in the cytoplasm; 4) the presence of lipid droplets; 5) the development of secretory organelles particularly rough endoplasmic reticulum and Golgi complexes; 6) the occurrence of basophilic secretory granules including cortical granules, and cosinophilic yolk granules, and their relative abundance; and 7) the presence of jelly coat surrounding the egg cells. By using these rather stringent morphological criteria, we have identified 5 stages of egg cells, starting from oogonia (Og) which are the smallest cells closely attached to the connective tissue trabecula. These cells could maintain a constant pool of early stem cells,

particularly those that are clustered towards the capsular side of trabeculae. During the spent period when most mature oocytes are released from the ovary and the connective tissues of trabeculae are breaking down, these cells are the only remaining group of germ cells. The restoration of gonadal structure during proliferative phase is carried out by the regeneration of connective tissues of trabeculae and the proliferation of this pool of oogonia.

The first stage of oocytes (Oc.) including cells of different sizes ranging from 20-24 µm. The most pronounced characteristics that they exhibit is the increasing basophilia or bluishness of their cytoplasm. And because of the similar degree of density between the cytoplasm on one hand, and the partially condensed chromatin and dense nucleoplasm on the other, the outline of nuclear membrane could not be easily discerned under LM. The nucleolus, while present, is not outstanding. All Oc. are surrounded by a single layer of flat follicular cells. Under TEM we found that there is increasing amount of ribosomes which reflects the intense cytoplasmic basophilia. While ribosomes are rapidly synthesized during the early stage of Oc, definite surge in the number and degree of development of Golgi complexes and RER are observed only in late Oc. These two subgroups of Oc, do not yet exhibit any secretory granules. Thus they may correspond to the presynthetic oocytes as described by Martin et al. when cells are preparing themselves for the onset of synthetic activities.

Oc, is the stage that first shows the presence of lipid droplets in the less intense basophilic cytoplasm. Due to the decondensation of most chromatin, and the increased translucence of the nucleoplasm, the nuclear boundary could be clearly observed under LM. For similar reasons the nucleolus also becomes more distinct; and because of its enlargement the nucleolar activities for tibusomal synthesis is believed to be on the increase<sup>24</sup>. Under TEM, a few definite SG<sub>1</sub> and SG<sub>2</sub> granules start to appear in this stage, by clustering around Golgi complexes. Thus Oc, could represent the initial phase of synthetic activities when jelly coat (SG<sub>1</sub>) and cortical granules (SG<sub>2</sub>) are first synthesized.

Oc, is the stage which cosmophilic yolk granules first appear, and later is nacressing in number; hence rendering the cytoplasm of Oc, more reddish in compast to that of Oc, while the basophilic or bluish 5G granules are seen scattered evenly between yolk granules and lipid draplets. We believed, therefore, that this is the stage where there is intense synthetic

activities, since under TEM numerous SG<sub>1</sub> and SG<sub>2</sub> as well as yolk granules appear in large numbers; particularly SG<sub>1</sub> and SG<sub>2</sub> were seen concentrating around Golgi complexes. Oc, is still surrounded by a single layer of follicular cells, which by this time consists of several cells because of the increase in size of the cell. In addition, Oc<sub>1</sub> is further detached from the connectives of trabeculae and assumes a pear or even tear-drop shape. The chromatin becomes completely euchromatic and the nucleolus is enlarged further as its chromatin are almost completely uncoiled; this implies the active transcriptional as well as translational activities.

Oc, is the stage where a thin jelly coat is first detectable, and it is sandwiched inbetween the egg cell membrane and the surrounding layer of follicular cells. Under LM the cytoplasm of Oc, becomes increasingly eosinophilic and appears more reddish due to the staining of numerous yolk granules by cosin. While the jelly coat is intensely PAS positive, the yolk granules are completely PAS negative. The contrasting feature implies that there may be very little or no carbohydrate moieties in the yolk granules, while these are the major constituent of the jelly coat. Under TEM the cytoplasm of Oc, is filled with SG1, SG2 and yolk granules, which reflect the near saturation of synthetic activities. The chromatin of Oc<sub>4</sub>, like that of Oc<sub>3</sub>, is completely in euchromatic state and the nucleolus is fully enlarged due to the complete uncoiling of its chromatin, and under LM it even appears eosinophilic. These indicate still high levels of both nuclear and nucleolar transcriptional activities. Another remarkable feature of Oc, under LM is the appearance of a narrow bluish stripe in the cytoplasm just underneath the cell membrane, while the bluishness of the remaining mass of cytoplasm is much decreased in comparison to Oc, and Oc. This could be due to the high concentration of basophilic SG, and SG, granules which are translocated to this area as observed under TEM. Some of the more electron SCI granules are also seen exocytosed to the cell's periphery, and thus is believed to contribute material to the formation of the jelly coat. In contrast, SG contains more electron lucent material than SG<sub>1</sub>. They may be the actual cortical granules that are concentrated in the narrow cytoplasmic zone underneath the plasma membrane, and thus are kept in reserve for cortical reaction upon fertilization of the egg by the sperm.

Oc, is the stage where the jelly coat becomes uniformly thick and deprived of surrounding layer of follicular cells. Under TEM the jelly coat is transformed from homogeneous in Oc, to fibrous

ilive

, ninte

g to ural rent iges. tron

the

with

d by

arc

y of usity the the the hich asni; nont

their coal tiner ified (Og) a the auld

clis,

Tical

C

gt

()

51

Ti

cl

51

all

51

11:

5:

1:1

81

13

ľξ

Ц:

SC

Sį

D

ſc

()(

Ti

11

Oi

d

b

():

11

la

()

(1

C:

1)

11

4

h

P

T

n

d

11

16

0

I'A

54

g

iı

Ci

1)

structure in Oc,. There is no division of this cell coat into jelly and vitelline layers as reported in other species. Thus Oc, appears completely mature and is fully detached from the trabeculae. The absence of follieular cells might allow the detachment of Oc. into space between trabeculae and ready them for release from the ovary. From this appearance it could be speculated that the major roles of follicular cells are protective and helping to maintain the adherence between oocytes and trabecula connective tissue, while the former are undergoing maturation. In addition, follicular cells could be involved in nutritive function for oocytes, and their roles in synthesizing the jelly coat could not yet be ruled out. Under LM the cytoplasm of Oc, is laden with reddish yolk granules. Based on the size of these yolk granules there could be 2 subgroups of Ocs: one containing small granules of uniform size while the other contains very large granules, both of which appear very electron opaque under TEM. It is still not possible to confirm whether these are two separate stages of Oc, or that the latter merely represent the final stage in which small yolk granules are coalesced to form larger ones. In any cases these two subgroups of Oc should represent fully mature cells. In comparison to the work of Martin et al,23 Oc, could represented the early postsynthetic cells and Oc, late postsynthetic cells; even though, judging from ultrastructural features certain degree of synthetic activities must still be carried out in these cells.

Up to now most studies have not rigorously categorize various spermatogenic cells of Haliotis; apart from suggesting broadly that there are 4 stages, ic, spermatogonia, spermatocytes, spermatids and spermatozoa<sup>18,18,20</sup>. In the present study, the male germ cells in H asinma could be classified into 13 specific stages according to the size, shape, appearance of chromatin and the presence or absence of nucleolus. Spermatogonium is the earliest cell whose nucleus contains almost all euchromatin which results in the nucleus being very clear and nucleolus is prominent. Spermatogonia divided mitotically to give rise to primary spermatocytes, which pass through 5 stages as In the first meiotic division of vertebrates' germ cells. 16 These prophase cells exhibit different forms of chromatin condensation, beginning with small to larger blocks of heterochromatin that are evenly scattered throughout the nucleus in 15c and ZSc. Heterochromatin blocks transform to thread-like pattern that are increasing in thickness and length, and become more entwined in PSc and DSc. Finally in diakinetic and MSc stages chromatin appears as pairs

of chromatids that are translocated to the equatorial region. Secondary spermatocytes are quite numerous in comparison to those in vertebrates and they have heterochromatin that exhibit checker-board or XY-ligure pattern.

Four stages of spermatids could be identified in H asining based on the nuclear size, shape and chromatin condensation. Under LM the first two stages exhibit finely granulated chromatin that appears homogeneous and evenly stained throughout the nuclei. Thus St, and St, could be distinguished by the difference in size (St. about 6 μm versus St, about 4 μm), and by the denser nuclear material in St,. The latter is due to the reduction of nuclear volume which results in the closer packing of chromatin fibers, even though each fibers still maintain their width of 30 nm. In the third stage (St,) the chromatin fibers begin to be tightly wound together into large dense blocks, particularly along the nuclear envelope, leaving clear areas between the blocks. At this stage individual fiber increases in size to 40 nm. Eventually, the decrease in volume of nucleus and its more ellipsoid shape results in the total condensation of chromatin mass in St,, and individual chromatin fiber is enlarged to 60 nm.

The two stages of spermatozoa are distinguished by their ellipsoid nuclei. Sz<sub>1</sub> also shows the initial formation of acrosome as a clear cap-like structure on one end of the nucleus, while exhibiting only short tail. Under TEM, there is the formation of axonemal complexes from centriolar pair that move to the neck area just distal to the nucleus. Later, three to five globular mitochondria become localized around the centrioles. In Sz<sub>2</sub> the nucleus is elongated further and chromatin appears completely dense with the outline of 60 nm fibers (or granules) barely discernible. Sz<sub>2</sub> exhibits a completely formed tail that is long and point outwards from each trabecula.

#### Reproductive Cycle

There have been a number of studies on the course of reproductive cycle in various abalone species by many investigators. The two methods that are frequently used for determining a reproductive cycle of a population are: 1) the measuring of the relative size of gonads with respect to the size of conical organ which is termed gonad indices (GI); and 2) the assessing of histological changes in the gonads. The GI is not always a valid index for development of the gonads because GI only relates gonad area to constant parameters (rg the size of conical organ) of the animal, and it does not take variation in bepatopanereas size into account.

99)

mil

1115

IVC

Y-

in

nd

WO

1111

cd

be

LO

car

of

ing

till

ige

nd

222

Tie

IZC

of

lie

nd

red

113

are

nly

of

WC

ree

.cd

ted

150

cly

731

lic

inc

List

ive

,he

61

il);

Hic

for

10%

edf

rice

The more precise index that can define of reproductive cycle better is the use of histological examination of gonad sections, which can give considerable details of cellular association and the time interval between successive phases<sup>17</sup>. Many investigators, including Tomita, <sup>15-16</sup> Lee, <sup>32</sup> Giorgi & DeMartini, <sup>33</sup> Ault, <sup>30</sup> classified the reproductive stages in various temperate species of *Haliotis* into 5 to 6 distinct phases which are more clearly defined in females. In the present study, these various phases were also observed in *Hasinina*. Histological examination of monthly samplings of the brooding stocks cultured in the land-based culture system reveal 5 distinctive gonadal patterns during the year, *ie*, proliferative, premature, mature, spawning and spent phase.

Proliferative phase is characterized by the regeneration of gamete cells for the new cycle. The gonads contain mostly early stage germ cells in both sexes, such as Og, Oc, Oc, in the ovary, and mainly Sg. PrSc without St and Sz in the testis Giorgi & DeMartini 33 and Ault, 30 on studying H rufescens, found that the ovary contained primarily small oocytes usually lesser than 50 jun in diameter; while Tomita, 19 on studying H discus hannai, reported that there were mainly oogonia, yolkless and oil drop oocytes in this stage. Another remarkable feature during this phase is the reciprocal relationship between the sizes of the gonads to the hepatopancreas, which is similar to that found in other Halioud.1317 That is the hepatopancreas is relatively large when compared to the total area of conical organ. Boolootian et al13 also reported that, in 11 crucherodii and Hrufescens, the size of hepatopancreas exhibits an inverse relationship to gonadal activity. During this phase, the hepatopancreas attains maximum size while the gonad activity is relatively quiescent. The precipitous drop in the size of hepatopanereas will occur during the subsequent phase when there is a rapid growth of the gonads. This implies that hepatopanereas may act as a nutrient storage that is necessary for gamete cells development; it becomes relatively depleted when the profileration of gonad cells start to surge. Another remarkable histological feature observed during this phase is the dilaration of the trabecular vessels which contain large amount of granular materials. This may represent the turgid state of the vessels that are supplying nutrients to the rapidly proliferating and growing gamete cells

Premature phase is the period of rapid increase in numbers and sizes of gamete cells. The ovary contains predominantly Og, Oc<sub>1</sub>, Oc<sub>2</sub>, Oc<sub>3</sub> and few Oc, which is similar to those reported in the premature stage of *H* discus hannai, <sup>13,44</sup> while Sg, Sc and only few of St and Sz are evident in the testis during this phase. Ault, <sup>30</sup> in studying *H* rujescens, also reported that there were numerous developing early germ cells in this stage. Hence the major events of development in this phase involve the rapid growth of the gonads due to fast proliferation of early germ cells.

Mature phase is characterized by a notable enlargement of the gonads which exhibit striking differences of color between both sexes: greenish in female and yellowish in male. The ovary contains mostly late stage germ cells, ic, Oc, with widely scattered Oc; and the testis is mostly filled with St and Sz. Before spawning occurs, Oc, are detached from trabeculae and released into the gonadal lumen. During the rapid development of the testis, each trabecula is surrounded successively by a few rows of Sg. PrSc which are closely bound to trabecular connectives, and middle Sc. Strappear further away, and Sz are completely detached from trabeculae. In comparison, during the differentiation of Oc, to Oc, from Og, the cells move along the trabeculae from capsular side towards the hepatopancreas side, until Oc, become detached from trabeculae.

Spawning phase is the time when gravid abalone start to release their ripened gametes. The period of spawning is the most important criterion for success of reproduction of various abalone species reared in close aquaculture system. 13-19.29,33,33-37 From many previous studies, spawning periods have been found to vary considerably among various species of abalone, and from year to year according to geographical locations, and local environment, such as food supply temperature and the day length. 17,34,3641 Thus, some investigators 13 36 have classified various Haliotid spp. into 3 groups according to their spawning season: those spawn during summer, those spawn during seasons other than summer, and those that exhibit year-round spawning. Earlier, Singhagraiwan & Doi12 reported the spawning period of some wild broodstocks of II asinina to peak around October, while the pond-reared broodstocks could spawning throughout the year with several minor peaks during March through September, In contrast, the spawning period of H asmina kept in land-based closed culture system in the present study occurs twice a year: around August to October and March to April in female, and around August to November and February to April in male. While this is the general pattern of spawning for most members of the population, some individual may show irregular periodic spawning throughout the year, especially in males animals.

Spent phase is characterized by the lacking of gamete cells and the breakdown of connective tissue in the gonads, which is similar to that previously finding in H infescens. According to Shepherd & Laws, appent phase is expressed when there is a complete discharge of gamete cells following spawning. Giese defined spent phase in marine invertebrates as a postspawning quiescent stage which is indistinguishable between male and female. In present study, it was observed that during the spent phase the gonads of H asinina are greatly reduced in size and become creamy in color, and the sexes of animals cannot be distinguished. In contrast, hepatopancreas is relatively increased in size which may be filled up with food reserve.

From the data collected during one year period, it could be concluded that the spawning of *H* asinina reared in the closed culture system can occur at least twice yearly providing that the culturing condition and food supply are optimal. And that each reproductive cycle, consisting of 5 phases of development, needs at least 5 to 6 months to complete itself.

#### Maturation of Gonads

In previous studies of the gonadal development in Hasinina, fecundity was observed in lemales with the shell length of at least 48 mm for the wild broodstock, and 44 mm of the hatchery-reared broodstock, which was about nine months old. 43-44 On the other hand, the mature gonad of males become obvious in animals with the shell length of at least 31 mm, which is about seven and a half months old. 12-14 The data collected in the present study indicate the same trend. Furthermore, detailed histological study indicated that definitive gonads become clearly separated from the hepatopanereas at 2 month. Testis and ovary could be distinguished by the presence of their initial stages of germ cells as early as 4 month. Testis tends to reach maturity quicker than ovary at 7 to 8 months, the time at which St and Sz are found to be abundant. Ovary tends to mature at 10 to 11 months when it starts to contain mature oocytes (Oc, and Oc,). Thus males tend to reach maturity and assume remoductive cycle much earlier than lemales.

# **ACKNOWLEDGEMENTS**

This investigation was supported by the Thailand Research Fund (Contract BRG-4080004 and Senior Research Scholar I ellowship to Present Sobbon).

# REFERENCES

- Nateswathana A and Hylleberge J (1986) A survey on Thai abalone around Plucket Island and feasibility study of abalone culture in Thailand. That Fish Gazette 39, 177-190.
- Tookvinart S, Leknim W, Donyadol Y, Freeda Lampahuira Y and Pering mak P (1986) Survey on species and distribution of abalone (Huliotis spp.) in Surajthani, Nakornardhammaraj and Songkhla provinces. Technical Paper No. i/1986, National Institute of Coastal Aquaculture, Department of Fisheries, Ministry of Agriculture and Cooperatives, Thailand, 16p.
- Nateewathana A and Bussarawit S (1988) Abundance and distribution of abalones along the Andaman Sea Coast of Thailand. Kasetsart J (Nat Sci) 22, 8-15.
- Singhagraiwan T and Sasaki M (1991a) Breeding and early development of the donkey's ear abalone, Haliotis asinina Linne. Thai Mar Fish Res Bull 2, 83-94.
- 5 Singhagraiwan T and Sasaki M (1991b) Growth rate of donkey's car abalone, Haliotis asinina Linne, cultured in tank. Thai May 198h Res Bull 2, 95-100.
- Kakhai N and Petjamrat K (1992) Survey on species and broodstock collection of abalone (Haliotis spp.) in Chonburi, Rayong and Trad provinces. Technical Paper No.6/1992, Aquaculture Station, Coastal Aquaculture Division, Department of Fisheries, Ministry of Agriculture and Cooperatives. Thailand.
- Singhagraiwan T and Doi M. (1993) Seed production and culture of a tropical abalone, Haliatis asinina Linne. The Eastern Marine Fisheries Development Center, Department of Fisheries, Ministry of Agriculture and Cooperatives, Thailand, 33p.
- Sungthong S, Ingsrisawang V and Fujiwara S. (1991) Study on the relative growth of abalone. Haliotis asinina Linne, off Samet Island. Thai Man Fish Res Bull 2, 120
- 9 Bussenawit S, Kawintertwathana P and Nateewathana A (1990) Preliminary study on reproductive biology of the balone (Haliotis varia) at Phuket, Andaman Sca Coast of Thailand, Kasetsart I (Nat Sci) 24, 529-39.
- Jarayabhand P, Jew N, Manasoveta P and Choonhabandu 5 (1994)
   Gamerogenic cycle of abalone Haliotis ovina Carelin 1791 at ichanglan Island, Chon-buri province. That J April Sci 1, 43-42.
- Stephenson TA (1924) Notes on Haliotis tuberculata. J. Marin Biol Assoc UK 13, 480-495.
- Croft DR (1929) Huliotis LMBC mem, Liverpool University Press, 29, 174p.
- Boodonton RA, Furmandarmanan A and Gree AC (1962) On the reproductive cycle and breeding liabits of two western species of Hultons Bull Bull 122, 183-93.
- 14 Newman GG (1967) Reproduction of the South African abaloue Haliatis midas. Division of Sea Fisheries, Republic of South Africa, hive-stigational Report No. 94, 24p.
- 15 Iomita K (1967) The maturation of the ovaries of the abalone, Haliors discus human Inc., in the Rebun Island. Hokkaido. Japan. Sci Rep Holdaido Fish Exp Sta 7, 1-7.
- 16. Jounna K (1968) The resis maturation of the abalone, Halings discus hamon two, in the Rebuta Island, Hokkaido, Japan. Sci Rep Hokkaido Fish Exp Sta 9, 50-64.
- Wehher IIII and Giese AC (1969) Reproductive cycle and gametogenesis in the black abalone Haliotis cracherodii (gastropoda: presobranchiata). Mor Biol 4, 152-9.
- 1B. Young IS and DeMartin ID (1970) The reproductive cycle, gonadal histology and gametogenesis of the red abatone, United in Proceedings (Swamson), Calif Fish and Came 56, 208–309.
- Harrison AJ and Grant JJ (1971) Progress in abalous research. Justice fish for 5, 1–10.
- 20 Jakashima I, Okomo M, Nichimura K and Nomura M (1978) Gametogenesis and reproductive cycle in Hollotts diversicolor discontrolor Recyc. J. John Chay Ush 1, 1-6.

21

Than

tra Y ttion

vics,

early

tkey That

buri,

and stem

p ly on

thone land

1994) 91 at -3-42. -darin

Endoy Din

rican ilienf

atilo,

diwis n Sci

e and

tycké, ilimic, 2 100 auch

(978) lealar

- Brickey BE (1979) The histological and cytological aspects of cogenesis in the California abalones. (MS Thesis) California State University, Long Beach, California.
- Tuischultz T and Connell JH (1981) Reproductive biology of three species of analone (Hallastis) in southern California. The Veliger 23, 195-206.
- Martin GG, Romero K and Miller-Walker C (1983) Fine structure of the ovary in the red abalone Haliotis infescens (Mollineat gastropoda). Zuomorphology 103, 80-103.
- Schwarzacher (IC and Wachtler F (1993) The nucleolus. Anat Embryol 188, 515-36.
- Monzingo NM, Vacquier VD and Chandler DE (1995) Structural features of the abalone egg extracellular matrix and its role in gamete interaction during fertilization. Mol Reprod Dev 41, 493-502.
- Courot M, Hochereau-de Reviers M-T and Ortavant R (1970).
   The testis Johnson AD (cd) (1970). Academic Press, New York, 399n.
- Halin KO (1989) Handbook of culture of abalone and other matine gastropods. Hahn KO (ed)(1989). CRC Press, Boca Raton, Fiorida, p 13-39.
- Giese AC (1939) Comparative physiology: annual reproductive cycle of marine invertebrates. Ann Rev Physiol 21, 547-76.
- 29 Grant A and Tyler PA (1983) The analysis of data in studies of invertebrate reproduction. I. Introduction and statistical analysis of gonad indices and maturity indices. Int J Invertebr Reprod 6, 25%.
- Ault J (1985) Some quantitative aspects of reproduction and growth of jeel abalone, Haliotis infescens Swainson. J World Maricult Soc. 16, 398-425.
- Hahn KO (1981) The reproductive cycle and gonadal histology of the pinto abalone, Haliatis kaintschalkana Jonas, and the flat abalone, Haliatis walallensis Steams. Adv Investebr Reprod 2, 387.
- Lee TY (1974) Histological Study on gametogenesis and reproductive cycle of the Korean Coasts. Bull Pusan Fish Coll 14, 55.
- 33 Giorgi Al and CeMartini ID (1977) A study of the repro-

- duetive biology of the red abalone, Haliotis rufescens, Swainson, near Mendocino, California, Calif Fish and Game 63, 80-94.
- 34 Mugaya Y, Kohayashi J, Nishikawa N and Motoya 5 (1980). Gamadal matturation in the abulone, Hulions diseas humai at Lase (, Holckaudo, Bull Fac Uish Holdadio Univ 31, 306-13.
- 35 Poore GCB (1973) Leology of New Zealand abalones, Haliotis species (mollusca: gastropoda). New Zealand J Mar Freshwat Res 6, 534-59.
- Shepherd SA and Laws HM (1974) Studies on southern Australian abalone (Genus Halloris). II. Reproduction of five species. Aust J Mar Freshwar Res 35, 49-62.
- Girard A (1972) La reproduction de l'ormeau Huliotis tuberculata L. Rev Trav Inst Peches Marit 36, 163-84.
- Cox KW (1962) Review of the abalone of California. Calif Fish and Game 46, 381-406.
- 39. Uki N and Kikuchi S (1984) Regulation of maturation and spawning of an abalone, Haliotis (Gastropoda) by external environmental factors. Aquaculture 39, 247-61.
- Kinne O (1970) Marine ecology: A comprehensive integrated treatise on life in oceans and coastal waters. Vol.1, Kinne O. (ed) (1970). Wiley-Interscience, London, p 407-514.
- Shepherd SA (1973) Studies on southern Australian abalone (Genus Haliotis). I. The ecology of five sympatric species. Aust. J. Mar. Freshwat. Res. 24, 217-57.
- Singhagraiwan T and Dor M (1992) Spawning pattern and fecundity of the donkey's ear abalone, Haliatis asinina Linne, observed in captivity. That Mar Fish Res Bull 3, 61-9.
- 43. Singhagraiwan T (1989a) The experiment on breeding and nursing of Donkey's ear abalone (Haliotis asinina Linne) feelineal Paper No.21/1989a, The Fastern Marine Fisheries Development Center, Department of Fisheries, Ministry of Agriculture and Cooperatives, Thailand.
- 44, Singhagraiwan T (1991) Study on growth rate of donkey's ear abalone (Haliotis asinina Linne). Technical Paper No. 28/1991. The Lastria Marine Fisheries Development Center, Department of Fisheries, Ministry of Agriculture and Cooperatives, Thatland



# Structure and Development of the Testis of Bullfrog, Rana catesbeiana, and Their Changes during Seasonal Variation

Jittipan Chavadej $^{\alpha}$ , Aungkura Jerareungrattana $^{b}$ , Prapee Sretarugsa $^{\alpha}$  and Prasert Sobhon $^{a}$ 

- Department of Anatomy, Faculty of Science, Matridol University, Bangkok 10400, Thailand.
- Department of Clinical Microscopy, Faculty of Medical Technology, Mahidol University, Bangkok 10700, Thailand.
- Corresponding author.

Received 9 Nov 1999 Accepted 8 Mar 2000

Assiract. The testes of fully mature bulllrogs, Rana catesbeiana, were studied by light microscope. The germ cells in the developing testis can be classified into 12 stages based on nuclear characteristics. Primary(type A) and secondary(type B) spermatogonia are the earliest germ cells, with the former showing large and completely cuchromatic nuclei with prominent nucleoli and the latter with small blocks of heterochromatin distributed along the nuclear envelope. Spermatocytes consist of five stages; namely, leptotene, zygotene, pachytene, diplotene and diakinesis metaphase spermatocytes. Succeeding stages show increasing condensation of chromatin: from the coarse libers, that are evenly distributed throughout the nucleus in leptotene stage to the highly condensed blocks of heterochromatin in pachytene and diplotene stages. Nucleoli are not detected in any stages. Secondary spermatocytes have blocks of completely condensed heterochromatin attaching to the nuclear envelopes. There are three stages of spermatids: the early stage shows coarse chromatin granules occurs evenly over the nucleus, the middle stage has increased chromatin condensation over the entire oval nucleus while the nuclear size decreases. The late stage exhibits completely condensed chromatin in an elongated nucleus, and its cytoplasm becomes highly vacuolized and starts to degenerate. In fully mature spermatozoa, the nucleus becomes highly clougated and chromatin completely condensed. During development of the testis, sex cords in putative testis appear in two-month-old frogs. Seminilerous tubules containing primary spermatogonia appear in the definitive testis of four-month-old frogs while spermatocytes are present in five-monthold frogs. Spermiogenesis and full production of spermatozoa could be detected from the seventh month onwards. The frogs become fully nature about sixteen months when their testes undergo cyclical change. During breeding period (April-September), there are abundant spermatozoa, round spermatids in seminiferous tubules, while during non-breeding period (October-March), such cells are much lewer in number and most remaining cells are spermatogonia and primary spermatocytes.

KLYWORDS: Rana catesbeiana, spermatogenesis, male germ cells, testicular development.

#### INTRODUCTION

Amphibian male germ cells, especially in *Xenopus laevis*, have been studied by many investigators, using transmission electron microscope to investigate nuclear and cytoplasmic characteristics of various spermatogenetic stages, including spermatogonia, spermatocytes as well as cells in spermiogenesis. <sup>1,2</sup> H<sup>3</sup>-thymidine labelling and antoradiography have also been used for detecting the duration of the *X. leavis* male germ cells cultured in serum free media. Results showed that the time required for the premeiotic S-phase spermatogonia to develop to late zygotene spermatocyte, that later changed to spermatid, were 14 days and 28 days, respectively. <sup>3</sup> Labelling with H<sup>3</sup>-thymidine was also

performed in vivo to determine the duration of cells in meiotic prophase and spermiogenesis in X. laevis. And it has been shown that spermatocyte spent four days in leptotene, six days in zygotene, one day in diplotene, one day in meiotic phase; and 12 days was required for the completion of spermiogenesis.2 In Rana pipiens, male germ cells could be divided into nine stages, i.e., spermatogonia; spermatocytes which were divided into leptotene, zygotene, pachytene, diplotene, diakinesis; secondary spermatocytes; spermatids and spermatozoa." In addition, cells in spermiogenesis were classified into five stages based on nuclear characteristics.9 In bullfrogs, Rana catesbeiana, which is the species indigenous in North America, the stages of spermatogenesis and spermiogenesis have not yet

been studied in details. Thus, one of the primary purposes of this experiment is to classify various stages of germ cells in this species of frogs. Furthermore, bullfrogs had been imported and commercially cultured in Thailand for a number of years. As Thailand is a tropical country with distinctive wet and dry seasons the maturation and cyclical change of the testis may be quite different from frogs reared in North America. Therefore, the other aims of this study are to investigate maturation of the testis during the frogs' development, their breeding period, as well as the histological changes in testis that accompany seasonal variations.

# MATERIALS AND METHODS

#### 1. Experimental animals

R. catesbeiana were cultured in cement tanks at Faculty of Science, Mahidol University. They were maintained in an approximately 12 hour light/dark cycle, at 25°-35°C, with the relative humidity ranging from 45 to 95%. The culture water was changed at alternate days. The frogs were fed daily with pelleted feed in the afternoon.

#### 2. Light microscopic study

Mature male frogs aged more than 18 months old were anesthesized by placing in an ice bath for 5-10 minutes or until they became immobile. Then the spinal cords were pitched and the frogs were decapitated. Testes were dissected and immediately fixed in cold 4% glutaraldehyde plus 2% paraformaldehyde in 0.1 M phosphate buffer, and post-fixed in cold 1% Osmium tetroxide in 0.1 M phosphate buffer. After fixation specimens were washed and dehydrated in ethanol and embedded in Araldite 502. Semithin sections were cut at 0.5-1 µm and stained with methylene blue for light microscopic observations.

For paraffin procedure, the dissected testes were fixed in Bouin's fluid and dehydrated through increasing concentrations of ethyl alcohol, and embedded in paraffin, five to six-micron-thick sections were deparaffinized and stained with Harris's Haematoxylln and Eosin, and examined with an Olympus light microscope BH-2

# 3. Development of testes

Young frogs aged 1, 2, 3 up to 18 months old were bred and reared in cement tanks with food and general conditions as stated previously. At least ten trogs from each age group were used in this study. The testes were processed using parallin procedure.

as previously described in section 2.

# 4. Changes of testes during seasonal variation

Fully mature frogs aged more than 18 months old were used in this study. The testes were removed from the frogs at the end of each month throughout the year, and the testicular tissue was prepared using paraffin technique for light microscopic observation as described in section 2.

# RESULTS

# 1. Classification of spermatogenic cells

In semithin sections, the male germ cells of bullfrogs, *R. catesbeiana*, can be distinguished into 12 stages based on nuclear characteristics and sizes. Spermatogenesis in the frog takes place within follicular structures called spermatocysts that rest upon the basement membrane of the seminiferous tubules (Fig 1).

# 1.1 Primary spermatogonia (1°Sg)

Primary spermatogonia is the first stage germ cells in seminiferous tubules, and they constitute a high proportion of the cell population in the tubules of immature frogs. The cells are large and round in shape, and have round or oval nuclei with line and mostly euchromatic material. They are generally located close to the basement membranes of seminiferous tubules. The size of the nucleus is about 10-13 µm. Frequently, cells with large bilobed nuclei could be found which may be spermatogonial cells that are undergoing nuclear division. Each nucleus also possesses one or two nucleoli which are very prominent. The cytoplasm is generally lightly stained (Fig 1B).

# 1.2 Secondary spermatogonia (2°Sg)

Secondary spermatogonia are round, but in comparison to 1°Sg they are smaller cells whose nuclear diameter is about 9-12 µm. They can be distinguished from primary spermatogonia by the presence of small blocks of heterochromatin along the nuclear envelopes, and those that are scattered all over the nuclei which tend to have smaller-size. The nucleoli are still prominent. Each group of 2 Sg usually consists of 2 or 4 cells surrounded by follicular cells' processes which still lie close to the busement membrane (Fig 1C).

# 1.3 Leptotene spermatocytes (LSc)

These cells are round and larger than 2°Sg, and have large round nuclei with diameter about 11-



























Fig 1. A) Semintensis valudes, illustrating various stages of spermatogenic cells U.G. (High magnitudition of scientificous ridioles, drawing minute spermatogenia (1°5g), secondary spermatogenia (2°5g), hydrotese spermatogenia (2°5g), and photose spermatogenia (2°5g), and kellicular cell (1).

13 µm with a thin rim cytoplasm. Their chromatin begins to condense into loosely arranged blocks which are distributed evenly throughout the nucleus. In contrast to 2°5g, there is no heterochromatin blocks along the inner surface of the nuclear envelope. Small nucleoli are still present in this stage. Group of leptotene spermatocytes form large clusters of more than four cells each, that are surrounded by follicular cells (Fig. 1D). Leptotene spermatocytes are usually located towards the lumen of seminiferous tubules and seldom touch the basement membrane.

#### 1.4 Zygotene spermatocytes (ZSc)

The discriminating features of zygotene spermatocytes are the increased condensation of chromatin blocks and the change in size of the nuclei, which become smaller than that of leptotene spermatocyte. The heterochromatin blocks gradually become larger and perceptibly denser than in previous stage (Fig 1D).

#### 1.5 Pachytene spermatocytes (PSc)

The nuclei of these cells are still round and about 10-12 µm in size. The chromatin becomes condensed into long thick cords, that are intertwined into loops resembling "bouguet pattern". These cells are still aggregated in clusters, each of which is still surrounded by processes of follicular cells (Fig. 113).

# 1.6 Diplotene spermatocytes (DSc)

The general appearance of the cells in this stage is similar to PSc; however, the heterochromatin cords become denser and larger. Nuclear diameter is about 10-11 µm, and thus the nucleus appears smaller than in PSc. They are also fewer in number in comparison to PSc (Fig. 1F).

# 1.7 Diakinetic (Dia) and Metaphase spermatocytes (MSc)

The cells in these stages show thick chromosomes that are arranged close together in Dia, and later move to the equatorial region in MSc, when the nuclear boundaries disappear. They are so lew and transient that they are rarely observed within the seminiferous tubules (Fig. 1G).

#### 1.8 Secondary spermatocytes (2"Se)

These cells arise after the first melotic division, and the nuclear diameter becomes smaller. Dense blocks of heterochromatin distributed in carawheel or clock-faced pattern within the nucleus arise from the coarse clamping of chromatin along the nuclear envelope (Fig 1F).

#### 1.9 Early spermatids (ESt)

ESt arise after the second meiotic division, and they are markedly decreased in size and number within the tubules. They still have round nuclei which are also reduced in size to approximately 8-9 µm in diameter. The condensation of chromatin occurs evenly over the nucleus and the nucleus becomes eccentrically located within the cell. A small dark spot in the cytoplasm which may represent the Golgi complex can occasionally be seen at this stage of spermatid (Fig 2A).

# 1.10 Middle or round spermatids (RSt)

The nuclei of these cells show higher degree of chromatin condensation than in previous stages, and the condensation occurs uniformly throughout the nuclei which are reduced in diameter to about 6-7 µm. Each nucleus tends to be oval in shape. A small dark bar adhered to the nucleus which may represent the centrioles can be found. RSt is the most numerous cells in the tubules, probably due to their long duration (Fig 2B).

#### 1.11 Late spermatids (LSt)

The nucleus of this late stage spermatid is characteristically reduced in size and begins to clongate. Chromatin becomes completely condensed throughout the nucleus. The cells usually move close to the lumen of seminiferous tubules, while they are stilled grouped together in clusters (Fig 2C).

# 1.12 Spermatozoa (52)

The mature spermatozoa exhibit highly clongated heads and tails. The head contains an ellipsoid nucleus with completely condensed chromatin which is deeply stained. Heads of several spermatozoa appear to be arranged in array that are embedded in the apical cytoplasm of Sertoli cells, while their tails point toward the seminiferous lumen (Fig. 2D).

Cells with varying size located in clusters between the seminiferous tubules are the interstitual cells (Ic). Those that lie at the periphery of the clusters usually have spindle shape, and are closely associated with the blood vessels (Fig 2E).

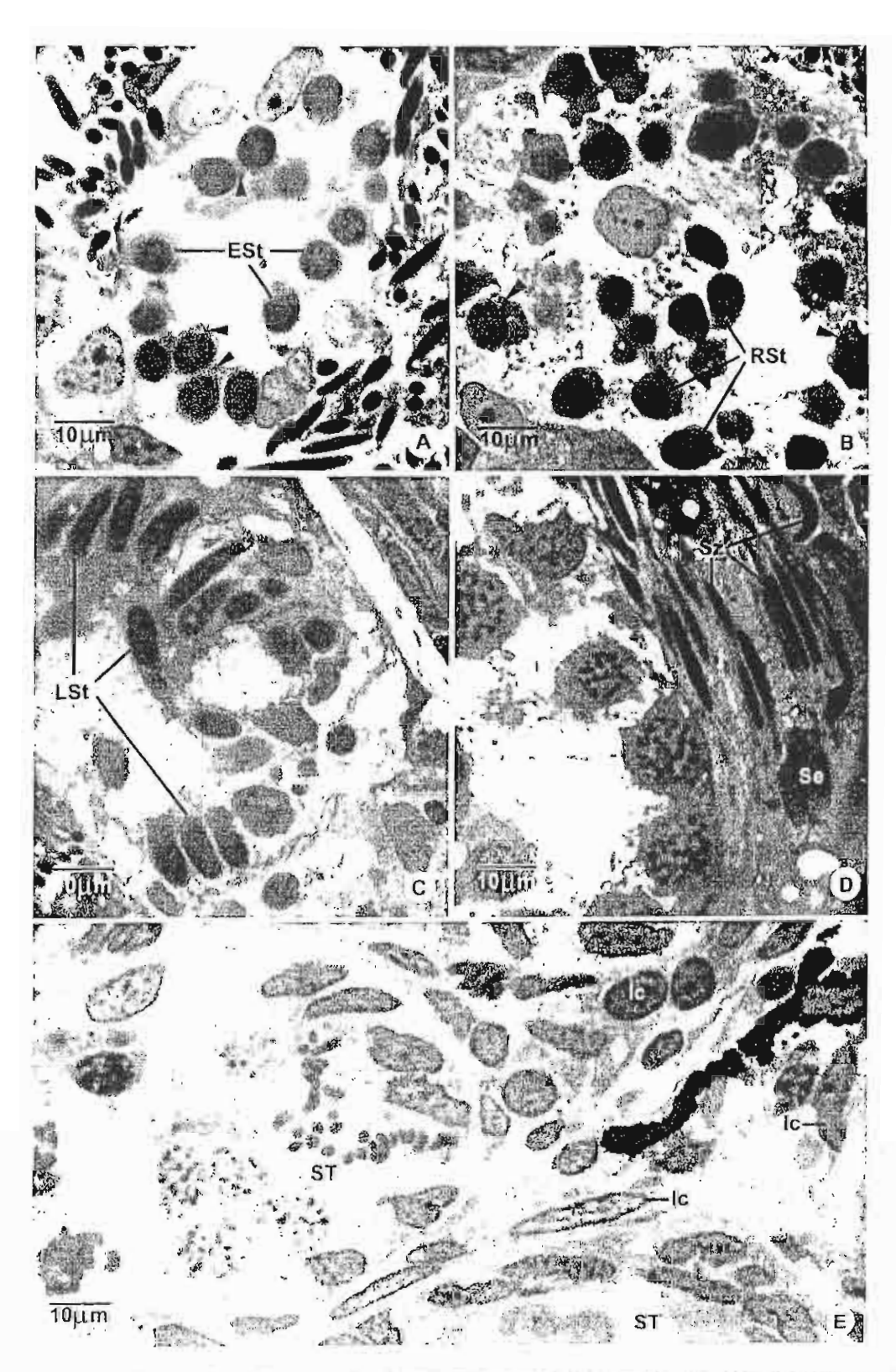
#### 2. Development of testes

Putative testis could be observed as a small avoid organ on the ventral surface of the kidneys when the frogs are around two months old. The testis is enclosed by peritoneal membrane and its vas deferens opens into the ureter.

Within the newly formed testis, the only principal

١).

U



Lig 2. A Dithigh magnification of seminificious tubules, showing cirtly spermatid (ESt), found spermatid (RSt), late spermatid (ESt), spermatoites (Eq.), and Seitoh cell (Se) In E section of the sura between seminificious tubules (SE), showing marishial cells (EE)

cell type is stromal cells with large round nuclei and spindle-shaped cytoplasm, characteristics which resemble undifferentiated mesenchymal cells. During 2-4 months, this cell type predominates in the sex cords located at the center, while some spermatogonia are present in those at the periphery (Fig 3A-C). Around the fourth month, all sex cords are enlarged and primary spermatogonia become dominant cell type.

In the fifth month, the seminiferous tubules become definitive entities and their walls start to contain other cell stages, including mainly primary spermatocytes. (Fig 3D). Spermatids could be identified in seven-month-old frogs and afterwards. Spermatozoa start to appear at the end of the seventh month (Fig 4A). By the end of the sixteenth month, the testis assumes similar appearance and cellular association as that of the fully mature male frogs (Fig 4B-D).

#### 3. Changes of testes during seasonal variation

Table 1. shows the changes in the body and testicular weights of adult male frogs collected over the period of 12 months. During post-breeding season (September-November), the testis shows decrease in weight, and the deepest drop is observed at the end of September or the beginning of October. During this period, the testis contains relatively few cell nests, and spermatogenetic activity is drastically decreased. Subsequently, testicular weights start to increase slightly in non-breeding period (December-January) when some early germ cells start to replenish the tubules which may still appear dilated and exhibit certain degree of degeneration of the epithelium (Fig 5B-D).

Spermatogenetic activities is clearly reactivated in February to March, which is designated as pre-

breeding period. The testicular weights significantly increase in comparison to earlier periods, and there is a rapid increase in the number of cell nests. Most of these cell nests transform into spermatozon during April to September which is the breeding period. The maximum testicular weight is observed in May, then it starts to decrease gradually until it reaches the minimum in September. During the breeding period, thick seminiferous epithelium contains numerous spermatocytes and round spermatids, while lumen are filled with fully mature spermatozoa. The maximal spermatogenetic activity is observed during the mid-breeding period around June (Fig 5A).

# DISCUSSION

#### Germ cell classification

In R. catesbeiana, the changes of nuclear characteristics could be used to divide germ cell into pre-mitotic stages which are composed of primary(typeA) and secondary(typeB) spermatogonia. The former is distinguished by the presence of completely euchromatic nuclei while the latter by the presence of small heterochromatin clumps along the nuclear envelope and nuclear center. After these cells enter meiosis I, the successive daughter cells consist of leptotene, zygotene, pachytene, diplotene and diakinesis- metaphase stage primary spermatocytes, respectively. Primary spermatocytes are characterized by the increased clumping of heterochromatin blocks or cords, that begin as loosely packed bodies of chromatin fibers in leptotene stage to the highly condensed heterochromatic cords in pachytene and diplotene stages, when they become intertwined to form bouquetfiked pattern.

When meiosis I is completed, the daughter cells

Table 1. Seasonal changes in the average body and testicular weights in R catesbelana during various months of the year.

Month	n	Body Weight (g) Mean ± SD	Testicular Weight (g) Mean ± SD	%Testicular Weight/Body Weight (GSI)
December-January		263.03 ± 36.05	$0.40 \pm 0.06$	0.15
February	8	$257.81 \pm 41.04$	$0.40 \pm 0.11$	0.15
March	8	$249.02 \pm 32.68$	$0.39 \pm 0.07$	0.16
April	7	$309.85 \pm 29.46$	$0.49 \pm 0.09$	0.16
May	4	$341.91 \pm 110.07$	$0.63 \pm 0.2$	0.18
June	5	$324.19 \pm 85.2$	$0.50 \pm 0.13$	0.15
July	5	$380.02 \pm 51.95$	$0.58 \pm 0.07$	0.15
August	5	292.19 ± 11.48	$0.33 \pm 0.12$	0.11
September	4	270.84 ± 29	$0.28 \pm 0.03$	0.11
October-November	1	249.87 ± 18.85	$0.32 \pm 0.04$	0.13

ly c st g ic n c

n e g

Fig. 3. A) Testis of one-month old long located serting to folding (180, illustrating genericals (Ge) and stromal cells (Sm). B) Bestis of two-month old long, illustrating the appearance of primary generals (pg). C) Testis of four month old long, illustrating a large month; of primary general cells (pg). D) Testis of five-month old frog, illustrating the long-ratio of committenes whites containing mostly only stages of generalists. Sg = specimalogonia, four = 35 pm.

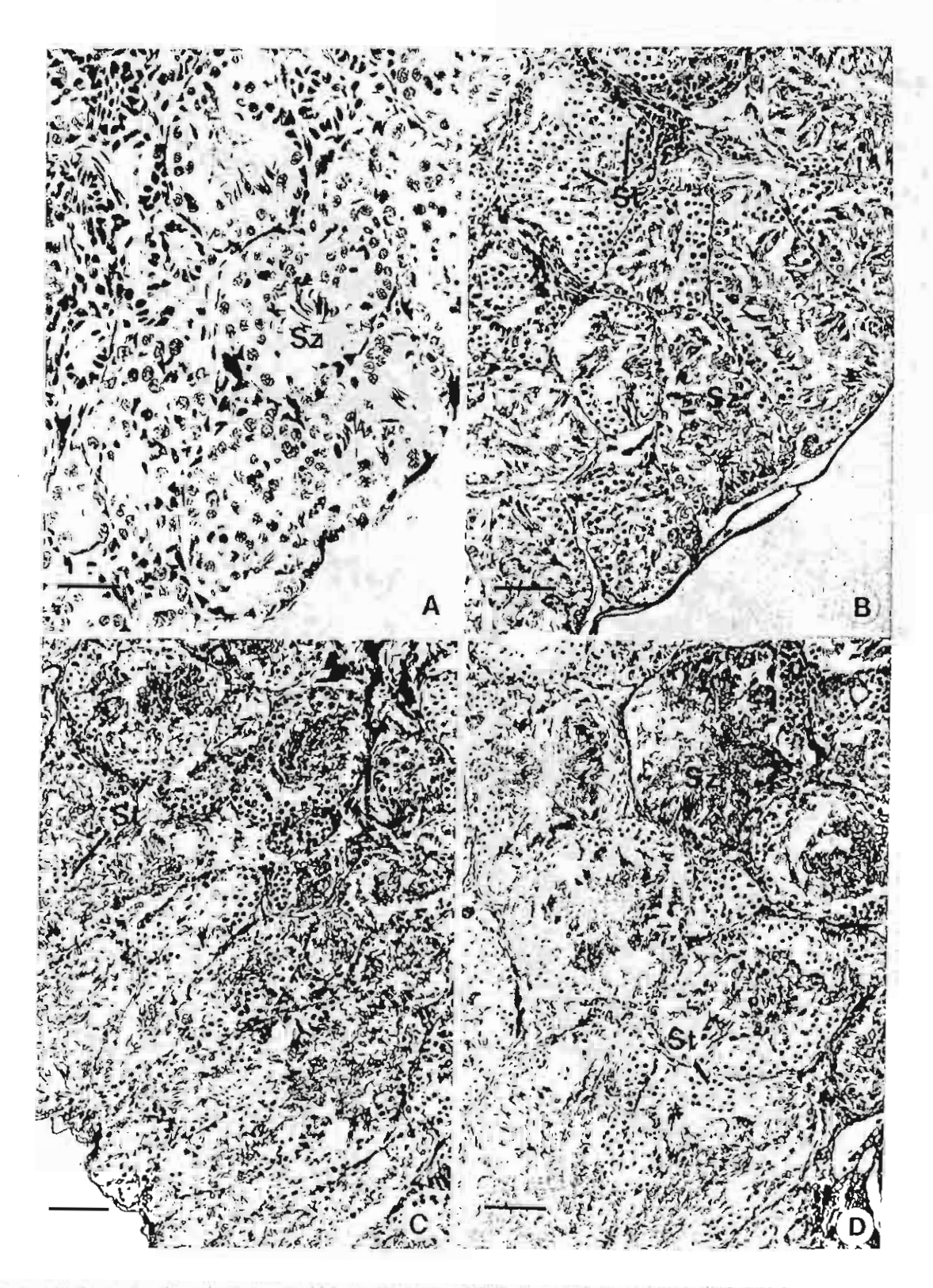


Fig 4. A, f) desire of eight and ion month-old frogs, illustrating definitive seminderons tubules which contain various stages of specimalogous cells, abundant sperimatals (5a) and sperimatozon (5a) for = 55 µm, C, D) festis of welve stud four term month old frogs, illustrating every stages of germ cells and a full number of sperimanish (5a) and sperimanism (5a). But = 110 µm.

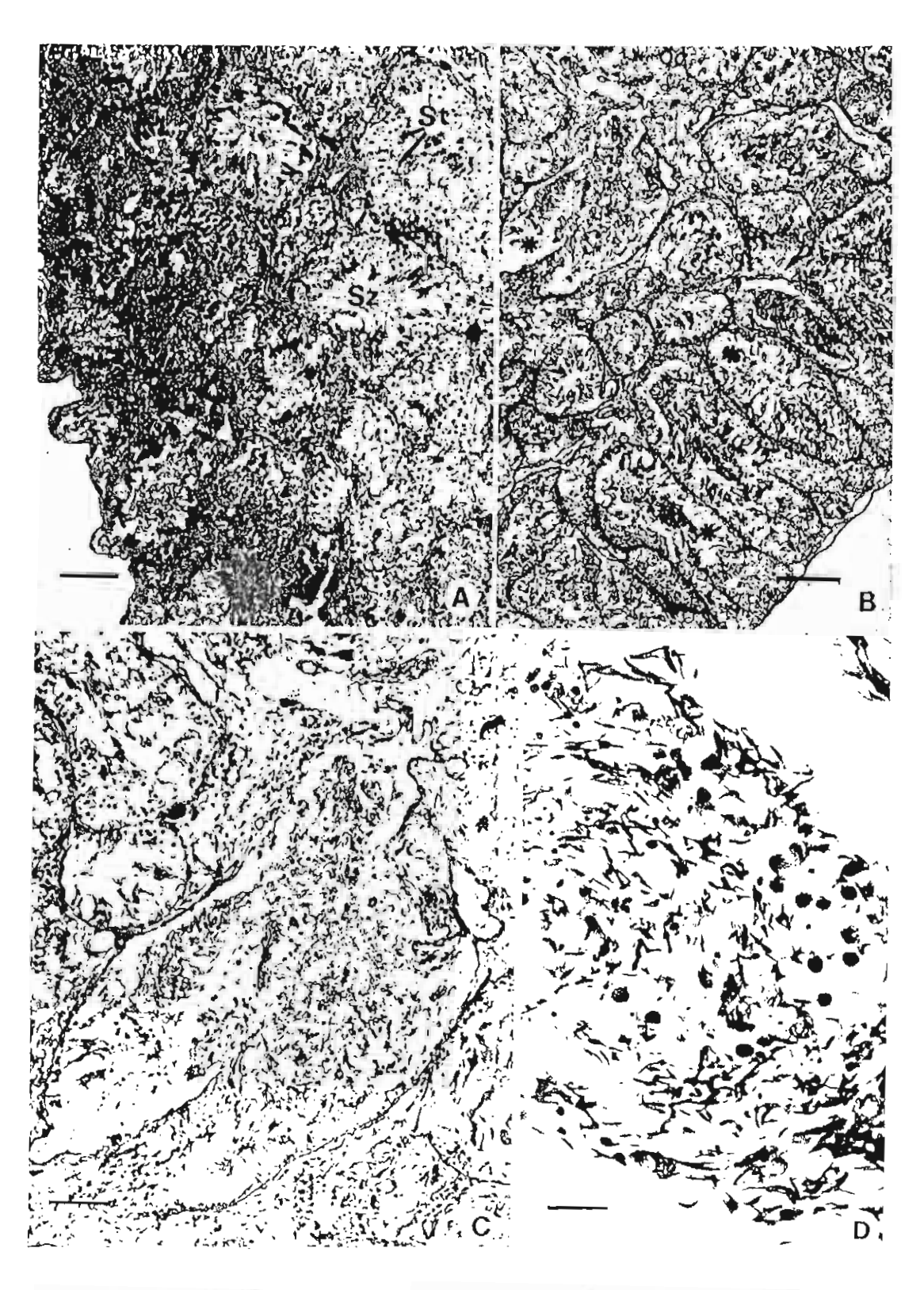


Fig 5. A) Tests of log during breading period, illustrating the thir k-walled seminiferous rundes containing surveys stages of germ cells especially a large manufact of seminiferous transfer and period, illustrating the desquarrance of lare stages of germ cells in the lumen of seminiferous tubules (asterisk). Some inhales are dilated and epithellium are thin t arrow local) and some break down (arrow), it is not a 400 pm, it is him a 100 pm, it has a 50 pm.

ol 1l1-

ScienceAsia 26 (2000)

are much reduced in size. Haploid secondary spermatocytes show nucleus with heterochromatin clumping along the nuclear periphery in a "cartwheel" pattern. These cells pass through meiosis II division, and consequently, transform into spermatids which are divided into early, middle and late spermatids. In early spermatid stage, the chromatin granules or libers become tightly packed within the round nuclei. These nuclei begin to transform into more clongated shape and are simultaneously reduced in size in middle and late spermatids, respectively. In addition, the small dark bar appearing in the cytoplasm could represent the beginning of the tail formation. After the condensation of chromatin and transformation of the nuclei are completed, the spermatozoa are derived.

In comparison to R. catesbeiana observed in the present study, Kalt<sup>2</sup> and Callard et al6 have studied testes of male X. laevis and found 11 stages of germ cells. They employed Ha-thymidine labelling and calculated the durations of various cell stages, including leptotene, zygotene, pachytene, diplotene and metaphase spermatocytes, whose durations were found to be 4, 6, 12, 1 and 1 days, respectively; and spermiogenesis needed 12 days to complete the process. In the toad, B. arenarum, Houssay could divide male germ cells into eight stages: namely two spermatogonia stages, spermatocyte l, spermatocyte II, three spermatid stages and spermatozoa. Afterwards, Rastogi et al. studied adult male Rana esculenta maintained at 18°C, and found 11 stages of spermatogenic cells, a situation comparable to the study of X. laevis by Kalt. However, it was noted that leptotene stage and spermiogenesis required longer periods than in R. esculenta. For a wrodele species, Triturus vulgaris, kept at 10°C, there were similar cell stages as identified in anurans. However, the duration of primary spermatocyte was longer while that of pachytene stage was shorter than both in X. laevis and R. esculenta.4

Radioisotope-labelling studies to determine the durations of male germ cells in *R. catesbeiana* have not yet been carried out. However, the relative durations of various cell stages could be inferred from the light microscopic observations. It is generally assumed that at any instant cells with longer duration should be present in more numerous number, while the scarce cells observed in each section should reflect the short duration or quick passage through that stage. From this generalization, it is suggested that sperinatogonta, pachytene spermatocytes, middle stage spermatids and differentiating.

spermatozoa had long durations; while secondary spermatocytes, diplotene and diakinesis-metaphase 1 spermatocytes have comparatively short durations.

#### Development of testes

Up to now, there have been many reports on the development of the testis. However, there have not yet been a common agreement on the origin of the testicular tissues in amphibians. Noble10 suggested that testes were derived from the kidney, while Spengel and Brauer found that testes apparently developed from a separate pair of gonadal ridges. Testis primordium as shown in R. sylvatica, consists of both medulla and cortex; and the inner medullary region was thought to be derived from the peritoneal covering of the genital ridge. 13 Sexual differentiation of gonads were thought to be controlled by two classes of substances: corticin that is localized in the cortex and stimulates the differentiation of female system, and medullarin which is localized in the medulla and stimulates the differentiation of male system. The predomination of the influence of one over the other was suggested to result in sexual differentiation of the gonads.13

In R. catesbeiana, a few large primordial germ cells could be observed in one-month-old frogs; and these cells were intermingled with mesenchymal cells in the region of putative testis or ovary. When the frogs were two months old, the sex cords appear in the gonads; afterwards, the definitive testis, which is ascertained by the presence of spermatogonia, could be discriminated in the fourth month, and spermatocytes appeared in five-month-old frogs. Seminiferous tubules with thick epithelium consisting of all stages of germ cells appeared on the seventh month, when there were abundant spermatids, especially middle or round stage, and a few spermatozoa. Thereafter, the number of mature spermatozoa increased gradually until they reached the maximum around the sixteenth month. Therefore, it appears that the sexual turning point or "puberty" in R. catesbeama reared in Thailand climate is around seven months old, and the complete sexual maturation is attained about sixteen months

#### Scasonal variation

Reproductive activities of most amphibians are greatly susceptible to environmental fluctuations, thus most of them exhibit markedly seasonal testicular cycle. Rastogi *et al.*<sup>14</sup> studied various environmental influences which could after the characteristics of internal morphology of the testis

try

use us.

he

101

lie

cd

ile

tly

CS.

515

try

no

vo he

11-

he

110

ne

tal

115

56

in

15

he

15

10

1d

111

10

111

re

:d

h.

111

141

10

11

I,C

S.

ari.

18

in *R. esculenta*, and found that these influences consist of rainfall, temperature and photoperiod. These factors cause cyclical external morphological changes as well as internal changes of the testis. For example, the toad, *B. arenarum* has maximum development of the thumbpad and testicular weight in spring, when the germ cells and spermatozoa were also markedly increased. *P. Rana ridihanda*, with continuous type spermatogenesis, show significantly increased number of spermatids during breeding season around April to June, while in winter, the number of spermatocytes was decreased and reach minimum in the coldest month. <sup>16</sup>

In the central and upper parts of Thailand, where the wet and dry seasons are quite distinct, R. catesbeiana show responses to seasonal change in both external appearance and reproductive capacity. During the breeding season (April-September), the secondary male characteristics such as thick greyish thumbpad are exhibited while the seminiferous tubules' production of spermatids and spermatozoa also come in full steam. In the non-breeding period (December-January), these tubules consist mainly of early spermatocytes with only few round spermatids; and some tubules are dilated and exhibit desquamation of the epithelium, in the pre-breeding period (February-May) there are numerous primary spermatocytes and spermatogonia in preparation for subsequent development, while during the postbreeding period (October-November) there appear spaces or vacuoles in the tubules from ruptured cell nests. Such cyclical change may depend on the availability of gonadotropins, as has been demonstrated in Rana temporaria that exogenous administration of these hormones or the elevation of environmental temperature could stimulate recordescence of spermatagenetic activity in the scasorally quiescent males. The toad, Bufo bufots, and greenfrog, R. esculentain, were the other two wellstudied species which showed similar cycles to seasonal variation. Another evidence supporting the response of the testis to seasonal changes is the gonadosomatic index (GSI) which correlates the changes of body weight and testicular weight. Kao et al. 24 showed that GSI in Rana rugulosa exhibited the rising phase in hibernation and pre-breeding season (January-March), while the maximum GSI were observed in the breeding period (April-June). On the other hand, GSI sharply decreased in the late breeding period (Jane-early July) and remained at the low level in post-breeding period (August-Octuber) In R. catesbeiana, the Changes of GSI also exhibited similar pattern as those of it, rugulosa and

it is interesting to note that in this species the reactivated spermatogenesis actually begins even before the rainy season which usually starts around middle of May. Furthermore decline of spermatogenesis commences before the end of rainy season which is around the end of October. Therefore, the present study demonstrated that *R. catesbeiana* does exhibit cyclical changes of the testis in response to seasonal variation.

## **A**CKNOWLEDGEMENTS

This research was supported financially by National Center for Genetic Engineering and Biotechnology, the National Science and Technology Development Agency (Grant # 01-35-006) and Thailand Research Fund (Senior Research Scholar Fellowship to Prasert Sobhon)

# REFERENCES

- Reed SC and Stanley HP (1972) Fine structures of spermatogenesis in the South African elawed toad Xenopus lacvis Daudin, J Ultrastruct Res 41, 277-95.
- Kali MR(1976) Morphology and kinetics of spermatogenesis in Xempus lacvis, J Exp 2nal 195, 393-408.
- Risley MS, Miller A and Bunicrot DA (1987) In vitro maintenance of spermatogenesis in Xenopus lucvis testis explains cultured in scrain free media. Biol Reprod 36, 985-97.
- Rugh R (1951) The Irog: its reproduction and development.
   Ist ed. pp 31-43. Mr. Graw-Hill Book Company, New York.
- Zishin BR (1971) The line structure of nuclei during spermiogenesis in the leopard log, Radio pipinas, J Ultrastruct Res 34, 159-74
- Callard IP, Callard GV, Cance V, Bolaffi JL and Rosser JS (1978) Testicular regulation in nonmammalian vertebrates. Biol Perpod 18, 16-43.
- Houssay BA (1954) Hormonal regulation of the sexual function of the male road. Acta Physiol Latin-amer 4, 1-41.
- 8 Rastogi RK, Icla L, Di Meglio M, Di Mauco L, Minucci S and Izzo-Vitiello 1 [1983] Initiation and kinetic probles of sperimogenesis in the Irog Rana esculenta (Amphibian). Zool Lond 201, 515-25.
- Callao HC and Taylor #1 (1968) A radioautographic study of the time course of male meioses in the newt friturus vulgaris. J Cell Sci 3, 635-27.
- Noble GK (1931) The Biology of Amphibia: The Urogenital System. Isted pp272-281. Mc Graw-Hill Company, New York.
- Spengel JW (1976) Das mogenital system der amphibien. I theil. Der austomische han des etrogenital system. Acheir Ausdem Zoof Inst. Warzburg 3, 24: 114.
- 12 Brance A, Bertrag zur Le meinis der Luxuschlung und Anatomie der Gymnophionen III (1902) Univerklung der Excretionsorgane, Zool Jahrb Anat 3, 1-176
- 13. Wischi E (1929) Studies on sex differentiation and sexelectromation in implifibilities. It sex reversal in Female 32/50/es of Rum sylvatic following the application of high temperature. J Exp 250/ 52, 267-92.
- 14. Rastogi RK, Jehel, Och io L. Dinegho M, Russo A and Chieffi G. (1978) Environmental influence on resemble activity in the green long Resembnute J Exp 2001/206, 49-64.

- Burgos MII (1950) Regulación hormonal de los caracteres sexuales secundarios en el sapo macho. Rev Soc Aigent Biol 26, 359-71.
- to Loumbourdis NS and Kyriakoponton-Sklavoumm P (1991) Reproductive and lipid cycles in the male frog Runn rillihimhi in northern Greece. Comp Biochem Physiol 99, 357-83.
- 17 Van Oordi PGWJ (1960) The influence of internal and external factor in the regulation of the spermatogenetic cycle in Amphilia. Symp Zool Soc Lond 2, 29-52.
- 18 Jorgenson CB, Larsen Lo and Lotts B (1979) Annual cycles of fat bodies and gonads in the toad Bufo bufo (L.), compared with cycles in other temperate zone anurans. Biologiske Skrifter K. Danske Videnskubomes Sciskab 22, 1-37.
- Lofts B (1964) Seasonal changes in the functional activity of the interstitual and spermatogenetic tissue of the green frog, Rana escalenta. Gen Comp Enduction 4, 550-62.
- Kao YH, Alexander PS, Cheng Yang VV, and Yu JYL (1993)
   Annual patterns of testicular development and activity in the Chinese bullfrog (Rana rugulosa Wiegmann). Zond Sci 10, 337-51.

# ULTRASTRUCTURE OF SPERMATOZOA IN THE TESTIS OF HALIOTIS ASININA LINNAEUS

Somjai Apisawetakan<sup>1</sup>, Prasert Sobhon<sup>1</sup>, Chaitip Wanichanon<sup>1</sup>, Vichai Linthong<sup>1</sup>, Maleeya Kruatrachue<sup>2</sup>, E. Suchart Upatham<sup>2,3</sup>, Padermsak Jarayabhand<sup>4</sup>, Tanate Pumthong<sup>5</sup> and Jintana Nugranad<sup>5</sup>

#### **ABSTRACT**

When studied by TEM and SEM, the head of a spermatozoa of *Haliotis asinina* Linnaeus appears as a cone-shaped cell whose size is about 3 x 1-1.5 µm, with a long tail. The acrosome is an inverted cup-shaped structure covering the indented anterior end of the head and containing a homogeneously dense matrix. There is an acrosomal core with a crystalline structure occupying the concave subacrosomal space, with its base resting in the indention of the anterior tip of the nucleus. The nucleus contains chromatin granules, about 60 nm in diameter, that are densely packed together, and a few nuclear vacuoles. At the posterior end of the nucleus, there are 3-5 globular-shaped mitochondria that are adhered to the nucleus by dense plaques of outer membranes, and linked to the posterior half of the sperm membrane by zig-zag filaments. A pair of centrioles are located in the middle of the mitochondria, with the proximal horizontal centriole tightly attached to the nucleus by thickened double plates, and the distal vertical centriole gives rise to a long tail. An axoneme of 9+2 doublets of microtubules makes up the entire core of the tail, whose membrane in the proximal part is crenulated, while that in the remaining distal part is tightly fitted around the axoneme.

Key words: Spermatozoa, ultrastructure, Haliotis asinina.

#### INTRODUCTION

As in mammalian species, mollusk sperm are either cone-shaped or highly elongated with some appearing spiral; they conform to the typical architecture of flagellated animal sperm in possessing an acrosome (absent in some), a head, a mid piece and a tail. In spite of the general similarity, however, there are unique features in the sperm of various mollusk species. By and large, sperm of externally-fertilizing mollusks are considered primitive, by virtue of having cone-shaped heads and long tails that do not have a middle piece. Instead, their mitochondria are located at the base of the nucleus (Franzen, 1955). In contrast, sperm of the internally-fertilizing mollusks, especially among neogastropods of freshwater, marine and even terrestrial species, possess long slender heads, and elongated middle pieces where helical or long straight mitochondria are concentrically arranged around the axonemes (Walker & MacGregor, 1968; Walker, 1970; Franzen, 1970; Kitajima & Paraense, 1976; Huaquin & Bustos-Obregon, 1981; Healy, 1983; Healy & Willian, 1984; Azevedo & Corral, 1985; Jaramillo et al., 1986; Hodgson, 1986; Gallardo & Garrido, 1989; Sretarugsa et al., 1991; Al-Hajj & Attiga, 1995; Pastisson & Lacorre, 1996). Abalone are prosobranch gastropods, which are considered to be rather primitive and reproduce by external fertilization. Thus,

<sup>&</sup>lt;sup>1</sup>Department of Anatomy, Faculty of Science, Mahidol University, Rama VI Road, Bangkok 10400, Thailand.

<sup>&#</sup>x27;Corresponding author and reprint request.

<sup>&</sup>lt;sup>2</sup>Department of Biology, Faculty of Science, Mahidol University, Rama VI Road, Bangkok 10400, Thailand.

<sup>&</sup>lt;sup>3</sup>Department of Biology, Faculty of Science, Burapha University, Chonburi, 20131, Thailand.

<sup>&</sup>lt;sup>4</sup>Department of Marine Science, Faculty of Science, Chulalongkorn University, Bangkok 10330, Thailand.

<sup>5</sup>Coastal Aquaculture Development Center, Department of Fisheries, Ministry of Agriculture and Cooperatives, Klong Wan, Prachuapkhirikun, 77000, Thailand.

their sperm belong to the first type. However, even within their own genus, spermatozoa of abalone exhibit species-specific characteristics. In the present study, we report the ultrastructure of spermatozoa in *Haliotis asinina*, a species commonly found in the coastal waters of tropical regions, including Thailand.

## MATERIALS AND METHODS

#### Collection of Haliotis asinina specimens

Abalone from a land-based culture system were provided by the Coastal Aquaculture Development Center, Prachaubkirikhun Province, and Marine Biological Station, Chulalongkorn University, Angsila, Chonburi Province. They were kept in concrete tanks housed in the shade, that were well flushed with mechanically circulated filtered sea water and aerated by air delivery system to maintain the controlled environment. The optimum level of salinity was about 22.5-32.5 ppt, and the temperature was about 22-26°C (Singhagraiwan & Doi, 1993). They were fed with a diet of macroalgae (usually *Gracilaria* spp. and *Laminaria* spp.) and supplemented with artificial food for abalone.

#### Electron microscopic study

Small pieces of the testis were prefixed with 3% glutaraldehyde in 0.1 M sodium cacodylate buffer, pH 7.4, at 4°C overnight, then prepared for electron microscopic observations by conventional transmission electron microscopic (TEM) and scanning electron microscopic (SEM) methods.

For TEM studies, the specimens were post-fixed in 1% osmium tetroxide in the same buffer at 4°C for 2 hours, then dehydrated in a graded series of ethanol, and embedded in Araldite 502 resin. Ultrathin sections were cut and stained with lead citrate-uranyl acetate and viewed under a Hitachi TEM H-300 at 75 kV.

For SEM studies, the specimens were post-fixed, ethanol-dehydrated, critical-point dried in liquid CO<sub>2</sub>, and coated with Platinum-Paladium in an ion-sputtering apparatus. Finally, they were examined with a Hitachi S-2500 scanning electron microscope at 15 kV.

#### RESULTS

# Scanning electron microscopy (SEM)

Under SEM, a testicular sperm has a cone-shaped head, whose size is about 3  $\mu m$  in length, 1.5  $\mu m$  in width at the base of the nucleus and 1  $\mu m$  at the acrosomal-nuclear junction (Fig. 1A-D). Compared to earlier stages of germ cells, the surface of spermatozoa appears smooth (Fig. 1B, C). The anterior end is covered by a cup-shaped acrosome, and the posterior end by five spherical mitochondria of similar size. Projecting from the middle of mitochondria is a long, slender, and uniform tail (Fig. 1B, C, D).

#### Transmission electron microscopy (TEM)

Under TEM, the acrosome appears as an inverted cup, whose concavity separates it from the anterior border of the nucleus, which is also indented. This subacrosomal space contains a crystalline acrosomal core embedded in a more homogeneous material (Fig. 2B, E, F). The acrosomal matrix itself appears homogeneous with varying degree of electron opacity (Fig. 2E, F).

The nuclei of most spermatozoa contain completely condensed chromatin which appears electron opaque except for clear areas of intranuclear vacuoles where there seems to be little chromatin material. Vacuoles vary in size and are distributed randomly throughout the nucleus. In a few spermatozoa, the nuclear chromatin still appears granular with numerous round granules tightly packed together, with each

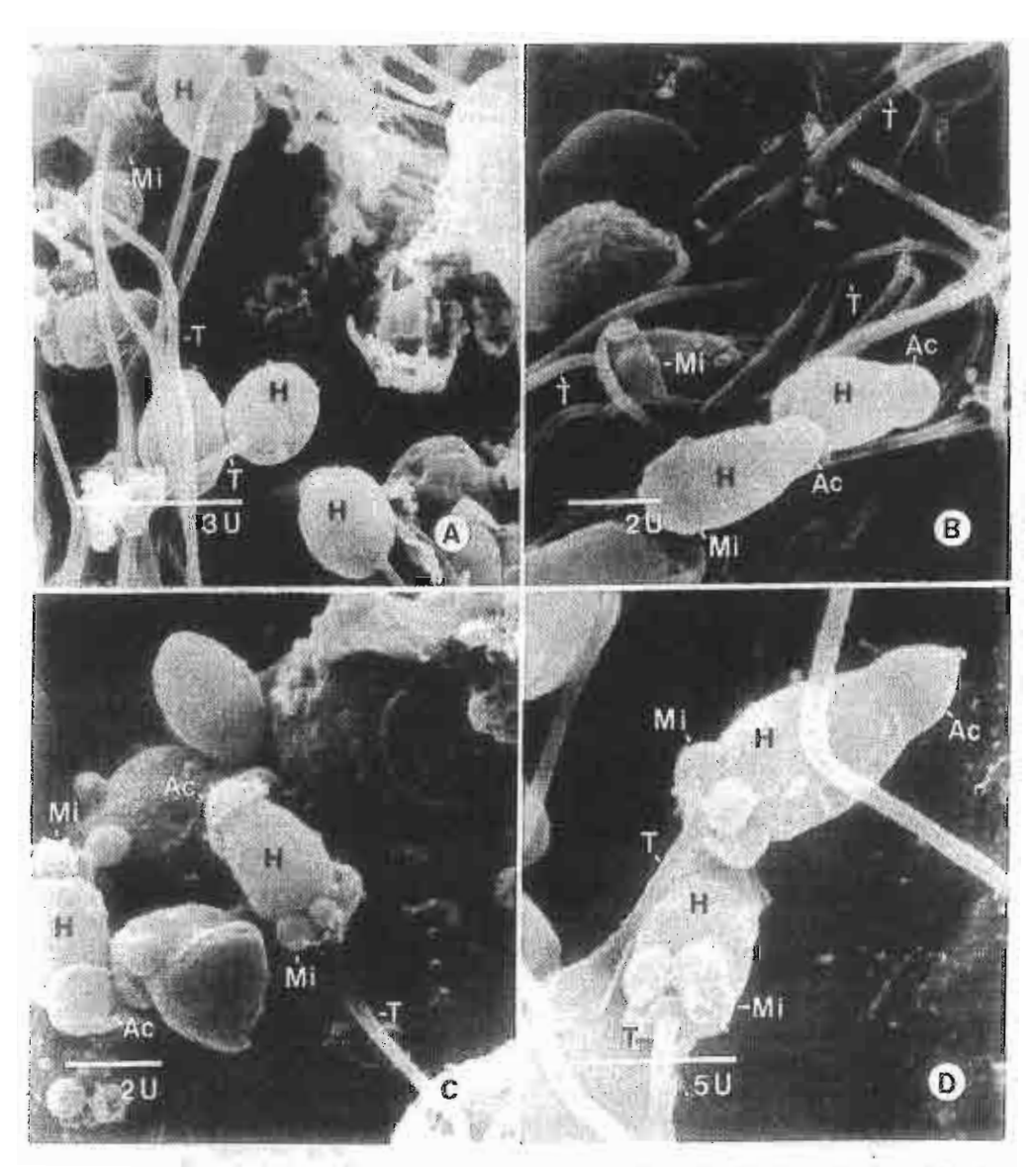


FIG. 1. Scanning electron micrographs of spermatozoa in the testis showing cone-shaped heads (H) and rod-shaped tails (T) (A, B). Five globular mitochondria (Mi) at the base of the head surrounds the proximal region of the tail (C, D), and a cup-liked acrosome (Ac) covers the anterior end of the head (C, D).

"granule" about 60 nm in diameter (Fig. 3B, D). These granules are of similar size and characteristics as those observed in earlier stage spermatids where chromatin is not yet completely condensed.

The posterior border of the nucleus is flanked by large, spherical mitochondria. In a longitudinal thin section of the nucleus, usually two to three mitochondria could be observed (Fig. 2A, B, C). However, in fortuitous cross-sections at the level of mitochondria, there appears to be five of these bodies arranged in a circle surrounding the centriole (Fig. 2A, B). Each mitochondrion is tightly apposed to the nucleus at which